QUASI-HOMOGENEOUS GOLD AND BIMETALLIC NANOPARTICLE CATALYSTS

A thesis submitted to

The College of Graduate Studies and Research

In Partial Fulfillment of the Requirements

For the Degree of Master of Science

In the Department of Chemistry

University of Saskatchewan

Saskatoon

By

Wenbo Hou

PERMISSION TO USE

In presenting this thesis in partial fulfillment of the requirements for a Postgraduate degree from the University of Saskatchewan, I agree that the Libraries of this University may make it freely available for inspection. I further agree that permission for copying of this thesis in any manner, in whole or in part, for scholarly purposes may be granted by the professor or professors who supervised my thesis work or, in their absence, by the Head of the Department or the Dean of the College in which my thesis work was done. It is understood that any copying or publication or use of this thesis or parts thereof for financial gain shall not be allowed without my written permission. It is also understood that due recognition shall be given to me and to the University of Saskatchewan in any scholarly use which may be made of any material in my thesis.

Requests for permission to copy or to make other uses of materials in this thesis in whole or part should be addressed to:

Head of the Department of Chemistry

University of Saskatchewan

Saskatoon, Saskatchewan, S7N5C9

Canada

ABSTRACT

The research in this thesis involves the synthesis and characterization of nanoparticle catalysts for oxidation reactions. It includes two projects: 1) polymer-stabilized Au, Pd and bimetallic AuPd nanoparticle catalysts for alcohol oxidation reactions, and 2) oxidative stabilities and catalytic activities of thiolate- and dithiolate-protected Au monolayer-protected clusters (MPCs).

In the first project, alcohol oxidations under mild conditions using polyvinylpyrrolidone (PVP)-stabilized Au, Pd and bimetallic AuPd nanoparticle catalysts in aqueous solutions have been investigated. The catalytic activities of the nanoparticles towards the oxidation of benzyl alcohol, 1-butanol, 2-butanol, 2-buten-1-ol and 1,4-butanediol indicate that bimetallic 1:3 Au:Pd nanoparticles have higher catalytic activities than Au, Pd and other bimetallic AuPd nanoparticles, and that selectivities towards specific products can often be tuned using bimetallic particles. In addition, advantages and disadvantages for the use of such nanoparticle catalysts as mild, environmentally-friendly oxidation catalysts have been examined. This work has recently been published in the *Journal of Catalysis*.

In the second project, 1-dodecanethiolate-, dithiolate-, and 1:1 mixed 1-dodecanethiolate/dithiolate-protected Au MPCs have been synthesized and their thermal stability, oxidative stability in the presence of oxygen and cyanide anions have been studied. These systematic investigations reveal the stability of Au MPCs can be tuned by choosing different thiolate ligands and oxidation conditions. Partially-oxidized thiolate-protected Au MPCs which have substrate-accessible surfaces and are stabilized by

residual thiolate ligands show indications they will be promising catalysts. The catalytic activities of 1-dodecanethiolate-, dithiolate-, and 1:1 mixed 1-dodecanethiolate/dithiolate-protected Au MPCs for catalytic 4-nitrophenol reduction with sodium borohydride were investigated, and all the Au MPCs showed high catalytic activity for this reaction.

ACKNOWLEDGEMENTS

I would like to thank Dr. Robert W. J. Scott for his invaluable help and guidance. I greatly appreciate all of his time and hard work he invested in me. He is the best supervisor I ever met. I would also like to thank Dr. Ian Burgess, my advisory committee member, for his great suggestions about my research work. Thanks to Nicole A. Dehm for her wonderful basic work about polymer-stabilized Au, Pd and bimetallic AuPd nanoparticle catalysts for alcohol oxidation reactions. Thanks to Mita Dasog for teaching me how to synthesize thiolate-protected Au MPCs. Finally, thanks to all of members in Dr. Scott's, Dr. Burgess', Dr. Paige's and Dr. Palmer's groups for all of their help.

In addition, thanks to NSERC, the University of Saskatchewan and Department of Chemistry for financial support and Ken Thoms and the Saskatchewan Structural Science Centre for help with GCMS measurements.

TABLE OF CONTENTS

LIST OF TABLES

LIST OF FIGURES

LIST OF SCHEMES

LIST OF ABBREVIATIONS

AOT	Sodium Bis(2-ethylhexyl) Sulfosuccinate
BINAP	2,2'-Bis-(diphenylphosphino)-1,1'-Binaphthyl
BMIM	1-n-Butyl-3-Methylimidazolium
CLS	Canadian Light Source
DMA	Dimethylacetamide
EDS	Energy Dispersive Spectroscopy
EXAFS	X-ray Absorption Fine Structure Spectroscopy
GC	Gas Chromatography
GCMS	Gas Chromatography-Mass Spectrometry
HBTU	2-(1H-Benzotriazole-1-yl)-1,1,3,3-Tetramethyluronium Hexafluorophosphate
HOBT	N-Hydroxybenzotriazole
HPLC	High Performance Liquid Chromatography
HRTEM	High Resolution Transmission Electron Microscopy
MPCs	Monolayer-Protected Clusters
NIPA	Poly(N-isopropylacrylamide)
NMR	Nuclear Magnetic Resonance
PAMAM	Poly(amidoamine)
PDMS	Poly(dimethylsiloxane)
PEO	Poly(ethylene oxide)
PhIO	Iodosylbenzene
PLC	Poly(ε-caprolactone)

PPI	Poly(propylene imine)
PVA	Poly(vinylalcohol)
PVP	Poly(N-vinyl-2-pyrrolidone)
SPA	Sodium Poly(acrylate)
TEM	Transmission Electron Microscopy
TEMPO	2,2,6,6-Tetramethyl-Piperidyl-1-Oxy
TGA	Thermal Gravimetric Analysis
THF	Tetrahydrofuran
TOAB	Tetraoctylammonium Bromide
TOFs	Turnover Frequencies
UV-Vis	UV-Vis Spectroscopy
XRD	X-ray Diffraction
XPS	X-ray Photospectroscopy

CHAPTER 1

Literature Survey-"Quasi-homogeneous" Nanoparticle Catalysts

1.1 Introduction of Nanoparticle Catalysts

A catalyst is a species which is added to a chemical reaction but does not get consumed. It works by providing an alternative reaction pathway in which the activation barriers of a reaction are lowered and the reaction rate is increased [1]. Catalysts are used widely in chemical reactions and in industry. Metal nanoparticles are promising catalysts for a variety of reactions, for example, oxidation, hydrogenation and C-C coupling reactions [2], given they have a very large surface-to-volume ratio. Metal nanoparticles (colloids, clusters) have been used as catalysts since the 19^{th} century [3], and industrial and petrochemical catalysis have involved nanoparticles since the beginning of the 20^{th} century [4, 5]. A major achievement in nanoparticle catalysis came with Haruta's report that oxide-supported gold nanoparticles were an effective catalyst for low-temperature oxidations of H_2 and CO in 1989 [6]. Since then, nanocatalysis has attracted more and more attention and an exponential growth has been seen in the number of publications in the literature [3].

"Naked" metal nanoparticles are unstable and tend to aggregate, agglomerate, and even precipitate out of solution and lose their catalytic activities. Therefore metal nanoparticles traditionally need to be supported on solid surfaces (*e.g.* oxide, carbon) [3] to form heterogeneous catalysts. The advantages of heterogeneous catalysts are that they

are easy to separate from the reactants and products for recovery and reuse. Also, they can be used at high temperatures and pressures. However, they often have poor catalytic activities and selectivities compared to many homogeneous catalysts [7]. An alternative method to stabilize metal nanoparticles is using polymers, block copolymers, dendrimers, surfactants, or organic ligands as stabilizers [3]. Polymer- or ligand-stabilized metal nanoparticles can be uniformly dispersed in organic solvents or water and mixed with reactants and products in a way resembling a homogeneous catalytic system [8]. Such catalytic systems are often called "quasi-homogeneous" nanoparticle catalysts. Quasi-homogeneous catalysts can have high catalytic activities and selectivities. However, insufficient stability and high costs, due to difficulties in recovery and reuse, are major drawbacks [9]. In this thesis, I will focus on the use of quasi-homogeneous nanoparticle catalysts. The use of different stabilizers and how the stabilizers affect the catalytic activity will be discussed.

1.2 "Quasi-homogeneous" Nanoparticle Catalysts

Quasi-homogeneous metal nanoparticles (metal colloids) can be synthesized using five general methods: (1) chemical reduction of metal salts, (2) thermal, photochemical, or sonochemical decomposition, (3) ligand reduction and displacement from organometallics, (4) metal vapor synthesis, and (5) electrochemical reduction [2]. Among them, chemical reduction of metal salts is the most frequently used method. This method is pretty straightforward; metal salts are reduced in the presence of stabilizers, *e.g.* polymers or surfactants [10]. Sodium borohydride is commonly used as the reducing agent, and often the metal salts and stabilizers can be dissolved in the same solvent and

reduced *in-situ*. Two-phase methods are a proven alternative. A typical Brust-Schiffrin synthesis involves $AuCl_4^-$ transfer from aqueous solution to toluene using tetraoctylammonium bromide (TOAB) as a phase-transfer reagent, followed by reduction with aqueous sodium borohydride in the presence of dodecanethiol [11]. In the following sections, the types of stabilizers and the effect of the stabilizers on the size, shape, and catalytic activity of metal nanoparticles will be elucidated.

1.2.1 Polymer-stabilized Nanoparticle Catalysts

Polymers can stabilize metal nanoparticles through the steric bulk of their framework, but also by binding weakly to the nanoparticle surface through heteroatoms that play the role of ligands [3]. Poly(N-vinyl-2-pyrrolidone) (PVP) is a popular polymer for nanoparticle stabilization; Hirai and coworkers first reported the use of PVP as a stabilizer for metal nanoparticles in 1979 [12]. PVP-stabilized metal nanoparticles are known to be weakly stabilized through multiple coordination of the amido sites of the PVP (Scheme 1.1), and are stable even in boiling water for short time periods [13, 14]. PVP-stabilized metal nanoparticles have been used as catalysts for a variety of reactions [3]. El-Sayed *et al.* showed that PVP-stabilized Pd nanoparticles are efficient catalysts for Suzuki C-C coupling reactions in aqueous media [15, 16]. Another interesting paper utilizing PVP-stabilized Pd nanoparticles was reported by Gniewek *et al*., who investigated the effect of the type of reducing agent and reduction conditions on the morphology and size distribution of palladium nanoparticles, and found that the sizes and shapes of the Pd nanoparticles, as well as the molecular weight of PVP used for their stabilization, play decisive roles in the catalytic activity toward the

methoxycarbonylation of iodobenzene [10]. Tsunoyama *et al.* reported the first successful application of PVP-stabilized gold nanoparticles toward the aerobic oxidation of benzylic alcohols in water at ambient temperatures [13]. In 2007, they showed that PVP-stabilized Au nanoparticles also have a high catalytic activity toward the aerobic oxidation of various kinds of primary and secondary alcohols in aqueous solution under ambient conditions [17].

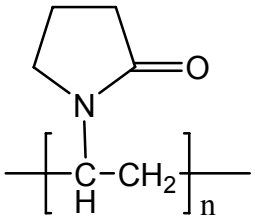

Poly(vinylpyrrolidone) (PVP)

Scheme 1.1. Poly(vinylpyrrolidone) stabilizer for metal nanoparticle catalysis.

There are two major advantages of using PVP as a stabilizing agent: (1) PVP is commercially available and is relatively low cost, and (2) PVP-stabilized metal nanoparticles can be dispersed in water and used as quasi-homogeneous catalysts to catalyze aqueous reactions [13, 15-17]. Water is an ideal "green" solvent due to environmental, economical, and safety reasons [16]. However, it should be pointed out that PVP-stabilized metal nanoparticles do have drawbacks; often agglomeration, aggregation and even precipitation happen during or after the reaction, particularly when a substrate or product can bind strongly to the nanoparticle surface [15]. Thus, PVP-stabilized metal nanoparticle catalysts can seldom be recycled and reused.

Besides PVP, a variety of other polymers have been used as stabilizing agents to stabilize metal nanoparticles in order to improve either the catalytic activity and/or the recyclability of the catalysts. One example of a system showing improved catalytic activity is the work of Liu *et al.*, who found that poly(N,N-dialkylcarbodiimide)-stabilized Pd nanoparticles were a robust catalyst for the Suzuki coupling reaction [18]. They postulated that catalyst exhibited a high catalytic activity due to the weak coordination between poly(N,N-dialkylcarbodiimide) and the Pd nanoparticle surfaces. Other groups have shown systems with improved recyclability. For example, Kanaoka *et al.* prepared thermosensitive vinyl ether star polymer-stabilized Au nanoparticles and found that they were catalytically active toward the aerobic oxidation of phenylic alcohols [19]. The clusters were easily separated from the reaction mixture by utilizing their thermosensitive nature, allowing for separation and reuse. Mertens *et al.* reported PVA (poly(vinylalcohol))-stabilized Au nanoparticles are active and chemoselective catalysts for the oxidation of aliphatic 1,2-diols in alcohol media [20], and the Au nanoparticle catalysts could be recycled by filtering through poly(dimethylsiloxane) (PDMS) membranes with excellent preservation of activity [20]. However, it is likely that the alcohols which were used as the reaction media were also oxidized during the reaction. Chauhan *et al.* showed that polymethylhydrosiloxane-stabilized Pd nanoparticles are recyclable and chemoselective hydrogenation catalysts for functional conjugated alkenes, and showed that polymethylhydrosiloxane had functions both as a reducing agent and a stabilizer during the synthesis [21]. Polyurea-stabilized Pd nanoparticles were proven to be effective recyclable catalysts for Suzuki coupling reactions [22]. Finally, Biffis *et al.* synthesized N, N-dimethylacrylamide-based soluble

cross-linked polymer microgel-stabilized Pd nanoparticles and found they were remarkably active catalysts for the aerobic oxidation of benzylic secondary alcohols in water [23]. The nanoparticle catalysts were readily separated from the reaction products and could be reused, albeit to a limited extent. Unfortunately the catalytic activity for the oxidation of aliphatic secondary alcohols was quite poor.

Block copolymers have been effectively used as stabilizers as well. Pd nanoparticles which were stabilized by 5-arm star-shaped block copolymers with a poly(ethylene oxide) (PEO) core and a poly(ε-caprolactone) (PLC) corona were a highly active catalyst for Heck cross-coupling reactions [24]. In addition, Pd nanoparticles stabilized in polystyrene-co-poly(ethylene oxide) were shown to be an effective catalyst for reactions of C-C and C-heteroatom bond formation [9]. The catalyst had a much higher stability than the low-molecular-weight palladium complexes and could be recycled by thermomorphic separation from products. Thermomorphic separations, in which a solvent system reversibly changes from biphasic to monophasic with mild heating, are also possible using block copolymers [25]. For example, Bergbreiter and coworkers used Pd nanoparticles stabilized by polystyrene-co-poly(ethylene oxide) in a thermomorphic heptane-10% aqueous DMA (2:1) mixture which was biphasic at room temperature and homogeneous when heated to 90 ^{o}C. After the solution was cooled to room temperature, the catalyst remained in the polar layer and the hydrophobic product stays in heptane, allowing them to be easily separated from each other [9].

Many of the polymers or copolymers used as stabilizers in the above paragraphs were used mainly in order to improve the recyclability of catalysts [19-21, 23]. The poor recyclability of PVP-stabilized metal nanoparticles is a major drawback for their use as

catalysts. In addition, some of the above polymers or copolymers also improved the catalytic activity or chemoselectivity of the nanoparticles [18, 21]. However, many of these polymers and block co-polymers are not commercially available and are difficult to synthesize and characterize, and thus have an increased cost.

The extent to which different polymers can influence the morphologies and catalytic properties of platinum and palladium nanoparticles has been investigated by several groups [26-28]. For example, Pt nanoparticles which were hexagonal, square and triangular in shape and had average sizes 6.9, 13.6 and 14.6 nm, respectively, were synthesized using the polymer stabilizers PVP, poly(N-isopropylacrylamide) (NIPA), and sodium poly(acrylate) (SPA) [26]. The catalytic activity and selectivity were found to be strongly influenced by the morphology and size of nanoparticles [26, 28]. Narayanan and El-Sayed also synthesized tetrahedral, cubic, and spherical platinum nanoparticles using SPA, PVP and oxalate as stabilizing agents [28, 29]. They tested the catalytic activities of the Pt nanoparticles for electron transfer reactions between hexacyanoferrate (III) ions and thiosulfate ions to form hexacyanoferrate (II) ions and tetrathionate ions and found that tetrahedral Pt nanoparticles had the highest activity while cubic Pt nanoparticles had a lowest activity. They postulated that the catalytic activity was dependent on the fraction of surface atoms on the corners and edges; the tetrahedral Pt nanoparticles had the highest fraction of surface atoms on its corners and edges, and therefore had the highest catalytic activity. On the other hand, the cubic nanoparticles have the lowest fraction of surface atoms on their corners and edges and thus had the lowest catalytic activity [28, 29].

1.2.2 Dendrimer-stabilized Nanoparticle Catalysts

Dendrimers are discrete, well-defined macromolecules with a polydispersity (a measure of the distribution of molecular mass in a given polymer sample) of 1.0 [3, 30]. They look like trees or cauliflowers and become globular after a few generations [3]. They have following advantages for stabilizing metal nanoparticles for catalysis: (1) dendrimers have a fairly uniform composition and structure, and therefore yield well-defined nanoparticles; (2) they can protect nanoparticles from agglomeration or aggregation, due to their steric bulk; (3) as they can't pack tightly on the surface of nanoparticles, substantial free surface area is accessible to catalytic substrates, leading to high catalytic activity; (4) the dendritic branches can serve as gates to control the access of substrates to the nanoparticle and therefore improve the selectivity of a catalytic reaction; and (5) the terminal groups of the dendrimers can be tailored to provide the desired solubility in organic, aqueous, or fluorous media [3, 30].

There are two families of dendrimers which have been extensively used to stabilize metal nanoparticles: poly(amidoamine) (PAMAM) and poly(propylene imine) (PPI) dendrimers (Scheme 1.2) [30]. The number of functional groups on the dendrimer surface increases exponentially as a function of generation. This means higher generation dendrimers have higher steric crowding on the periphery [30]. For a particular generation the PPI dendrimers are substantially smaller than PAMAM dendrimers (2.8 nm vs 4.5 nm for G4, respectively) [30].

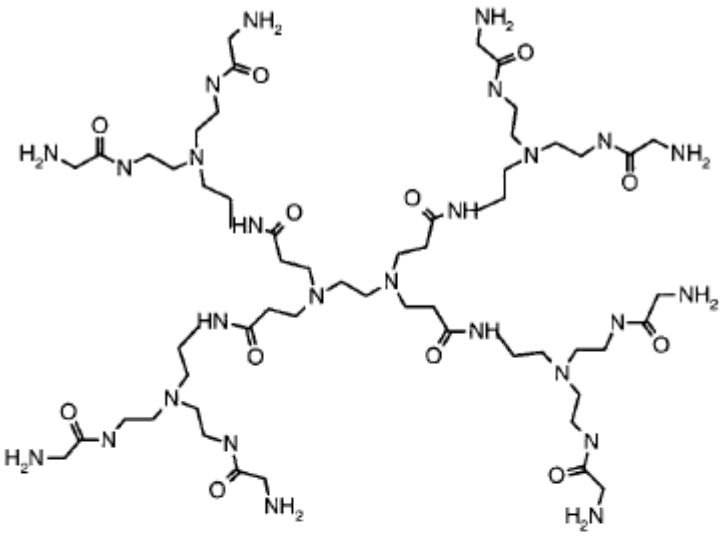

G1 PAMAM Dendrimer

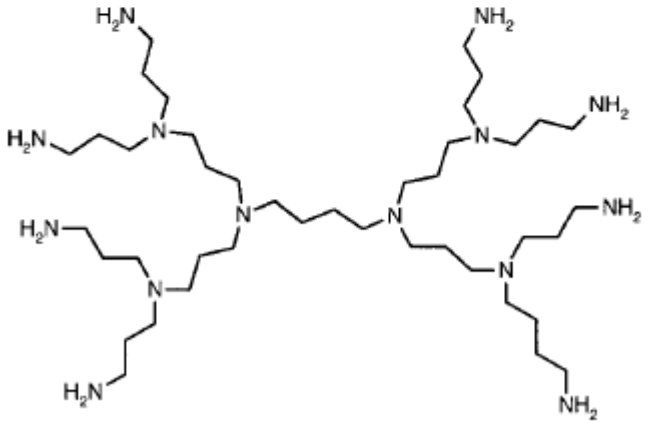

G1 PPI Dendrimer
(not to scale)

Scheme 1.2. The structures of PAMAM and PPI dendrimers. (Reprinted with permission from [30]. Copyright (2001) American Chemical Society.)

Dendrimer-stabilized Cu[31], Ag[32, 33], Au[34], Pt[33], and Pd[33, 35-37] nanoparticles have been synthesized by several groups. Amongst them, dendrimer-stabilized Pd nanoparticles have been shown to have high catalytic activities for the hydrogenation of alkenes in aqueous solution by Crooks and co-workers[37]. It is

noteworthy that the hydrogenation rate can be controlled by using dendrimers with different generations[37]. El-Sayed and co-workers also showed that dendrimer-stabilized Pd nanoparticles can catalyze Suzuki reactions in aqueous solution[35, 36], while Esumi *et al.* found PAMAM- and PPI-stabilized Ag, Pt, and Pd nanoparticles are effective catalysts for the reduction of 4-nitrophenol. The rate constants for the reduction reaction of 4-nitrophenol catalyzed by these nanoparticles are very similar between PAMAM and PPI dendrimer-stabilized Ag nanoparticles, whereas the rate constants for PPI dendrimer-Pt and dendrimer–Pd nanoparticles were greater than those for the corresponding PAMAM dendrimer nanoparticles [33].

In a very interesting study, El-Sayed and co-workers compared the catalytic activity of Pd nanoparticles stabilized by PAMAM-OH dendrimers of different generations to PVP-stabilized Pd nanoparticles and polystyrene-b-poly(sodium acrylate) block copolymer-stabilized Pd nanoparticles for Suzuki cross-coupling reactions [28, 36]. They found that 3rd generation PAMAM-OH dendrimer-stabilized Pd nanoparticles, PVP-stabilized Pd nanoparticles and block-copolymer-stabilized Pd nanoparticles were all effective catalysts for Suzuki reactions and had comparable catalytic activities. On the other hand, 2nd generation dendrimer-stabilized Pd nanoparticles were unstable and precipitated out of the solution after the Suzuki reaction, while 4th generation dendrimer-stabilized Pd nanoparticles had the lowest catalytic activity of all the stabilized-Pd nanoparticles studied. They postulated that the higher generation dendrimer allowed lower accessibility of substrates to the nanoparticle surface [28, 36]. However, while the 4th generation dendrimer-stabilized Pd nanoparticles had the lowest catalytic activity, they were much more easily recycled than PVP-Pd nanoparticles [28, 35]. Thus high

generation dendrimer-stabilized metal nanoparticles had better stability, but with a low catalytic activity; whereas the low generation dendrimer-stabilized metal nanoparticles had higher catalytic activities with poor stability. How to balance these two extremely important factors is a key to use dendrimers (and other polymers) as stabilizers for quasi-homogeneous catalysis [28].

1.2.3 Ligand-stabilized Nanoparticle Catalysts

Organic ligands, such as amine, phosphine, and thiol molecules, also can be used as stabilizers. Au [11, 38-40], Ni [41], Pd [39, 42-46], and Pt [47] nanoparticles stabilized by amines, phosphines, and thiols have been prepared. It is worth mentioning that chiral phosphine-stabilized Pd nanoparticles can be highly-selective catalysts for asymmetric reactions. For example, an asymmetric allylic alkylation reaction catalyzed by chiral diphosphite-stabilized phosphite Pd nanoparticles mainly proceeded with only one enantiomer of the substrate reacting [43]. Tamura *et al.* also showed that chiral biphosphine BINAP (2,2'-bis-(diphenylphosphino)-1,1'-binaphthyl)-stabilized Pd nanoparticles are an effective catalyst for the asymmetric hydrosilylation of olefins under mild conditions [39]. However, phosphine stabilizers are quite toxic and tend to be expensive; thus in recent studies, phosphines have been used sparingly as ligands to stabilize metal nanoparticles.

Alkylthiols and alkylthiolates are well known as poisons that inhibit the catalytic activity of metal nanoparticles, due to strong bonding between the thiolate group and the electrophilic nanoparticle surface. The coordination of thiolates to the nanoparticle decreases the number of surface atoms available for catalysis [45, 48]. However, Astruc

and coworkers showed that palladium-dodecanethiolate nanoparticles are stable and recyclable catalysts for the Suzuki-Miyaura reaction of aryl halides under ambient conditions, even though they are not as active as molecular palladium catalysts [45]. Eklund *et al.* have prepared a variety of thiolate-stabilized Pt nanoparticles and shown they are indeed catalytically active toward hydrogenation reactions, although the hydrogenation rates are quite low [47]. The Kaifer group showed that thiolated β-cyclodextrin (HS-β-CD)-stabilized Pt and Pd nanoparticles are active catalysts for the hydrogenation of allylamine in aqueous solution [49], and that HS-β-CD-Pd nanoparticles are also effective catalysts for Suzuki cross-coupling reactions between aryl halides and phenylboronic acid [46]. Fox's group used bulky dendritic thiolate ligands to stabilize nanoparticles [50, 51]. The advantage of this method is there were very few thiolate bonds on the metal surface due to the bulky dendrons, thus most of the nanoparticle surface remains unpassivated (Scheme 1.3). 3rd generation thiolated dendrimer-stabilized Pd nanoparticles (Pd-G-3) were shown to have efficient catalytic activity for Heck and Suzuki reactions [50]. Unfortunately, such catalysts were found to be inert for hydrogenation reactions, and the synthesis of the thiolated dendritic ligands is quite time and labour intensive. Finally, Murakami *et al.* found that dodecanethiol-stabilized Au nanoparticles displayed a remarkable co-catalyst effect on olefin oxidation reactions catalyzed by a manganese-porphyrin complex [52]. They speculated that the dodecanethiol-stabilized Au nanoparticles mediated regeneration of the active Mn(III) complex from a catalytically ineffective Mn(IV) species. All of these examples show that thiolate-stabilized metal nanoparticles can be used as promising catalysts. It is also noteworthy that thiols bonding on the surface of nanoparticles can be easily oxidized and

detached from the surface [52, 53], leaving, in theory, surface sites after oxidation that are available for catalysis. If the oxidation of thiols from the surface can be controlled, partially-oxidized thiolate-stabilized metal nanoparticles could show unique activity and selectivity [52].

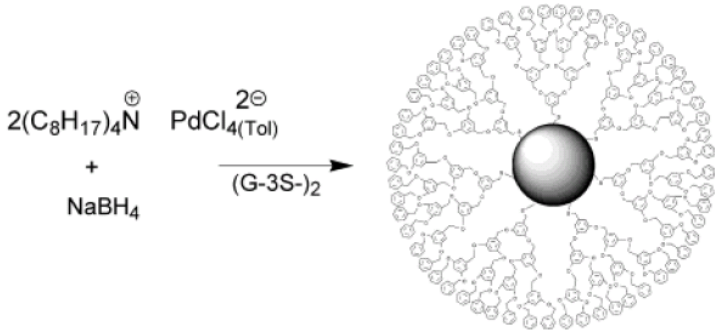

Scheme 1.3. Synthesis of Pd-G-3, in which seven of the fourteen G-3 wedges are shown. (Reprinted with permission from[50]. Copyright (2003) American Chemical Society.)

Polymers, dendrimers, and ligands sometimes have been combined by other groups in order to stabilize metal nanoparticles with novel activities, selectivities, and recycling potentials. For example, phosphine terminated dendrimer-stabilized Pd nanoparticles were found to be highly effective for Suzuki coupling reactions with excellent reusability [54]. Furthermore, these Pd nanoparticles were efficient and selective catalysts for hydrogenation reactions. In addition, poly(ethylene glycol), 2,2'-bipyridine, and 2,2,6,6-tetramethyl-piperidyl-1-oxy (TEMPO) were combined to support copper nanoparticles, and the resulting particles were shown to catalyze the selective

oxidation of primary alcohols to the corresponding aldehydes in an environmentally friendly manner [55].

1.2.4 Surfactant-stabilized Nanoparticle Catalysts

Several surfactants, for example, tetraoctylammonium bromide (TOAB) [56] and sodium bis(2-ethylhexyl) sulfosuccinate (AOT) [8], have been reported to stabilize metal nanoparticle catalysts. However, TOAB-stabilized metal nanoparticles had unsatisfactory long-term stability, though Isaacs *et al.* found that the use of thiosulfate anions instead of bromide anions can greatly improve both the chemical and thermal stability of tetraoctylammonium-stabilized Au nanoparticles [56]. The water/AOT/n-hexane microemulsion-stabilized Pd nanoparticles were shown to be an efficient catalyst for hydrogenation of olefins in organic solvents [8] (Scheme 1.4). Surfactants are generally not preferred stabilizers for nanoparticle catalysts as the catalytic activity of metal nanoparticles is typically inhibited by them [48]. Indeed, Sato *et al.* reported that the hydrogenation activity of Pd nanoparticles was inhibited by the AOT surfactant [57].

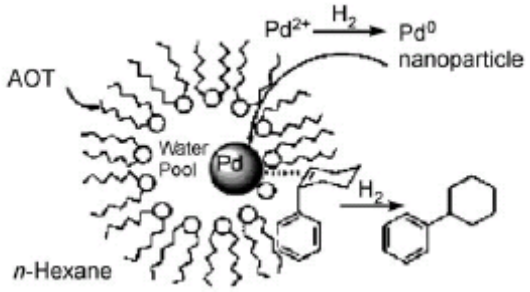

Scheme 1.4. Hydrogenation of olefins catalyzed by Pd nanoparticles in water/AOT/n-hexane microemulsion [3]. -Reproduced with permissions of Wiley-VCH Verlag GmbH & KGaA and The Royal Society of Chemistry.

1.2.5 Ionic Liquids as Media for Nanoparticle Catalysts

Ionic liquids are solvents that are composed entirely of ions. Room temperature ionic liquids are generally salts of organic cations such as tetraalkylammonium, tetraalkylphosphonium, N-alkylpyridinium, 1,3-dialkylimidazolium and trialkylsulfonium cations, paired with highly diffuse anions (Scheme 1.5) [58].

cations:

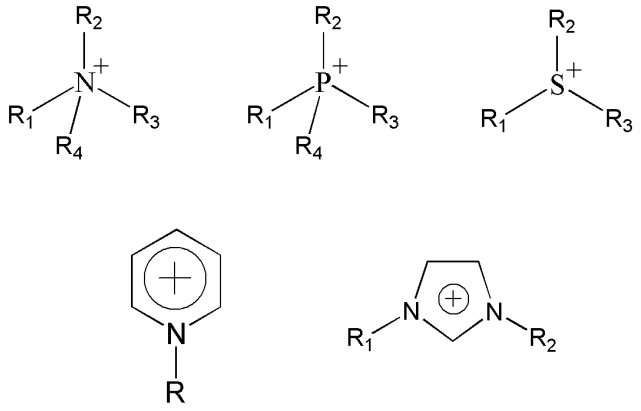

anions: BF_4^-, PF_6^-, SbF_6^-, NO_3^-, $CF_3SO_3^-$, $(CF_3SO_3)_2N^-$,

$ArSO_3^-$, $CF_3CO_2^-$, $CH_3CO_2^-$, $Al_2Cl_7^-$

Scheme 1.5. Structures of ionic liquids [58].

Ionic liquids have been shown to provide "electrosteric" stabilization for metal nanoparticles (Figure 1.1) [3, 48], which is similar to the stabilization mode of surfactants. This mode of stabilization is known as "electrosteric" as the anions of the ionic liquid offer an electrostatic stabilization for the electrophilic nanoparticle surface and the cations offer a steric stabilization due to their bulky volume [3, 48]. The major difference between ionic liquid and surfactant stabilizers is the former are liquids and are used as the dispersion media, while the latter are used as stabilizers in other solvents. It has been reported by a number of groups that no additional stabilizers are needed when metal nanoparticles are synthesized in the ionic liquids [48, 59-65], which can benefit catalytic reactions over the nanoparticle surface in the ionic liquid due as more free surface area is exposed on the surface of nanoparticles.

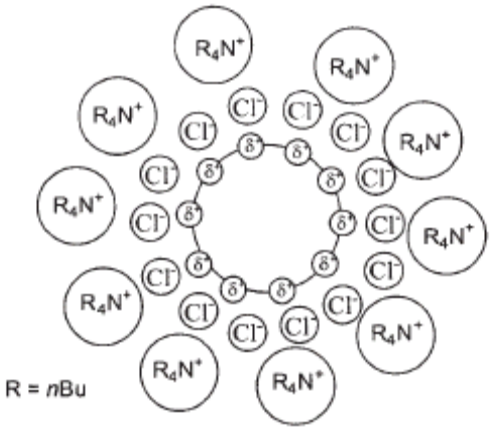

Figure 1.1. Pictorial representation of "electrosterically" stabilized nanoparticles [3]. - Reproduced with permission of Wiley-VCH Verlag GmbH & KGaA.

Au [65-67], Pt [60, 61, 66, 68], Pd [62, 63, 68], Ru [64], Rh [68] and Ir [59] nanoparticles have been synthesized in ionic liquid solvents, and their catalytic activities

have been investigated. Ru nanoparticles in imidazolium ionic liquids catalyzed the partial hydrogenation of benzene to cyclohexene, though the cyclohexene yield and selectivity were quite low [64]. Pd nanoparticles in imidazolium ionic liquids were effective catalysts for the selective hydrogenation of 1,3-butadiene to 1-butene [63]. The size and shape modifications of Pd nanoparticles dispersed in imidazolium ionic liquids during the Heck coupling reaction have been demonstrated by Cassol *et al.,* who found the size of Pd nanoparticles dispersed in imidazolium ionic liquids increased from 1.7± 0.3 nm to 6.1 ± 0.7 nm after the Heck reactions [62]. The catalytic activity of Pt nanoparticles in imidazolium ionic liquids for the hydrogenation of cyclohexene has been published by Scheeren *et al.*; they postulated that the catalytic activity is determined by the nature of the anion of the ionic liquids rather than the mean diameter of the nanoparticles [61]. Pt nanoparticles dispersed in 1-n-butyl-3-methylimidazolium tetrafluoroborate with a larger mean diameter (3.4 nm) had a higher catalytic activity than those dispersed in 1-n-butyl-3-methylimidazolium hexafluorophosphine (2.3 nm), since the BF_4^- anions show weaker coordination to the Pt surface than the PF_6^- anions.

A major reason for using ionic liquids to stabilize metal nanoparticles is increasing the reusability of the quasi-homogeneous metal nanoparticle catalysts. A major disadvantage of homogeneous catalysis is the problematic separation of the catalytic particles from the products and unused reactants at the end of the reaction. Incorporation of nanoparticles in ionic liquids gives nanoparticles which have free surface area available for catalysis; and catalytic reactions can occur at the interface between the ionic liquid and the reactants in an immiscible liquid phase. At the end of the reaction, the reaction mixture may be separated from the ionic liquid by simple

decantation and/or removal by vacuum [68]. Several studies have shown that ionic liquid-stabilized metal nanoparticle catalysts have good reusability. For example, Ir nanoparticles in imidazolium ionic liquids were shown to be recyclable catalysts for hydrogenation reactions [59]. PVP-stabilized Pt, Pd and Rh nanoparticle catalysts in 1-n-butyl-3-methylimidazolium (BMIM) ionic liquids could be recycled by a simple decantation procedure without loss of activity after hydrogenation reactions [68]. Pt nanoparticles in BMIM ionic liquids have high catalytic activity for the hydrogenation of alkenes and arenes under mild reaction conditions and can be reused several times without any significant loss in catalytic activity [60]. Our group has also recently found that PVP-stabilized Au, Pd and bimetallic AuPd nanoparticles in BMIM ionic liquids have decent catalytic activity and selectivity for hydrogenation reactions, and that these catalysts could be recycled then reused for further catalytic reactions with only a minimal loss in activity [69].

1.3 Au and Bimetallic Nanoparticle Catalysts

Since Haruta and coworkers found that Au nanoparticles are an effective catalyst for the oxidation of CO at low temperatures [6], the applications of Au nanoparticles in catalysis have attracted great attention and been extensively investigated [3]. Most gold nanoparticle catalyst systems are heterogeneous systems in which gold nanoparticles are supported on a metal oxide support, such as Al_2O_3, TiO_2, Fe_2O_3, Co_2O_3 and La_2O_3 etc [3, 70]. Metal-support interactions are very important for the catalytic activity and selectivity [70]. Different catalytic reactions need different supports, for example, only titania and titania-silicates were found to act as effective supports for Au nanoparticles

for the selective oxidation of hydrocarbons in the co-presence of O_2 and H_2 [70]. Several quasi-homogeneous Au nanoparticle catalyst systems have recently been reported [13, 51], although the examples of such systems are much fewer in number than those of heterogeneous catalyst systems involving Au nanoparticles. However, monometallic Au nanoparticles still do not have satisfactory activity and selectivity for many reactions.

Bimetallic nanoparticle catalysts provide a way to enhance the activity of gold-based catalysts. Bimetallic nanoparticles, composed of two different metal elements, can have improved activity as well as selectivity towards desired products due to synergetic electronic interactions between two different metal atoms in the individual nanoparticles. The catalytic activities and selectivities towards specific products can often be tuned by changing the composition of bimetallic nanoparticle catalysts [71]. There are two general methods to synthesize bimetallic nanoparticles, co-reduction and successive reduction. Co-reduction strategies require simultaneous reduction of two metal salts in the presence of stabilizing agents. Bimetallic nanoparticles that are synthesized using this method typically have an alloy structure if both metals are reduced at similar rates. Successive reduction strategies are an effective method to prepare core-shell structure bimetallic nanoparticles. One of the metal salts is reduced first to form the core, then a second metal is deposited on the surface of pre-formed monometallic nanoparticles to form the shell [71]. However, care must be taken to avoid galvanic exchange reactions using such strategies. For example, this method is not typically suitable to synthesize Pd/Au core/shell structure bimetallic nanoparticles, due to the redox potentials of Pd and Au ions. When Au^{3+} ions are added to solutions containing Pd nanoparticles, some Pd^0 atoms on the nanoparticles are oxidized and reduce the Au^{3+} ions to Au^0 atoms. After the

reduction of Au^{3+} ions, the oxidized Pd ions are reduced again by the reducing agent. This process may form particles with a "cluster-in-cluster" structure, or other structures altogether [71].

Bimetallic nanoparticles can have many different internal structures; three commonly encountered structures are random alloy, core-shell, and cluster-in-cluster structures (Figure 1.2). Amongst them, core-shell bimetallic nanoparticles are interesting because they can minimize the amount of precious metals that are required for catalytic applications [72]. Furthermore, they provide a method to design catalysts with desired activity and selectivity towards specific products. For example, Sales *et al.* found the desired product hex-1-ene selectivity was improved when a PdAg bimetallic system was used as a catalyst instead of monometallic Pd catalysts for the hydrogenation of hexa-1,5-diene, since palladium atoms were diluted by silver atoms, which prevented the isomerization of hexa-1,5-diene [73]. Xia *et al.* reported that a PdAu alloy had a higher catalytic activity than core/shell Pd/Au nanoboxes for the decolorization of methyl red, as the Au shell was not an active hydrogenation catalyst, and prevented the methyl red from accessing Pd atoms surface below [74].

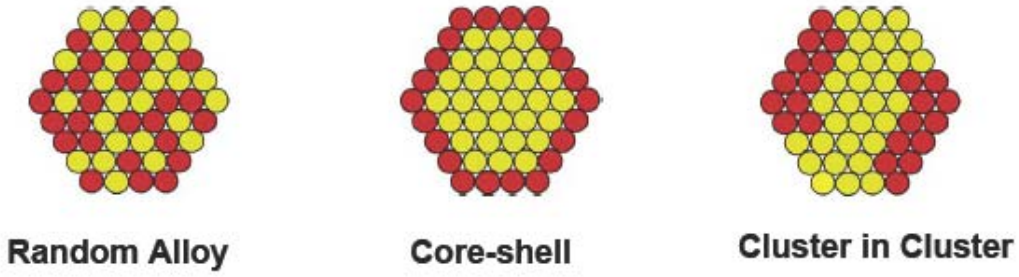

Figure 1.2. Several structures of bimetallic nanoparticles.

Bimetallic nanoparticles can be characterized using transmission electron microscopy (TEM), UV-Vis spectroscopy, X-ray diffraction (XRD), X-ray photoelectron Spectroscopy (XPS), and extended X-ray absorption fine structure (EXAFS) spectroscopy [71]. TEM studies can give the information about the size and shape of each bimetallic nanoparticle. In addition, Energy Dispersive Spectroscopy (EDS) results collected during TEM imaging can quantitatively give compositions of individual nanoparticles, and thus show if all nanoparticles are bimetallic without separate formation of pure monometallic nanoparticles. High resolution TEM (HRTEM) can also provide information on the atomic crystallinity of bimetallic nanoparticles [71]. Comparison of UV-Vis spectra of bimetallic nanoparticles with those of physical mixtures of the respective monometallic particle dispersions can also help confirm a bimetallic structure of the nanoparticles [71]. Monitoring UV-Vis spectral changes during successive reductions can provide important information about the formation core-shell structure bimetallic nanoparticles [71]. Powder XRD can show that bimetallic nanoparticles are formed and not a mixture of monometallic nanoparticles, since the diffraction pattern of physical mixtures of metallic nanoparticles would consist of overlapping lines of the two individual monometallic nanoparticles, and is clearly different from that of the bimetallic nanoparticles [71]. By quantitative analysis of XPS spectra of bimetallic nanoparticles, which elements are rich on the surface of the particles can be elucidated, as well as possible shifts of electron density from one element to the other [71].

The techniques mentioned above usually give average information about bimetallic nanoparticles except TEM, which can give information about the size and

shape of every single nanoparticle. Moreover, many of these methods can only prove that nanoparticles are bimetallic and cannot elucidate their actual structures (random alloy, core-shell, cluster-in-cluster, or others) with confidence. EXAFS spectroscopy is a powerful method to characterize the structure of bimetallic nanoparticles. For example, Toshima and co-workers published several papers determining the structure of bimetallic nanoparticles using EXAFS spectroscopy [75, 76]. They found that a Pt core structure was formed in Pd/Pt (4:1) bimetallic nanoparticles formed by co-reduction in refluxing alcohol solutions, in which 42 Pd atoms are on the surface and 13 Pt atoms are in the core. In contrast, PdPt (1:1) bimetallic nanoparticles had a cluster-in-cluster structure, in which 28 Pt atoms connect directly with each other and are located both in the core and on the surface, while the 27 Pd atoms form islands on the surface of bimetallic nanoparticles [75]. They observed similar results for AuPd bimetallic nanoparticles, and found that Au/Pd (1:4) bimetallic nanoparticles had a Au core-Pd shell structure while AuPd (1:1) nanoparticles had a cluster-in-cluster structure [76].

Improved catalytic hydrogenation activity and selectivity of desired products of bimetallic nanoparticles containing gold as one substituent were reported in the early 20^{th} century by Toshima [76]. Toshima and co-workers showed that PVP-stabilized AuPd bimetallic nanoparticles had higher catalytic activity than pure Au or Pd monometallic nanoparticles for the selective partial hydrogenation of 1,3-cyclooctadiene at 30 ^{o}C under 1 atm of hydrogen. The initial rate of hydrogenation was dependent on the metal composition of the bimetallic nanoparticles, with the maximum catalytic activity achieved at a Au:Pd ratio of 1:4. At this ratio, the Au/Pd bimetallic nanoparticles had a core-shell structure [76]. Toshima and coworkers also showed that PVP-stabilized

AuPt bimetallic nanoparticles could act as catalysts for visible light-induced hydrogen evolution, with the bimetallic system having a Au:Pt ratio of 2:3 being the most active catalyst [77]. Scott *et al.* reported that both alloy PdAu and core-shell Pd/Au bimetallic nanoparticles stabilized by hydroxyl-terminated PAMAM dendrimer had enhanced catalytic activity for the hydrogenation of allyl alcohol [72]. Our group has recently shown that PVP-stabilized AuPd bimetallic nanoparticles in imidazolium ionic liquids have higher catalytic activities for hydrogenation reactions [69]. The catalytic activity and selectivity towards specific products can be tuned by changing the composition of bimetallic nanoparticles and 1:3 Au: Pd ratio bimetallic nanoparticles have the highest activity.

Bimetallic nanoparticles containing gold as one substituent also have enhanced activity and selectivity for desired products for oxidation reactions. Enache *et al.* found that the addition of Au to Pd nanoparticles improved the selectivity towards aldehydes for the oxidation of alcohols, even though the activity was decreased [78]. AuPd and AuPt bimetallic nanoparticle catalysts with enhanced catalytic activity for the selective oxidation of various primary alcohols under mild conditions also was published by Dimitratos *et al.* [79]. Chaki *et al.* provided a mechanism for the aerobic oxidation of alcohol catalyzed by Au nanoparticles by comparing the catalytic activities of pure Au nanoparticles and AuAg bimetallic nanoparticles [80]. They argued that the partial anionic character of the Au core was important for aerobic oxidation reactions, and since the less electronegative Ag atoms donates partial electron density to Au atoms in AuAg bimetallic nanoparticles, the AuAg bimetallic nanoparticles have an enhanced activity for aerobic oxidations of p-hydroxybenzyl alcohol. AuPd bimetallic nanoparticles have

also been shown to be significantly more active for the direct synthesis of H_2O_2 from molecular H_2 and O_2 [81].

1.4 Goals for My Research

Research involving metal nanoparticle catalysts has attracted a great deal of attention and gained numerous achievements in the past ten years. However, catalytic activity, selectivity and reusability still need to be improved for many systems for commercial applications. Goals for my research mainly focus on two aspects: (1) the design of water-soluble metal nanoparticle catalysts for the aerobic oxidation of a wide range of alcohols; (2) to exploit the catalytic potential of thiol-stabilized Au nanoparticles.

Traditionally, alcohol oxidations have been performed using stoichiometric additions of oxidizing agents, which leads to the generation of large amounts of waste. Thus routes that allow for efficient and selective catalytic oxidation of alcohols to their respective aldehydes, ketones, or acids in aqueous solution using O_2 as the oxidizing agent are desirable alternatives. Supported Au nanoparticles have been proven to be effective catalysts for oxidation reactions [3, 70]. However, heterogeneous catalysts usually (but not always) have poor activities and cannot easily be used with solution phase substrates. With that in mind, we wished to synthesize water-soluble quasi-homogeneous Au nanoparticle catalysts by choosing a suitable stabilizer. Tsunoyama and coworkers had shown that PVP-stabilized Au nanoparticles could be successfully used for the aerobic oxidation of benzylic alcohols in water [13]. However, Au monometallic nanoparticles often have lower catalytic activity and poor selectivity for

desired products for alcohol oxidation reactions than bimetallic nanoparticles containing Au as a constituent [78-80]. Thus we synthesized PVP-stabilized AuPd bimetallic nanoparticles in the first project, and investigated these bimetallic nanoparticles as efficient and highly selective catalysts for a wide range of alcohol oxidation reactions. The results of these experiments will be documented in Chapter 2.

For the second project, we have noted that alkylthiols are well known as poisons that inhibit the catalytic activity of metal nanoparticles, due to strong bonding between the thiolate group and the electrophilic nanoparticle surface. However, several groups have reported that thiolate-stabilized Pt or Pd nanoparticles indeed have catalytic activities for hydrogenation and Suzuki cross-coupling reactions [46, 47, 49, 50]. To date, however, no publications have shown the direct catalytic activities of thiolate-stabilized Au nanoparticles. However, Murakami *et al.* recently demonstrated co-catalyst effects of dodecanethiolate-capped gold clusters in the enhanced activity of Mn-porphyrin catalysts for olefin oxidation reactions. They postulated that partially-oxidized thiolate-protected Au clusters, which were oxidized by iodosylbenzene (PhIO), are responsible for the improved activity of Mn-porphyrin catalyst (Scheme 1.6) [52].

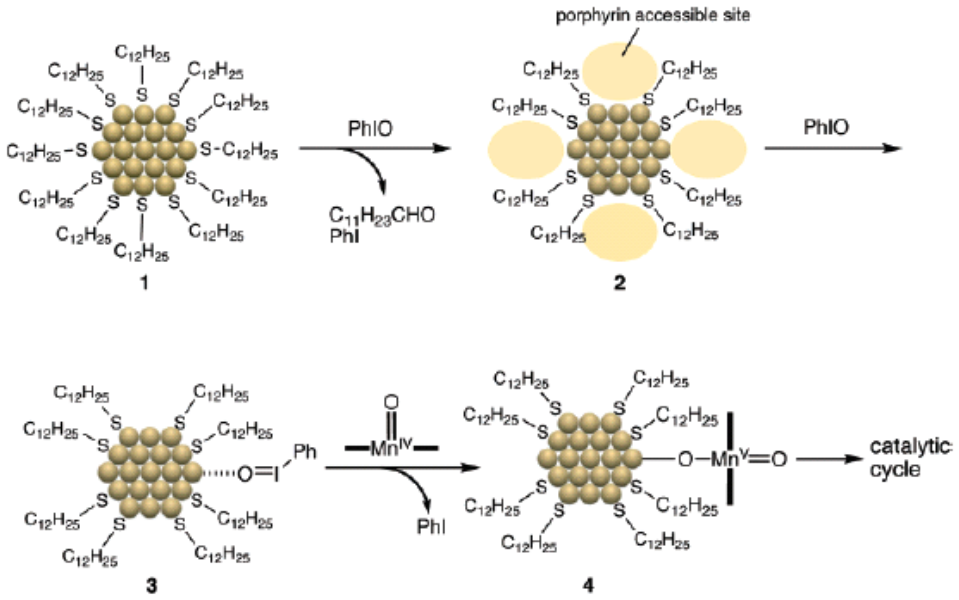

Scheme 1.6. Schematic illustration of a possible catalytic mechanism in the Au:SC_{12}/Mn(TPP)Cl system. (Reprinted with permission from [52]. Copyright (2007) American Chemical Society.)

In addition, our group [53] and other groups [82, 83] have also reported that alkylthiolates attached to gold surfaces can be oxidized to disulfide or sulfonate groups, along with the oxidation of Au^0 atoms to Au^{3+} species under appropriate oxidation conditions (Scheme 1.7). Thus the second project (Chapter 3) that I undertook in this thesis is to attempt to control the oxidation of alkanethiolates to form partially-oxidized thiolate-protected Au clusters which possess substrate-accessible Au surfaces but are still protected from aggregation by residual ligands. Furthermore, attempts to show that partially-oxidized thiolate-protected Au nanoparticles have accessible surface areas, and thus can show catalytic activity for some reactions will be detailed.

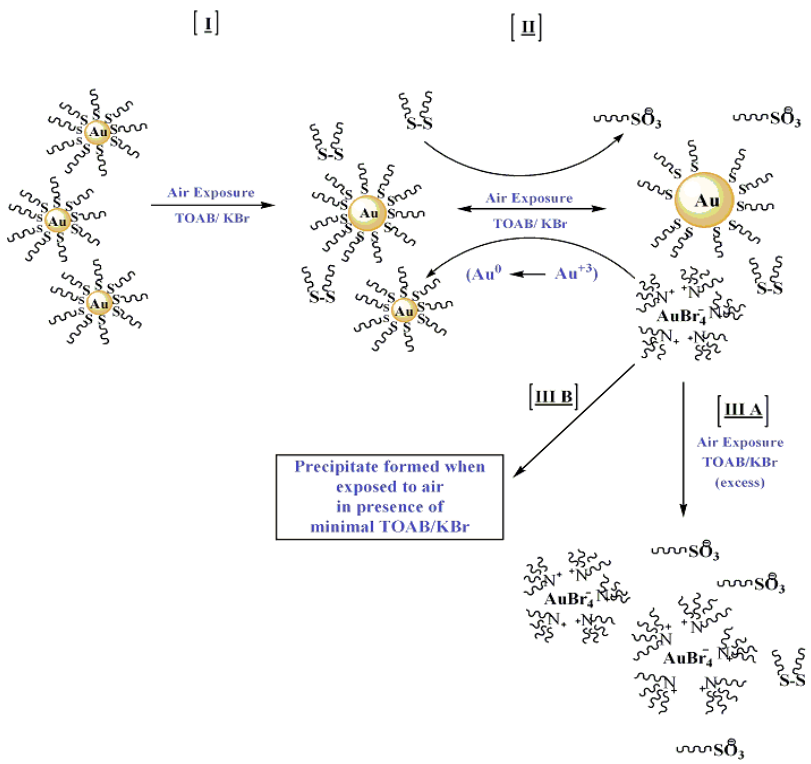

Scheme 1.7. Schematic illustration of the oxidative stability of 1-dodecanethiol-stabilized Au nanoparticles in the presence of halide ions under ambient conditions. (Reprinted with permission from [53]. Copyright (2007) American Chemical Society.)

1.5 References

[1] P. Atkins, and J.D. Paula, Physical Chemistry. Oxford University Press, 2002, 908.

[2] A. Roucoux, J. Schulz, and H. Patin, Chem. Rev. 102 (2002) 3757-3778.

[3] D. Astruc, F. Lu, and J.R. Aranzaes, Angew. Chem. Int. Ed. 44 (2005) 7852-7872.

[4] N. Pernicone, Cattech 7 (2003) 196-204.

[5] G.A. Somorjai, and Y.G. Borodko, Catal. Lett. 76 (2001) 1-5.

[6] M. Haruta, N. Yamada, T. Kobayashi, and S. Iijima, J. Catal. 115 (1989) 301-309.

[7] R. Nishio, M. Sugiura, and S. Kobayashi, Org. Lett. 7 (2005) 4831-4834.

[8] B. Yoon, H. Kim, and C.M. Wai, Chem. Comm. (2003) 1040-1041.

[9] I.P. Beletskaya, A.N. Kashin, A.E. Litvinov, V.S. Tyurin, P.M. Valetsky, and G. van Koten, Organometallics 25 (2006) 154-158.

[10] A. Gniewek, J.J. Ziolkowski, A.M. Trzeciak, and L. Kepinski, J. Catal. 239 (2006) 272-281.

[11] M. Brust, M. Walker, D. Bethell, D.J. Schiffrin, and R. Whyman, J. Chem. Soc., Chem. Commun. (1994) 801-802.

[12] H. Hirai, J. Macromol. Sci., Chem. A13 (1979) 633-649.

[13] H. Tsunoyama, H. Sakurai, Y. Negishi, and T. Tsukuda, J. Am. Chem. Soc. 127 (2005) 9374-9375.

[14] H. Tsunoyama, H. Sakurai, N. Ichikuni, Y. Negishi, and T. Tsukuda, Langmuir 20 (2004) 11293-11296.

[15] R. Narayanan, and M.A. El-Sayed, J. Am. Chem. Soc. 125 (2003) 8340-8347.

[16] Y. Li, X.M. Hong, D.M. Collard, and M.A. El-Sayed, Org. Lett. 2 (2000) 2385-2388.

[17] H. Tsunoyama, T. Tsukuda, and H. Sakurai, Chem. Lett. 36 (2007) 212-213.

[18] Y.B. Liu, C. Khemtong, and J. Hu, Chem. Comm. (2004) 398-399.

[19] S. Kanaoka, N. Yagi, Y. Fukuyama, S. Aoshima, H. Tsunoyama, T. Tsukuda, and H. Sakurai, J. Am. Chem. Soc. 129 (2007) 12060-+.

[20] P.G.N. Mertens, I.F.J. Vankelecom, P.A. Jacobs, and D.E. De Vos, Gold Bull. 38 (2005) 157-162.

[21] B.P.S. Chauhan, J.S. Rathore, and T. Bandoo, J. Am. Chem. Soc. 126 (2004) 8493-8500.

[22] C. Ramarao, S.V. Ley, S.C. Smith, I.M. Shirley, and N. DeAlmeida, Chem. Comm. (2002) 1132-1133.

[23] A. Biffis, and L. Minati, J. Catal. 236 (2005) 405-409.

[24] M.A.R. Meier, M. Filali, J.F. Gohy, and U.S. Schubert, J. Mater. Chem. 16 (2006) 3001-3006.

[25] P.L. Osburn, and D.E. Bergbreiter, Prog. in Poly. Sci. 26 (2001) 2015-2081.

[26] A. Miyazaki, I. Balint, and Y. Nakano, J. Nanoparticle Res. 5 (2003) 69-80.

[27] A.B.R. Mayer, and J.E. Mark, J. Polym. Sci. Part a-Polym. Chem. 35 (1997) 3151-3160.

[28] R. Narayanan, and M.A. El-Sayed, Top. Catal. 47 (2008) 15-21.

[29] R. Narayanan, and M.A. El-Sayed, Nano Lett. 4 (2004) 1343-1348.

[30] R.M. Crooks, M.Q. Zhao, L. Sun, V. Chechik, and L.K. Yeung, Acc. Chem. Res. 34 (2001) 181-190.

[31] L. Balogh, and D.A. Tomalia, J. Am. Chem. Soc. 120 (1998) 7355-7356.

[32] L. Balogh, D.R. Swanson, D.A. Tomalia, G.L. Hagnauer, and A.T. McManus, Nano Lett. 1 (2001) 18-21.

[33] K. Esumi, R. Isono, and T. Yoshimura, Langmuir 20 (2004) 237-243.

[34] K. Esumi, A. Suzuki, N. Aihara, K. Usui, and K. Torigoe, Langmuir 14 (1998) 3157-3159.

[35] R. Narayanan, and M.A. El-Sayed, J. Phys. Chem. B 108 (2004) 8572-8580.

[36] Y. Li, and M.A. El-Sayed, J. Phys. Chem. B 105 (2001) 8938-8943.

[37] M.Q. Zhao, and R.M. Crooks, Angew. Chem. Int. Ed. 38 (1999) 364-366.

[38] M.J. Hostetler, J.E. Wingate, C.J. Zhong, J.E. Harris, R.W. Vachet, M.R. Clark, J.D. Londono, S.J. Green, J.J. Stokes, G.D. Wignall, G.L. Glish, M.D. Porter, N.D. Evans, and R.W. Murray, Langmuir 14 (1998) 17-30.

[39] M. Tamura, and H. Fujihara, J. Am. Chem. Soc. 125 (2003) 15742-15743.

[40] W.W. Weare, S.M. Reed, M.G. Warner, and J.E. Hutchison, J. Am. Chem. Soc. 122 (2000) 12890-12891.

[41] N. Cordente, M. Respaud, F. Senocq, M.J. Casanove, C. Amiens, and B. Chaudret, Nano Lett. 1 (2001) 565-568.

[42] E. Ramirez, S. Jansat, K. Philippot, P. Lecante, M. Gomez, A.M. Masdeu-Bulto, and B. Chaudret, J. Organomet. Chem. 689 (2004) 4601-4610.

[43] S. Jansat, M. Gomez, K. Philippot, G. Muller, E. Guiu, C. Claver, S. Castillon, and B. Chaudret, J. Am. Chem. Soc. 126 (2004) 1592-1593.

[44] S.U. Son, Y. Jang, K.Y. Yoon, E. Kang, and T. Hyeon, Nano Lett. 4 (2004) 1147-1151.

[45] F. Lu, J. Ruiz, and D. Astruc, Tetrahedron Lett. 45 (2004) 9443-9445.

[46] L. Strimbu, J. Liu, and A.E. Kaifer, Langmuir 19 (2003) 483-485.

[47] S.E. Eklund, and D.E. Cliffel, Langmuir 20 (2004) 6012-6018.

[48] L.S. Ott, and R.G. Finke, Coordination Chem. Rev. 251 (2007) 1075-1100.

[49] J. Alvarez, J. Liu, E. Roman, and A.E. Kaifer, Chem. Comm. (2000) 1151-1152.

[50] K.R. Gopidas, J.K. Whitesell, and M.A. Fox, Nano Lett. 3 (2003) 1757-1760.

[51] K.R. Gopidas, J.K. Whitesell, and M.A. Fox, J. Am. Chem. Soc. 125 (2003) 14168-14180.

[52] Y. Murakami, and K. Konishi, J. Am. Chem. Soc. 129 (2007) 14401-14407.

[53] M. Dasog, and R.W.J. Scott, Langmuir 23 (2007) 3381-3387.

[54] L. Wu, B.L. Li, Y.Y. Huang, H.F. Zhou, Y.M. He, and Q.H. Fan, Org. Lett. 8 (2006) 3605-3608.

[55] C.W.Y. Chung, and P.H. Toy, J. comb. Chem. 9 (2007) 115-120.

[56] S.R. Isaacs, E.C. Cutler, J.S. Park, T.R. Lee, and Y.S. Shon, Langmuir 21 (2005) 5689-5692.

[57] H. Sato, T. Ohtsu, and I. Komasawa, J. Chem. Eng. Jpn 35 (2002) 255-262.

[58] R. Sheldon, Chem. Comm. (2001) 2399-2407.

[59] J. Dupont, G.S. Fonseca, A.P. Umpierre, P.F.P. Fichtner, and S.R. Teixeira, J. Am. Chem. Soc. 124 (2002) 4228-4229.

[60] C.W. Scheeren, G. Machado, J. Dupont, P.F.P. Fichtner, and S.R. Texeira, Inorg. Chem. 42 (2003) 4738-4742.

[61] C.W. Scheeren, G. Machado, S.R. Teixeira, J. Morais, J.B. Domingos, and J. Dupont, J.Phys. Chem. B 110 (2006) 13011-13020.

[62] C.C. Cassol, A.P. Umpierre, G. Machado, S.I. Wolke, and J. Dupont, J. Am. Chem. Soc. 127 (2005) 3298-3299.

[63] A.P. Umpierre, G. Machado, G.H. Fecher, J. Morais, and J. Dupont, Adv. Synth. Catal. 347 (2005) 1404-1412.

[64] E.T. Silveira, A.P. Umpierre, L.M. Rossi, G. Machado, J. Morais, G.V. Soares, I.L.R. Baumvol, S.R. Teixeira, P.F.P. Fichtner, and J. Dupont, Chem. Eur. J. 10 (2004) 3734-3740.

[65] S. Guo, F. Shi, Y.L. Gu, J. Yang, and Y.Q. Deng, Chem. Lett. 34 (2005) 830-831.

]66] K.S. Kim, D. Demberelnyamba, and H. Lee, Langmuir 20 (2004) 556-560.

[67] H. Itoh, K. Naka, and Y. Chujo, J. Am. Chem. Soc. 126 (2004) 3026-3027.

[68] X.D. Mu, D.G. Evans, and Y.A. Kou, Catal. Lett. 97 (2004) 151-154.

[69] P. Dash, N.A. Dehm, and R.W.J. Scott, J. Mol. Catal. A: chem. 286 (2008) 114-119.

[70] M. Haruta, Cattech 6 (2002) 102-115.

[71] N. Toshima, and T. Yonezawa, New J. Chem. 22 (1998) 1179-1201.

[72] R.W.J. Scott, O.M. Wilson, S.K. Oh, E.A. Kenik, and R.M. Crooks, J. Am. Chem. Soc. 126 (2004) 15583-15591.

[73] E.A. Sales, B. Benhamida, V. Caizergues, J.P. Lagier, F. Fievet, and F. Bozon-Verduraz, Appl. Catal. A 172 (1998) 273-283.

[74] C.M. Cobley, D.J. Campbell, and Y.N. Xia, Adv. Mater. 20 (2008) 748-752.

[75] N. Toshima, M. Harada, T. Yonezawa, K. Kushihashi, and K. Asakura, J. Phys. Chem. 95 (1991) 7448-7453.

[76] N. Toshima, M. Harada, Y. Yamazaki, and K. Asakura, J.Phys. Chem. B 96 (1992) 9927-9933.

[77] T. Yonezawa, and N. Toshima, J. Mol. Catal. 83 (1993) 167-181.

[78] D.I. Enache, J.K. Edwards, P. Landon, B. Solsona-Espriu, A.F. Carley, A.A. Herzing, M. Watanabe, C.J. Kiely, D.W. Knight, and G.J. Hutchings, Science 311 (2006) 362-365.

[79] N. Dimitratos, A. Villa, D. Wang, F. Porta, D. Su, and L. Prati, J. Catal. 244 (2006) 113-121.

[80] N.K. Chaki, H. Tsunoyama, Y. Negishi, H. Sakurai, and T. Tsukuda, J.Phys. Chem.C 111 (2007) 4885-4888.

[81] A.A. Herzing, A.F. Carley, J.K. Edwards, G.J. Hutchings, and C.J. Klely, Chem. Mater. 20 (2008) 1492-1501.

[82] M.H. Schoenfisch, and J.E. Pemberton, J. Am. Chem. Soc. 120 (1998) 4502-4513.

[83] A.C. Templeton, M.J. Hostetler, C.T. Kraft, and R.W. Murray, J. Am. Chem. Soc. 120 (1998) 1906-1911.

CHAPTER 2

Alcohol Oxidations in Aqueous Solutions using Au, Pd, and Bimetallic AuPd Nanoparticle Catalysts

The contents of this chapter were recently published as a full paper in the *Journal of Catalysis*, and is reprinted from: Journal of Catalysis, 253 (1), W. Hou, N.A. Dehm, R.W.J. Scott, Alcohol oxidations in aqueous solutions using Au, Pd, and bimetallic AuPd nanoparticle catalysts, p 22-27, Copyright 2008, with permission from Elsevier. In addition, all co-authors have given their permission for use of this paper in this thesis.

The experimental work in this project was completed by both myself and Nicole Dehm, and the first draft of the final manuscript was written by myself. Nicole found that polyvinylpyrrolidone (PVP)-stabilized Au, Pd and bimetallic AuPd nanoparticle catalysts in aqueous solutions can be used as effective catalysts for the benzyl alcohol oxidation reaction under mild conditions. Building on her work, I studied the kinetics of the above reaction, and examined the catalytic activities of bimetallic 1:3 Au:Pd nanoparticles for a wide range of alcohol oxidation reactions (benzyl alcohol, 1-butanol, 2-butanol, 2-buten-1-ol and 1,4-butanediol), and optimized the conditions to maximize the catalytic activities for different substrates.

2.1 Introduction

Oxidation of alcohols to their respective aldehyde or ketone is a useful and fundamental organic reaction [1, 2]. Traditionally, this oxidation is performed using stoichiometric amounts of oxidants, such as permanganate [3], chromate [2, 4], or bromate [5]. These methods produce a large amount of waste, and are unacceptable in view of green chemical practices. Recently, transition metal nanoparticle-catalyzed aerobic alcohol oxidations have been investigated, and many have shown high catalytic activities and good selectivities [6-17]. However, despite this progress, there are still persistent problems in this field. First, many oxidation reactions are conducted in organic solvents or solvent-less conditions [6, 7, 10, 12, 13], and the resulting mixtures of the organic substrates, products, solvents and molecular oxygen can be quite dangerous. Also, some oxidation reactions have to be performed under severe conditions, such as high temperature and high oxygen pressure [6, 7, 14]. Finally, a number of catalysts have only been shown to be active for specific types of alcohols. For example, Biffis *et al.* [8] have shown that microgel-stabilized Pd nanoclusters are effective for the selective oxidation of secondary alcohols, while Abad *et al.* [6, 7] have noted out that ceria-supported Au nanoparticle catalysts are most suitable for the aerobic oxidation of allylic alcohols and can effectively prevent the isomerization and hydrogenation of C=C double bonds. Therefore there is still significant demand for catalyst systems which can activate a wide range of substrates and can be used under mild, aqueous conditions [15, 16, 18].

Herein, we show that polyvinylpyrrolidone (PVP)-stabilized bimetallic AuPd nanoparticle catalysts in aqueous solutions can be used as effective catalysts for a wide

range of alcohol oxidation reactions under mild conditions. This work builds on the earlier observations by Tsunoyama and coworkers [18] that PVP-stabilized Au nanoparticles could be successfully used for the aerobic oxidation of benzylic alcohols in water. The Au nanoparticles had high catalytic activities, and the PVP stabilizer effectively prevented the agglomeration of nanoparticles during the course of the catalytic oxidations in aqueous solution. Several groups have also recently examined supported-bimetallic PdAu nanoparticles as catalysts with increased activity and product selectivity for alcohol oxidation reactions. Specifically, Enache *et al.* [10] and Dimitratos *et al.* [19] have both observed that supported-AuPd bimetallic catalysts have an improved activity and selectivity of desired products for aerobic oxidations of alcohol, presumably due to synergetic electronic interactions between Au and Pd atoms in the individual nanoparticles [20]. Thus we wished to investigate whether polymer-stabilized, solution-phase bimetallic AuPd nanoparticles would also show significantly enhanced activities and desirable product selectivities for aerobic alcohol oxidations. Herein we report the synthesis of PVP-stabilized Au, Pd and AuPd bimetallic nanoparticle catalysts, and show that the resulting nanoparticles can catalyze the oxidation of benzyl alcohol, 1-butanol, 2-butanol, 2-buten-1-ol and 1,4-butanediol in aqueous solutions under an oxygen atmosphere.

2.2 Experimental and Methods

2.2.1 Materials

Poly(N-vinyl-2-pyrrolidone) (M.W. 40,000), hydrogen tetrachloroaurate hydrate (99.9%), potassium tetrachloropalladate (99.99%), benzyl alcohol (99+%, ACS), 2-

butanol (99.9%), 1, 4-butanediol (99.9%) and 2-buten-1-ol (predominantly trans, 97%) were purchased from Alfa and were used without further purification. Sodium borohydride powder (98%) was obtained from Aldrich and was used as obtained. K_2CO_3 (anhydrous) was obtained from EMD Chemicals Inc. and was used without further purification. n-Butanol (ACS) was obtained from EM Science and was used without further purification. Deuterated solvents were purchased from Cambridge Isotope Laboratories. 18 MΩ·cm Milli-Q water (Millipore, Bedford, MA) was used throughout.

2.2.2 Preparation of PVP Stabilized 1:3 Au:Pd Nanoparticles

The following procedure was used to prepare PVP stabilized 1:3 Au:Pd nanoparticles [18]. First, 0.188 ml of a 10 mM potassium tetrachloropalladate solution (1.88×10^{-6} mol) and 0.062 ml of a 10 mM hydrogen tetrachloroaurate trihydrate solution (0.62×10^{-6} mol) was added to 2 ml of deionized water with stirring. Next, 0.5 ml of a 1.39 mM PVP solution (6.95×10^{-7}mol) was added. This mixture was then stirred for 30 minutes at room temperature ($20^{o}C \pm 2^{o}C$) in air. Finally, 0.25 ml of a fresh 0.10 M sodium borohydride solution (2.5×10^{-5} mol) was added. After stirring for an additional 30 minutes at $0^{o}C$ in air, the PVP stabilized 1:3 Au: Pd NPs were diluted to 5.0 ml. Au, Pd and other bimetallic Au:Pd nanoparticles were prepared as stated above keeping the total molar amount of metal salt constant.

2.2.3 Oxidation Reactions

The following procedure was used to oxidize benzyl alcohol [18]. First, 5.0 ml of the previously prepared nanoparticles, 51.9 mg of potassium carbonate (3.75×10^{-4} mol) and 2.5ml of deionized water were mixed together with vigorous stirring at 1080 rpm with a magnetic stir bar. Next, 129 μL of benzyl alcohol (1.25×10^{-3} mol) was added (for a substrate:catalyst ratio of 500:1). For alternative substrates the catalytic reactions were performed as above but substituting the benzyl alcohol with other alcohols. For these studies, both the nanoparticle catalyst and substrate amounts were increased by a factor of five, which necessitated a doubling of the PVP stabilizer in order to keep the particles stable during the oxidation of benzyl alcohol and 1-butanol.

NMR, GCMS and GC samples were prepared as follows: 1 ml of the solution was taken out from the oxidation reaction system and placed in a vial and 500 μL of 1.0 M hydrochloric acid (5×10^{-4} mol) was added. Then 1 ml of $CDCl_3$ was added, and the vial was shaken to transfer the substrates and products into the organic phase. The $CDCl_3$ was then extracted and characterized by ^1H NMR and/or GCMS, GC. Turnover frequencies (TOFs), conversions and selectivities were determined from NMR. Turnover frequencies (TOFs) were determined from the slope of linear plots of turnover (mol product (aldehyde+acid+benzoate)/mol Pd+Au) vs. time for initial studies and calculated using molar ratio of the converted substrate over the catalyst divided by the reaction time for subsequent studies. Turnover numbers generated from NMR results were verified by GC or GCMS for several substrates; in all cases, both methods gave comparable results. Control experiments in which no nanoparticles were present showed no background alcohol oxidation was occurring over 24 h.

2.2.4 Characterization

UV-Vis spectra were obtained using a Varian Cary 50 Bio UV-Visible Spectrophotometer with a scan range of 300-900 nm with an optical path length of 1.0 cm. ^{1}H-NMR spectra were obtained using a Bruker 500 MHz Avance NMR spectrometer; chemical shifts were referenced to the residual protons of the deuterated solvent. Transmission electron micrographs (TEM) were obtained with a Philips 410 microscope operating at 100 keV. To prepare samples for TEM, a drop of the solution containing the nanoparticles was placed on a carbon grid which had been pretreated by plasma discharge. Gas chromatography data was obtained using a HP 4890D Gas Chromatograph and a HP 3393A Integrator using pure acetophenone as an internal standard. The identity of products was confirmed by GC-MS (GC EI+ Magnet VG 70SE) in subsequent studies.

2.3 Results and Discussion

2.3.1 Synthesis of PVP-stabilized Au, Pd and Au:Pd Bimetallic Nanoparticles

Poly(N-vinyl-2-pyrrolidone) (PVP) stabilized Pd, Au, and bimetallic AuPd particles were synthesized via $NaBH_4$ reduction of aqueous solutions of the metal salts in the presence of the polymer. TEM images of the resulting Pd, Au, and AuPd nanoparticles stabilized with PVP are shown in Figure 2.1. The average size of the PVP- stabilized Au and Pd nanoparticles that were synthesized were measured through TEM was found to be 3.3 $\pm$ 0.8 nm and 3.9 $\pm$ 2.8 nm, respectively, while the bimetallic AuPd nanoparticles had average particle sizes of 2.7 $\pm$ 0.7 nm (Au:Pd = 1:3), 2.7 $\pm$ 1.2 nm (Au:Pd = 1:1) and 4.0 $\pm$ 1.7 nm (Au:Pd = 3:1). PVP-stabilized metal nanoparticles

are known to be weakly stabilized through multiple coordination of the amido sites of the PVP [18, 21]. Figure 2.2 shows representative UV-Vis spectra of the AuPd bimetallic series after reduction with sodium borohydride. UV-Vis spectra of the AuPd nanoparticles shows an exponentially increasing absorbance toward higher energy; this is a consequence of interband transitions of the newly formed bimetallic AuPd nanoparticles [22, 23]. In contrast, the PVP-stabilized Au nanoparticles show a broad plasmon band around 515 nm after reduction, which is in general agreement with TEM results (3.3 ± 0.8 nm). These results show that as-synthesized nanoparticles with similar particle sizes (2.5 – 4.0 nm) can be stabilized with the PVP stabilizers over all Au:Pd bimetallic ratios. Of note is the absence of any plasmon bands in the bimetallic nanoparticles, which suggests that all particles are bimetallic with no separate formation of pure Au nanoparticles [19].

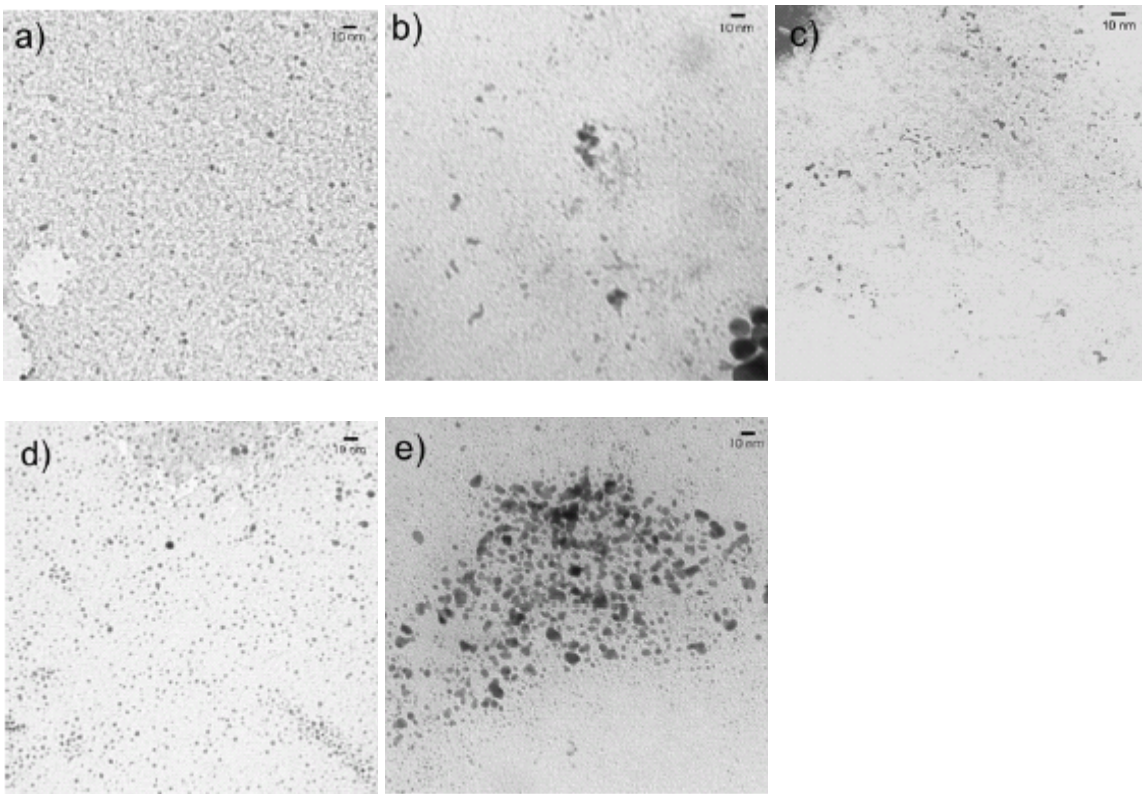

Figure 2.1. TEM images of PVP-stabilized a) Au nanoparticles, b) Pd nanoparticles, c) 1:3 Au:Pd nanoparticles, d) 1:1 Au:Pd nanoparticles, e) 3:1 Au:Pd nanoparticles.

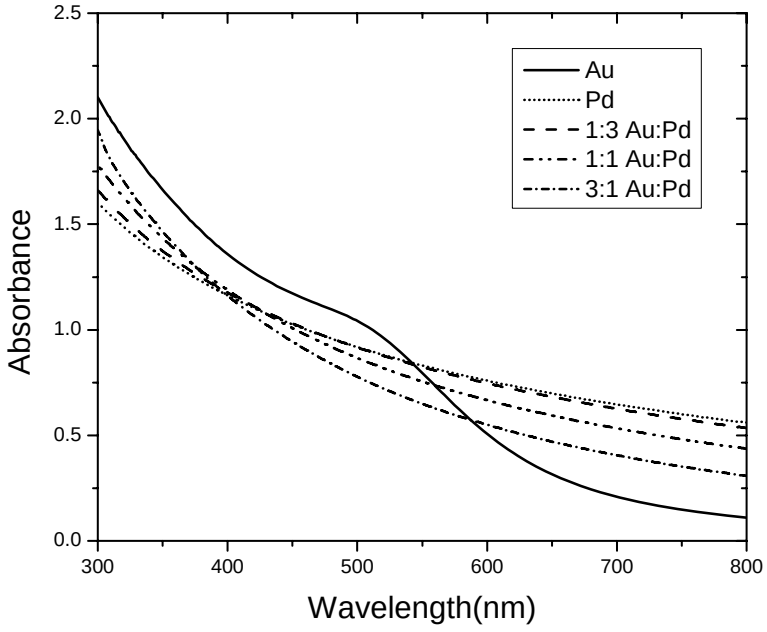

Figure 2.2. UV-Vis spectra of PVP-stabilized Au, Pd, and Au:Pd nanoparticles.

2.3.2 Catalytic Tests for Benzyl Alcohol Oxidation

The catalytic activity of the nanoparticles towards the oxidation of benzyl alcohol was measured over seven hours (see experimental section), and the formation of benzaldehyde and benzyl benzoate was observed. GC and GCMS results confirmed the presence of benzyl benzoate and absence of benzylic acid as a product. Quantitative yields and turnover frequencies of the two products were determined based on the integration of the respective integrations peaks of the pure alcohol, aldehyde and benzoate. For the PVP stabilized bimetallic nanoparticles (Table 2.1, entries 1-5) the 1:3 Au:Pd nanoparticles showed the highest turnover frequency for the oxidation of benzyl alcohol in air at room temperature. Such enhancements of catalytic activity have previously been seen for many AuPd systems [19, 24], and are thought to be due to synergistic electronic effects in which Au atoms draw electron density away from Pd atoms, thereby enhancing the interaction of Pd atoms with the substrate [20]. The selectivity of each oxidation reaction was also determined, and the results can be seen in Table 2.1 entries 1-5 for each different type of nanoparticle. When pure Au nanoparticles were used for the oxidation of benzyl alcohol, nearly equal amounts of benzaldehyde and benzyl benzoate were produced, in agreement with previous work by Tsunoyama *et al*. [18]. However, when Pd and AuPd bimetallic nanoparticles were used for the oxidation, benzaldehyde was produced preferentially with nearly 100% selectivity. Enache and co-workers [10] previously investigated the oxidation of benzyl alcohol at 373 K with O_2 as oxidant in the absence of solvent using TiO_2-supported PdAu catalysts, and also found that the bimetallic catalysts were very active for this reaction with high selectivity to benzaldehyde ($\geq$ 96%) at high conversion rates.

Table 2.1. Turnover frequencies and selectivities for benzyl alcohol oxidation with PVP stabilized Au, Pd and Au:Pd bimetallic nanoparticles.

Conditions: moles (Pd +Au) = 2.5 x 10^{-6} mol, Pd+Au:substrate = 1:500.

Entry	Type of NP	Conditions	Turnover Frequency (h^{-1})[1]	Selectivity	
				Benz-aldehyde	Benzyl Benzoate
1	Au	298 K, air	8.6	52.8	47.2
2	3:1 Au:Pd	298 K, air	8.6	86.1	13.9
3	1:1 Au:Pd	298 K, air	7.1	96.9	3.1
4	1:3 Au:Pd	298 K, air	11.5	97.9	2.1
5	Pd	298 K, air	6.2	100	0
6	Au	298 K, O_2	3.9	100	0
7	1:3 Au:Pd	298 K, O_2	26.2	98.1	1.9
8	Pd	298 K, O_2	3.7	100	0
9	Au	358 K, O_2	14.3	97.3	2.7
10	1:3 Au:Pd	358 K, O_2	57.3	100	0
11	Pd	358 K, O_2	32.0	100	0

[1] The turnover frequency is the mean value over 6 h measured by plots of mol product (aldehyde+acid+benzoate)/mol Pd+Au) vs. time. The values do not include alcohol consumed via esterification with benzoic acid to form the benzoate.

The conditions were varied in order to maximize the catalytic activity of the nanoparticles. Interestingly, it was found that the TOF for the oxidation of benzyl alcohol by the 1:3 Au:Pd nanoparticles increased to 26.2 h^{-1} from 11.5 h^{-1} upon replacing the atmosphere with pure O_2 at 298 K, while slight decreases were seen for both the pure Au and Pd nanoparticles (Table 2.1, entries 6-8). While we are still uncertain as to the origin of the decreasing catalytic activities for the pure Au and Pd nanoparticles, the results for the 1:3 Au:Pd nanoparticle catalysts suggest that under

these experimental conditions the solubility of oxygen in water was a rate-limiting step in the catalytic oxidation reaction. Increasing the reaction temperature to 358 K led to even further increases in the catalytic activity for all three catalysts (Table 2.1, entries 9-11), with the 1:3 Au:Pd nanoparticles showing a TOF of 57.3 h^{-1} with 100% selectivity towards benzaldehyde under these conditions, which is four times greater than the activity of the Au nanoparticles under these conditions and nearly two times greater than the corresponding Pd nanoparticles. Interestingly, for reactions under pure O_2, the selectivity of PVP-stabilized Au nanoparticles shifted nearly completely towards the formation of benzaldehyde, though we are still investigating the source of this selectivity change. Finally, the catalysts retained their activity over 24 h reaction cycles under these conditions, and no precipitation of the PVP-stabilized particles was seen over the course of the reaction. Indeed, after undergoing an oxidation reaction for 24 hrs under O_2 at 358 K; the particle size as determined by TEM increased only very slightly from 2.7 $\pm$ 0.7 nm to 2.8 $\pm$ 0.6 nm.

2.3.3 Kinetics of Catalytic Oxidation of Benzyl Alcohol

The kinetics of the above reaction were carefully examined to attempt to determine whether the final conditions used (1 atm O_2, 358 K) were kinetically-limiting at the catalyst concentration chosen, or if there was still a mass-transport limitation with respect to O_2 under these conditions. Lowering the stirring speed (from 1080 rpm to 720 rpm) led to falling TOFs over time (Table 2.2), suggesting that mass-transport limitations become quite strong at lower stirring rates. Attempts to lower the catalyst concentration to ensure the reaction was under kinetically-limiting conditions invariably

led to de-activation of the PdAu nanoparticle catalysts within an hour (Table 2.3). Indeed, others have previously shown for Pd and Pt nanoparticle catalysts that kinetically-limiting conditions can lead to over-oxidation (*i.e.* metal oxidation) and poisoning of the particle surface, and that alcohol oxidations can be considerably faster under mass-transport-limiting conditions, in which just enough oxygen is present to clean the surface but not to oxidize the metal surface [25, 26]. Thus it is likely that mild mass transport limitations exist for the reaction under these conditions. Such mass-transport-limited conditions appear unavoidable as nanoparticle stability is severely problematic under kinetically-limiting conditions.

Table 2.2. Turnover frequencies for benzyl alcohol oxidation with different stirring rates.Conditions: moles (Pd +Au) = 5.0 x 10^{-6} mol, Pd+Au:substrate = 1:250.

Time (h)	Turnover Frequency (h^{-1})	
	1080 rpm	720 rpm
1	20.0	18.4
2	17.8	7.89
3	21.2	4.64
4	18.7	3.16

Table 2.3. Turnover frequencies for benzyl alcohol oxidation with different ratios of substrate: Pd+Au.

Time (h)	Turnover Frequency (h^{-1})			
	1000:1[a]	500:1	250:1	125:1
1	28.8	10.7	20.0	13.5
2	12.5	2.70	17.8	13.9
3	8.13	1.93	21.2	11.3
4	6.10	1.13	18.7	11.1

[a] The ratio of substrate: Pd+Au.

Finally, the measured effective activation energy for the 1:3 Au:Pd nanoparticles was found to be *ca.* 14 kJ/mol (Figure 2.3), which is much lower than that seen previously for pure PVP-stabilized Au and Pd nanoparticles (20 and 33 kJ/mol, respectively) [18], which lends further support to the likelihood that mass-transport limitations exist under these conditions. Note the rate constant, k, was obtained via plots of ln[1-c] vs. time (where c is the total conversion), giving linear plots with a slope of -k.

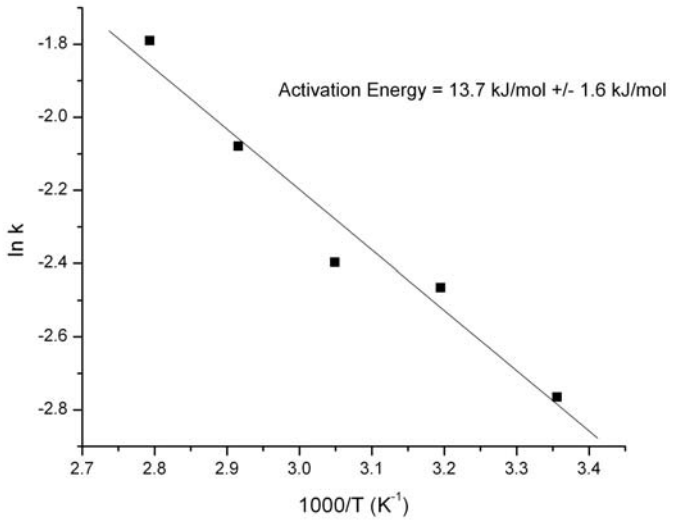

Figure 2.3. Arrhenius plot of PVP-stabilized 1:3 Au:Pd nanoparticles in 1 atm O_2.

2.3.4 CatalyticTests for Other Alcohol Substrates

Intrigued by these initial results, we wished to examine the generality of the alcohol oxidation reaction using the 1:3 Au:Pd catalysts at scaled-up conditions. The catalytic activity of the 1:3 Au:Pd nanoparticles toward other alcohol substrates (1-butanol, 2-butanol, 2-buten-1-ol and 1,4- butanediol) were subsequently examined under 1 atm O_2 at 335 K; the results are summarized in Table 2.4 and Scheme 2.1. For these studies, both the amount of nanoparticle catalyst and the substrate were increased by a factor of five from earlier studies; this necessitated a further doubling of the amount of PVP stabilizer in order to keep the particles stable during the oxidation of benzyl alcohol and 1-butanol. Substantial oxidations of all the alcohols studied were seen under these conditions. The rate of oxidation of benzyl alcohol and 1-butanol were quite similar after one hour, with conversions of 14.8%, but the oxidations of both substrates slowed considerably over time, likely due to mass-transport limitations at these higher catalyst

concentrations. In addition, we note that while after 1h, the major product for the benzyl alcohol oxidation was benzaldehyde (90.5%), a great deal of the aldehyde was subsequently oxidized to benzoic acid over 24 hours (final selectivity 39.7% for the aldehyde). Note that benzyl benzoate was a minor product under these new conditions; unlike the earlier room temperature reactions with PVP-stabilized Au nanoparticles in which benzyl benzoate was seen. Control experiments with benzaldehyde in the absence of nanoparticles indicate that disproportionation of the aldehyde over the course of 24 h occurs, and may be a source of the lowered selectivity of the benzyl alcohol oxidation.

Table 2.4. Turnover frequencies and selectivities for diverse substrate oxidations with PVP stabilized 1:3 Au:Pd bimetallic nanoparticles. Conditions: [Pd+Au] = 1.25×10^{-5} mol, Pd+Au:Substrate = 1:500.

Entry	Substrate	Conversion (%)		Turnover Frequency (h^{-1})[2]	Aldehyde or Ketone Selectivity (%)	
		1h	8h		1h	8h
1	Benzyl alcohol	14.8	33.6	74	90.5	39.7 [1]
2	1-Butanol	14.8	24.6	74	26.4	23.1
3	2-Butanol	25.0	65.0	125	100	100
4	2-Buten-1-ol	13.3	38.5	67	34.0	77.6
5	1,4-Butanediol	46.7	84.7 [3]	234	100 [4]	100

[1]After 24 h. [2]Turnover frequency was calculated over the first hour. [3]After 5h. [4]γ-butyrolactone selectivity.

Entry	Reaction
1	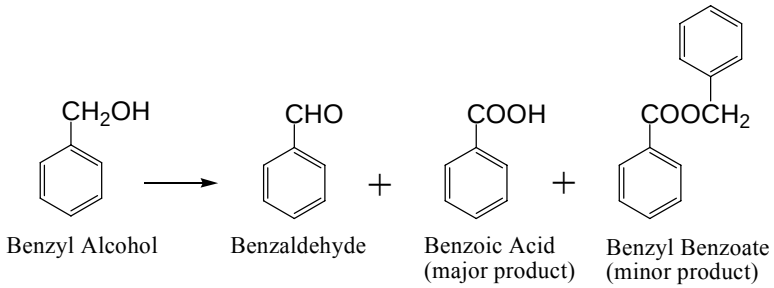
2	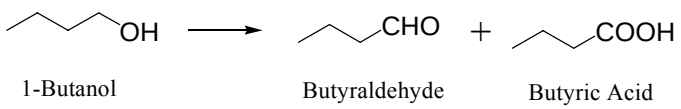
3	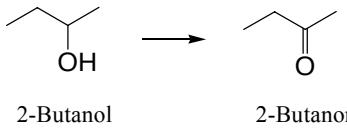
4	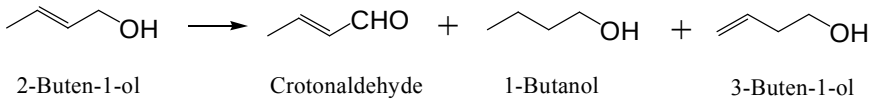
5	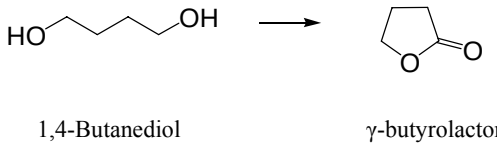

Scheme 2.1. Alcohol substrates oxidized using 1:3 Au:Pd catalysts and reaction products observed for each substrate.

No selectivity towards the aldehyde was seen at any point for the oxidation of 1-butanol, as butyric acid was always the predominant product (>75% butyric acid, negligible amounts of butyl butyrate were detected by GC). We speculate that the catalytic oxidation of benzyl alcohol and 1-butanol reactions slow down due to the buildup of benzoic acid and butyric acid on the surface of nanoparticles, lowering the

availability of catalyst sites for alcohol oxidation. Alternatively, acid buildup tends to lower the pH of the solution (typically around 11.5-11.6 to start), and we have found that alcohol oxidations over PVP-stabilized nanoparticles are much less effective at pHs below 11. We note that no nanoparticle precipitation was seen for either of these systems during the 24 hour reaction. Strong deactivation of the AuPd and AuPt catalysts owing to the carboxylic acid production was also observed by others [19]. Support for this conjecture is seen in the data for the oxidation of 2-butanol and 1,4-butanediol using the 1:3 Au:Pd nanoparticle catalysts; 100% selectivity towards 2-butanone and γ-butyrolactone, respectively, were seen at substantially higher TOFs than any of the other substrates, with only very gradual changes in the TOF over time.

The oxidation of 2-buten-1-ol using 1:3 Au:Pd nanoparticles shows some interesting features. Three separate reactions were seen: the oxidation reaction of 2-buten-ol to crotonaldehyde, the hydrogenation reaction of 2-buten-1-ol to 1-butanol and the isomerization of 2-buten-1-ol into 3-buten-1-ol. After one hour, the product selectivities were 34% crotonaldehyde, 26% 1-butanol, and 40% 3-buten-1-ol. After one hour, no further 3-buten-ol and very little 1-butanol were seen, as the reaction became much more selective towards the oxidation of 2-buten-ol to crotonaldehyde. Similar C=C double bond isomerization and hydrogenation products were reported by Abad *et al*. [6, 7], who suggested that Pd-H species were formed during the aerobic alcohol oxidation which promote C=C double bond isomerization and hydrogenation. We found that no isomerization and hydrogenation products were formed using PVP stabilized Au nanoparticle catalyst at the same conditions. However, it should be noted the pure Au nanoparticle catalyst has a low catalytic activity for this substrate, with a conversion of

2-buten-1-ol to crotonaldehyde of 1.7% was seen after one hour, followed by apparent deactivation of the catalyst.

2.3.5 Catalytic Mechanisms of Alcohol Oxidations

The actual mechanism of alcohol oxidation of the AuPd catalysts may involve several pathways, given that both pure Au and Pd nanoparticles show activity (albeit lower for the pure metals) for this reaction [6, 18, 27]. It has been postulated that alcohol oxidation over Pd nanoparticles involves β-H elimination of a dissociated alcohol on the Pd surface, followed by reaction of oxygen with Pd-H species [27], as shown in Scheme 2.2, while alcohol oxidation over Au surfaces involves primarily superoxo species via oxygen activation over the Au surface [18]. The appearance of the hydrogenation and isomerization products seen for the AuPd catalysts for the oxidation of 2-buten-1-ol above (which are not seen for pure Au catalysts), along with the maximum activity of bimetallic catalysts with high Pd contents, both suggest that surface Pd atoms are predominately the catalytically active species in these particles. This would be consistent with a synergetic electronic effect, which has been used to explain enhancements in other AuPd catalysts. However, it should be noted no further buildup of the hydrogenation and isomerization products of 2-buten-1-ol are seen after 1 hour, suggesting that other catalytic pathways (such as activation over Au atoms) may be more predominant over longer time scales. *In-situ* production of H_2O_2 over AuPd catalysts is another possible mechanism, particularly given the presence of Pd-H species during catalytic reactions. Others have observed the formation of hydrogen peroxide from H_2/O_2 over AuPd bimetallic nanoparticles [28], and that the addition of hydrogen

peroxide to PVP-stabilized AuPd nanoparticles led to significant increases in product turnovers over short (1 hr) time periods.

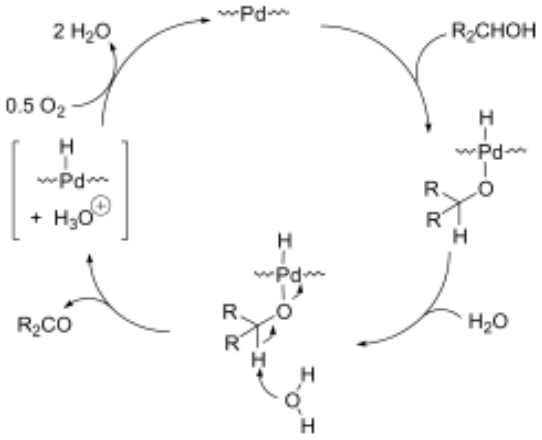

Scheme 2.2. Catalytic alcohol oxidation mechanism on Pd surface. (Reprinted from [27]. Copyright (2003), with permission from Elsevier.)

2.4 Conclusions

In summary, PVP-stabilized 1:3 Au:Pd nanoparticles have been shown to have higher catalytic activities than pure Au, pure Pd nanoparticles and other bimetallic nanoparticles for alcohol oxidation reactions. These particles have been shown to catalyze the aerobic oxidations of aliphatic, allylic, phenylic alcohols and diols in aqueous solution under mild conditions. In most cases, selective oxidations to aldehydes (or ketones) were seen; however, alkanoic acids were the major products for primary aliphatic alcohols and γ-butyrolactone was the only product observed for the oxidation of 1,4-butanediol. Future work will focus on how to prevent catalyst poisoning in this system, understanding structure-property relationships in AuPd bimetallic nanoparticles, as well as attempting to elucidate the mechanism(s) of alcohol oxidation reactions over bimetallic catalysts.

2.5 References

[1] J. March, Advanced Organic Chemistry: Reactions, Mechanisms, and Structure. Wiley, New York, 1992.

[2] K. Peter, C. Vollhardt, and N.E. Schore, Organic Chemistry: Structure and Function, 1999, 300.

[3] F.M. Menger, and C. Lee, Tetrahedron Lett. 22 (1981) 1655-1656.

[4] D.G. Lee, and U.A. Spitzer, J. Org. Chem. 35 (1970) 3589-3590.

[5] C.K. Lee, B.-S. Koo, Y.S. Lee, H.K. Cho, and K.-J. Lee, Bull. Korean Chem. Soc. 23 (2002) 1667-1670.

[6] A. Abad, C. Almela, A. Corma, and H. Garcia, Chem. Commun. (2006) 3178-3180.

[7] A. Abad, C. Almela, A. Corma, and H. Garcia, Tetrahedron 62 (2006) 6666-6672.

[8] A. Biffis, and L. Minati, J. Catal. 236 (2005) 405-409.

[9] K.-M. Choi, T. Akita, T. Mizugaki, K. Ebitani, and K. Kaneda, New J. Chem. 27 (2003) 324-328.

[10] D.I. Enache, J.K. Edwards, P. Landon, B. Solsona-Espriu, A.F. Carley, A.A. Herzing, M. Watanabe, C.J. Kiely, D.W. Knight, and G.J. Hutchings, Science 311 (2006) 362-365.

[11] Z. Hou, N. Theyssen, A. Brinkmann, and W. Leitner, Angew. Chem. Int. Ed. 44 (2005) 1346-1349.

[12] N. Kakiuchi, Y. Maeda, T. Nishimura, and S. Uemura, J. Org. Chem. 66 (2001) 6620-6625.

[13] B. Karimi, S. Abedi, J.H. Clark, and V. Budarin, Angew. Chem. Int. Ed. 45 (2006) 4776-4779.

[14] M.S. Kwon, N. Kim, C.M. Park, J.S. Lee, K.Y. Kang, and J. Park, Organic Letters 7 (2005) 1077-1079.

[15] Y. Uozumi, and R. Nakao, Angew. Chem. Int. Ed. 42 (2003) 194-197.

[16] Y.M.A. Yamada, T. Arakawa, H. Hocke, and Y. Uozumi, Angew. Chem. Int. Ed. 46 (2007) 704-706.

[17] P.G.N. Mertens, I.F.J. Vankelecom, P.A. Jacobs, and D.E. De Vos, Gold Bull. 38 (2005) 157-162.

[18] H. Tsunoyama, H. Sakurai, Y. Negishi, and T. Tsukuda, J. Am. Chem. Soc. 127 (2005) 9374-9375.

[19] N. Dimitratos, A. Villa, D. Wang, F. Porta, D. Su, and L. Prati, J. Catal. 244 (2006) 113-121.

[20] N. Toshima, and T. Yonezawa, New J. Chem. 22 (1998) 1179-1201.

[21] H. Tsunoyama, H. Sakurai, N. Ichikuni, Y. Negishi, and T. Tsukuda, Langmuir 20 (2004) 11293-11296.

[22] N. Toshima, M. Harada, Y. Yamazaki, and K. Asakura, J. Phys. Chem. 96 (1992) 9927-9933.

[23] J.A. Creighton, and D.G. Eadon, J. Chem. Soc. Faraday Trans. 87 (1991) 3881-3891.

[24] R.W.J. Scott, O.M. Wilson, S.K. Oh, E.A. Kenik, and R.M. Crooks, J. Am. Chem. Soc. 126 (2004) 15583-15591.

[25] T. Mallat, Z. Bodnar, P. Hug, and A. Baiker, J. Catal. 153 (1995) 131-143.

[26] C. Hardacre, E.A. Mullan, D.W. Rooney, and J.M. Thompson, J. Catal. 232 (2005) 355-365.

[27] J. Muzart, Tetrahedron 59 (2003) 5789-5816.

[28] P. Landon, P.J. Collier, A.J. Papworth, C.J. Kiely, and G.J. Hutchings, Chem. Commun. (2002) 2058-2059.

CHAPTER 3

Oxidative Stability and Catalytic Activity of Thiolate-Protected Au Monolayer-Protected Clusters

3.1 Introduction

Monolayer protected clusters are nanoparticles coated with a dense protecting layer consisting of, for example, alkanethiolate molecules. Alkanethiols are well known as poisons that inhibit the catalytic activity of metal nanoparticles, due to strong bonding between thiolate groups and electrophilic nanoparticle surfaces [1, 2]. However, several groups have reported that thiolate-protected Pt or Pd nanoparticles do indeed have catalytic activities for hydrogenation and Suzuki cross-coupling reactions, although their catalytic activities are low [2, 3]. Opening access to the surface of thiolate-protected metal nanoparticles is the key to improving their catalytic activities. The groups of Fox and Kaifer used thiolated dendritic ligands [4] and thiolated cyclodextrins [5, 6], respectively, to stabilize nanoparticles; as these systems have few metal-S bonds on the metal surface due to the bulky ligands used, much of the nanoparticle surface remained unpassivated [4]. Indeed, Fox and coworkers found that 3rd generation thiolated dendrimer-stabilized Pd nanoparticles have efficient catalytic activities for Heck and Suzuki reactions [4]. Kaifer and coworkers showed that thiolated β-cyclodextrin (HS-β-CD)-stabilized Pt and Pd nanoparticles were active catalysts for the hydrogenation of allylamine in aqueous solution [6], and that HS-β-CD-Pd nanoparticles are also effective catalysts for Suzuki cross-coupling reactions between aryl halides and phenylboronic

acid [5]. Unfortunately, the synthesis of such dendritic ligands is quite time consuming and costly.

To date, catalytic activity of thiolate-protected Au nanoparticles has not been documented. Indeed, most applications of thiolate-protected Au nanoparticles rely on the inertness of the Au surface. However, Murakami *et al.* demonstrated that dodecanethiolate-capped gold clusters could have the co-catalyst effects on the enhanced activity of Mn-porphyrin catalyst for olefin oxidation reactions [7]. They postulated that partially-oxidized thiolate-protected Au clusters are responsible for the improved activity of Mn-porphyrin catalyst (see Scheme 1.6). The postulated catalytic pathway involved oxidation of thiolate groups from the surface, opening up the surface for other species. Our group [8] and others [9, 10] have recently reported that alkanethiolates attached to gold surfaces can be oxidized to disulfide or sulfonate groups, along with the oxidation of Au^0 atoms to Au^{3+} species under appropriate oxidation conditions (see Scheme 1.7). Thus we wished to study the oxidative stability of thiolate-protected Au monolayer-protected clusters (MPCs) in more detail and determine if there were routes that could control the oxidation of alkanethiolates to form partially-oxidized thiolate-protected Au clusters, which would possess substrate-accessible gold surfaces. These surfaces would still be protected from aggregation by residual ligands remaining on the surface. If this strategy is successful, partially-oxidized thiolate-protected Au nanoparticles could be catalytically active for a number of different reactions.

Earlier studies in the group indicated that dodecanethiolate-protected nanoparticles are stable in air as pure solutions, but are readily oxidized in the presence of halides [8]. Several papers in the literature have reported that dithiols which contain

two mercapto groups were able to be bound to Au surface more strongly and irreversibly due to a chelation effect [11-13], thus suggesting that dithiolate-protected Au MPCs might be more stable than monothiolate-protected Au MPCs. We wished to study the stability of dithiolate-protected Au MPCs and compare them with monothiolate-protected Au MPCs. In addition, routes that allow for control of thiolate oxidation from MPC surface to leave partially-oxidized Au MPCs are desirable. We postulated that mixed thiolate/dithiolate systems would be interesting to study, if indeed one ligand was more stable to oxidation than the other. Disulfide ligands based on (±)-α-lipoic were synthesized as ligands that show strong, irreversible binding to gold nanoparticle surfaces. Dithiolate-, 1-dodecanethiolate-, and mixed 1-dodecanethiolate/dithiolate-protected Au MPCs were synthesized and characterized by UV-Vis, TEM and thermal gravimetric analysis (TGA). The oxidative stability of each of these Au MPC samples was studied in the presence of oxygen and cyanide anions, in order to determine their relative stabilities towards oxidation. Finally, the Au MPCs were studied as catalysts for the reduction of 4-nitrophenol.

3.2 Experimental

3.2.1 Materials

All solvents (HPLC grade toluene, chloroform, acetone, acetonitrile, tetrahydrofuran (THF), and ethanol) and KCN were purchased from EMD Chemicals Inc. and used as received. Deuterated solvents were purchased from Cambridge Isotope Laboratories. Tetraocytlammonium bromide (TOAB), 1-dodecanethiol, butylamine, dodecylamine, (±)-α-lipoic acid, 4-nitrophenol and sodium borohydride were purchased from Aldrich, while hydrogen tetrachloroaurate (III) trihydrate and triethylamine were

purchased from Alfa Aesar. 2-(1H-Benzotriazole-1-yl)-1,1,3,3-tetramethyluronium hexafluorophosphate (HBTU) and N-Hydroxybenzotriazole (HOBT) were purchased from Advanced ChemTech. All the chemicals were used without further purification.

3.2.2 Synthesis of Disulfide Ligands

Disulfide ligands were synthesized via amide conjugation between (±)-α-lipoic acid and amines, as shown in Scheme 3.1 [14]. A typical synthesis is as follows: 2.02 g of (±)-α-lipoic acid, 5.84 g of HBTU, 2.21 g of HOBT and 20 ml of triethylamine were stirred in 120 ml of chloroform for 1h. 1.0ml of butylamine (for short chain ligands) or 2.40g of dodecylamine (for long chain ligands) was added. The solution was then stirred at the room temperature for approximately 72 hours until it turned clear. The mixture was washed sequentially three times with saturated $NaHCO_3$ solution and 10% citric acid solution. The organic layer was then collected and concentrated. The crude product was subjected to silica gel column chromatography. Elution with 40% ethyl acetate and 60% chloroform solvent mixture (for short-chain disulfides) or 10% ethyl acetate and 90% chloroform (for long-chain disulfides) gave compound **1**, the short-chain disulfide (0.68 g, 26.6% yield), or compound **2**, the long-chain disulfide (0.804 g, 63.1% yield).

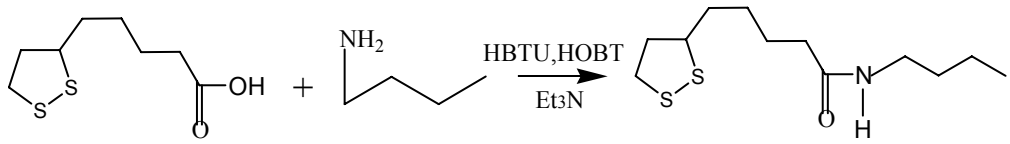

(±)-α-Lipoic acid Butylamine Short-chain disulfide ligand, **1**

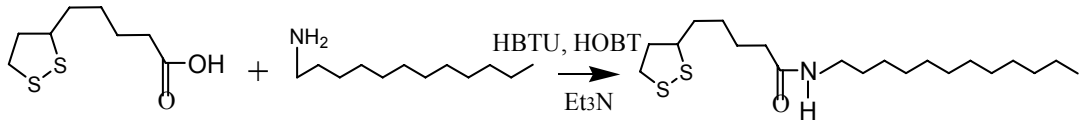

(±)-α-Lipoic acid dodecylamine Long-chain disulfide ligand, **2**

Scheme 3.1. Amide conjugation between (±)-α-lipoic acid and butylamine or dodecylamine to form disulfide ligands **1** or **2**.

3.2.3 Synthesis of Au MPCs

1-dodecanethiolate-protected Au MPCs were synthesized via a modified Brust-Schiffrin method using standard literature procedures [15]. All solvents were degassed with N_2 (Praxair) and reactions were kept under an N_2 atmosphere unless otherwise noted. A typical synthesis is as follows: 30 ml of an aqueous solution of $HAuCl_4.3H_2O$ (0.40 g) was stirred with a solution of tetraoctylammonium bromide (TOAB, 0.34 g) in 80 ml of toluene until all the $HAuCl_4$ was transferred to the organic layer and the water layer became colorless. 0.17 g of 1-dodecanethiol was then added to the organic phase. After stirring for several minutes, 25.0 ml of a freshly prepared 0.40 M $NaBH_4$ solution was added over 20 minutes and the solution was stirred for the next 24 h. Excess thiol, free disulfide and TOAB impurities were removed by sequential washing with ethanol, acetonitrile, and acetone.

Dithiolate-protected Au MPCs (from compounds **1** and **2**) were synthesized via a one-phase method, which is similar to the method reported by Huang [12, 16]. A typical synthesis is as follows: 5 ml of chloroform solution of $HAuCl_4.3H_2O$ (0.039 g, 1.0×10^{-4} mol) was added into 50 ml of chloroform solution of disulfide (0.053 g of **1** or 0.076 g of **2**, 2.0×10^{-4} mol). Then 50 ml of a fresh aqueous solution of $NaBH_4$ (0.077 g, 2.0×10^{-3} mol, 20 times excess) was added dropwise. The solution turned from bright orange to dark purple with the addition of $NaBH_4$, indicating the formation of Au MPCs. After addition, the mixture was stirred for 2 h. The organic layer was extracted and washed with a 80% ethanol and 20% acetone mixture twice.

3.2.4 Ligand Exchange Reactions

0.050 g of 1-dodecanethiolate- or dithiolate-**2**-protected Au MPCs (~ 8.7×10^{-5} mol of ligands attached on the surface of Au MPCs) and 15 ml of chloroform were placed in a 25ml round bottom flask. A 100 times excess (8.7×10^{-3} mol) of **2** or 1-dodecanethiol was added. The mixture was stirred at room temperature for 24 hours.

3.2.5 MPC Oxidation Studies

Oxidation reactions were carried out by bubbling oxygen (Praxair) through 6.0 ml of solution of the 0.10 M Au MPCs (concentration with respect to gold) in d8-THF. 1.0 ml of this solution was removed for NMR measurements at certain time intervals.

3.2.6 MPC Cyanide Etching Studies

0.50 ml of a freshly prepared aqueous solution of KCN (10 mM) was added to a 3.0 ml solution of Au MPCs in THF (1.0 mM in Au). The decay in absorbance at 520 nm was monitored every minute by UV-Vis until the solution became colourless. The decomposition rate data were fit to a general first-order kinetics equation, $y=ae^{-bx}$, in which y is the absorption and x is the time (min).

3.2.7 Catalytic Reactions with Nitrophenol

The reduction of 4-nitrophenol by $NaBH_4$ was studied as a model reaction to probe the catalytic activity of the Au MPCs. In a typical catalytic reaction, 2.65 ml of THF was mixed with 0.15 ml of Au MPCs solution in THF (1.0 mM with respect to Au), followed by the addition of 0.10 ml of 4-nitrophenol aqueous solution (1.5 mM), and finally 0.10 ml of a freshly prepared $NaBH_4$ aqueous solution (1.5 M). Thus the final concentrations of 4-nitrophenol was 0.050 mM, and that of $NaBH_4$ was 0.050 M. Immediately after the addition of $NaBH_4$, UV-Vis spectra of the sample were recorded every minute between 250-550 nm until the yellow solution became colorless. The rate constant of the reduction process was determined by measuring the change in absorbance of the initially observed peak at 400 nm, which corresponds to the nitrophenolate ion, as a function of time [17]. A control experiment was carried out at the same conditions in the absence of Au MPCs.

3.2.8 Characterization of Au MPCs

Absorption spectra were recorded on a Varian Cary 50 Bio UV-Vis spectrometer with an optical path length of 1.0 cm. Transmission electron micrographs (TEM) were obtained with a Philips 410 microscope operating at 100 keV. Samples were prepared by placing a drop of solution on a holey-carbon-coated Cu TEM grid (400 mesh) and allowing the solvent to evaporate in air. ^{1}H NMR and 2D COSY NMR were recorded on a Bruker 500 MHz Avance spectrometer; chemical shifts were referenced to the residual protons of the deuterated solvent. The relative amounts of bound **1** or **2** ligands as well as oxidized disulfide molecules were calculated from ^{1}H NMR data using the integrated areas of methylene α-H (proton 9 in Figure 3.1 below) signals from the disulfide species and methyl signals from both species. TGA was performed on a TGA Q5000IR (TA Instruments). The Au MPCs were placed in a ceramic TGA pan and heated from the room temperature (about 25 ^{o}C) to 600 ^{o}C at a rate of 10 ^{o}C min^{-1} under a nitrogen atmosphere, and the weight loss was recorded as a function of temperature.

3.3 Results and Discussion

3.3.1 Synthesis of Disulfide Ligands, 1 and 2

Short-chain (compound **1**) and long-chain (compound **2**) disulfide ligands were synthesized according to Scheme 3.1. ^{1}H NMR ($CDCl_3$ 500 MHz) analysis indicates the desired disulfide ligands were formed. Figure 3.1 shows representative NMR spectra of the two ligands.

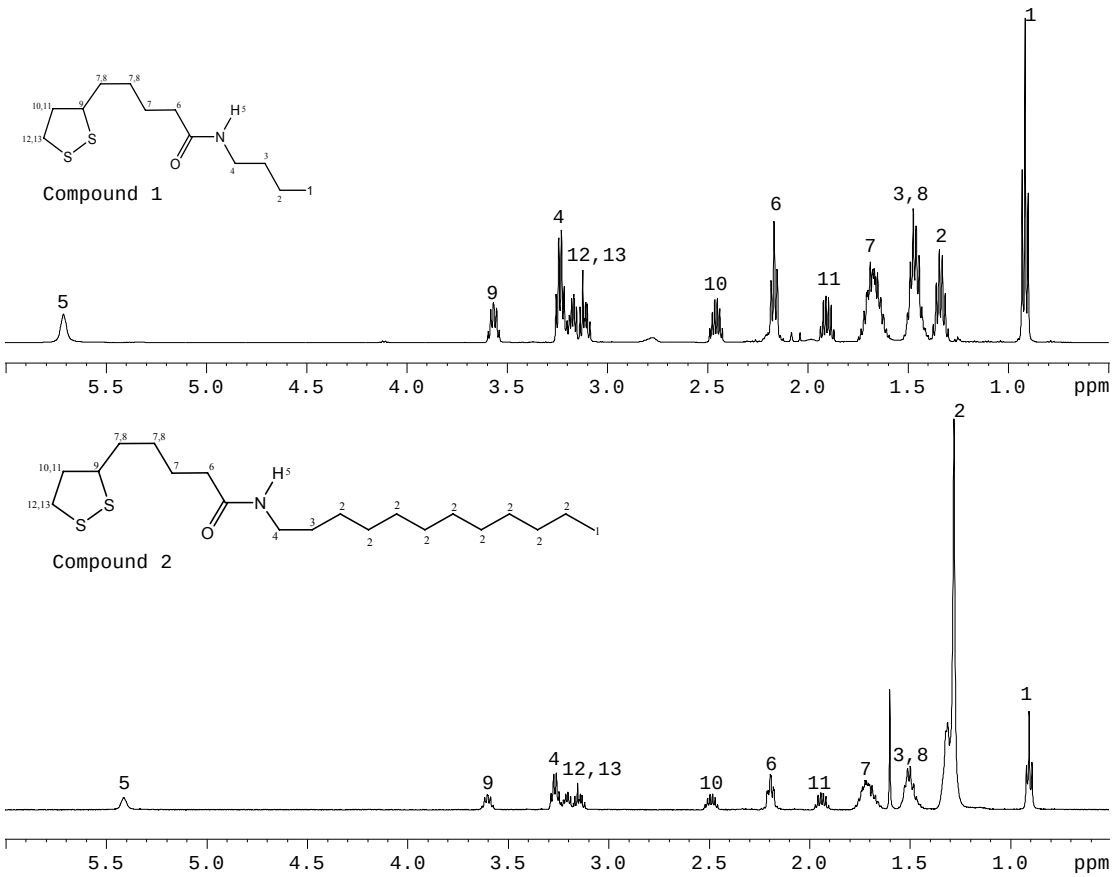

Figure 3.1. ^{1}H NMR of compound **1** (top) and compound **2** (bottom). Assignments were verified by 2D COSY NMR.

3.3.2 Synthesis of 1-dodecanethiolate-protected Au MPCs

1-dodecanethiolate-protected Au MPCs were synthesized via a modified Brust-Schiffrin method [15]. Figure 3.2 shows UV-Vis spectra of the 1-dodecanethiolate-protected Au MPCs solution in chloroform; the very weak plasmon shoulder indicates the size of Au MPCs is quite small (below 2 nm) [8, 18]. TEM measurements show the average particle size of 1-dodecanethiolate-protected Au MPCs is 1.8 ± 0.4 nm (Figure 3.3).

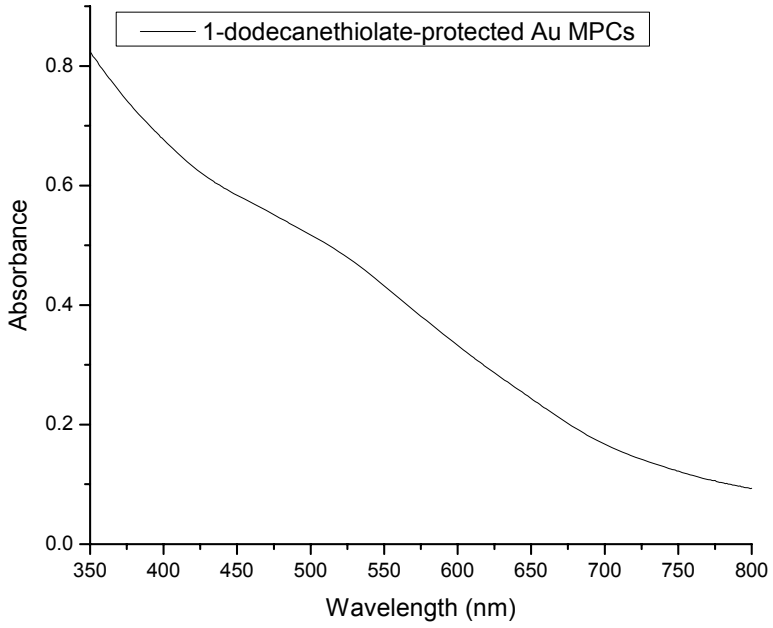

Figure 3.2. UV-Vis spectrum of 1-dodecanethiolate-protected Au MPCs.

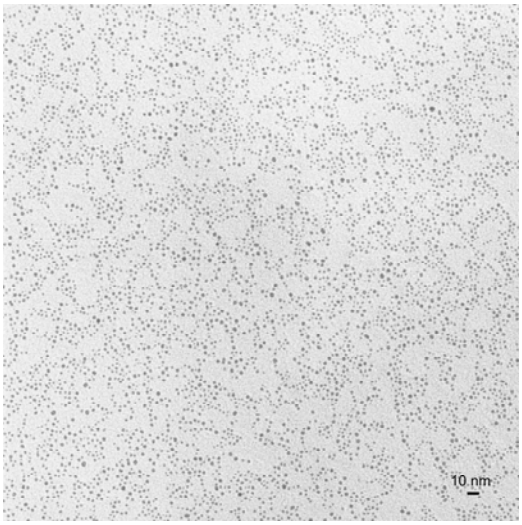

Figure 3.3. TEM image of 1-dodecanethiolate-protected Au MPCs.

3.3.3 Synthesis of Dithiolate-protected Au MPCs

The Brust-Schiffrin method was not feasible for the synthesis of dithiolate-protected Au MPCs, as it was found that the phase transfer agent, TOAB, attached strongly to the surface of the Au MPCs and could not be removed from the Au MPCs. Thus dithiolate-protected Au MPCs were synthesized using a one-phase method, in which tetrachloroauric acid was reduced by sodium borohydride in the presence of the disulfide ligand in chloroform according to a modified procedure reported by Huang *et al.* [16] and Rotello *et al.* [12]. Roux *et al.* have noted that dithiolate-protected Au MPCs can be made from either disulfide (thioctic acid) or dithiol (dihydrolipoic acid) and that the resulting Au MPCs are both stabilized by dithiolates [13]. Figure 3.4 shows UV-Vis spectra of dithiolate **1** and **2**-protected Au MPCs. The plasmon bands of the Au MPCs are both near 523 nm, which indicates they have similar size. Weak plasmon bands such as these are typically indicative of Au MPCs between 2-4 nm [19-21]. This is in general agreement with TEM results, shown in Figure 3.5, which indicate that Au MPCs stabilized by compound **1** have an average size of 3.1±1.0 nm, while those stabilized by compound **2** have an average size of 3.0 ±1.0 nm.

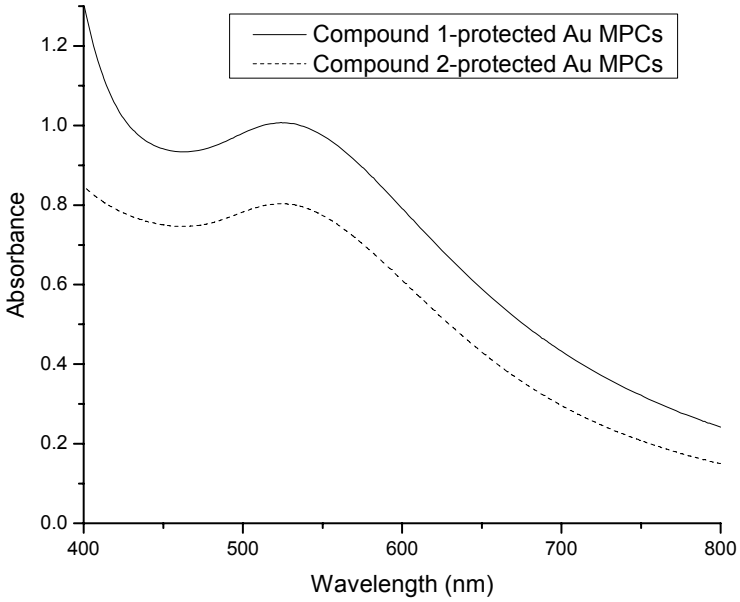

Figure 3.4. UV-Vis spectra of Au MPCs stabilized by disulfide compounds **1** (solid line) and **2** (dotted line).

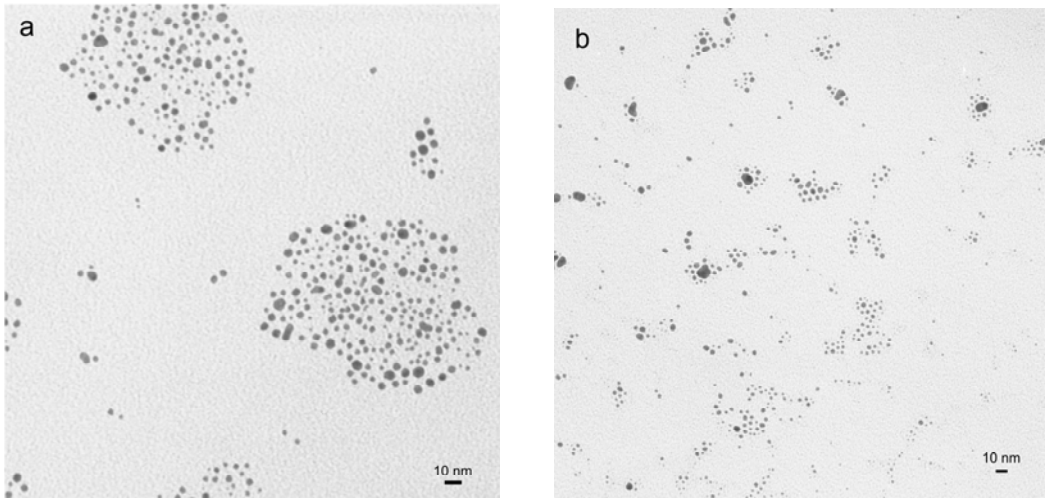

Figure 3.5. TEM images of Au MPCs stabilized by disulfide compounds (a) **1** and (b) **2**.

Au MPCs stabilized by compound **1** were found to be poorly soluble after purification, and are not completely soluble in many common deuterated solvents. Thus it was difficult to monitor their stability using ^{1}H NMR. For this reason, only the stability of Au MPCs stabilized by compound **2** were studied, and the Au MPCs will be referred to as dithiolate-protected Au MPCs hereafter. The NMR spectra of free compound **2** and compound **2**-stabilized Au MPCs are shown in Figure 3.6. It should be noted that the peaks in compound **2** for proton 9 disappeared, proton 5 was shifted to about 6.6 ppm and became a very broad peak and the positions of protons 10, 11, 12, and 13 were shifted when the ligand was attached on the Au surface. The disappearance of proton 9 upon ligand attachment to the Au surface is likely due to broadening effects due to its proximity to the gold surface, such that it cannot undergo rotational motion. Similar effects have been seen for other groups on thiols in close proximity to gold surfaces [22]. We are not certain as to the reason for the NMR downfield shift of proton 5; two possibilities include hydrogen bonding with the adjacent ligands on the particle surface, or weak back-bonding of amide groups to the Au surface.

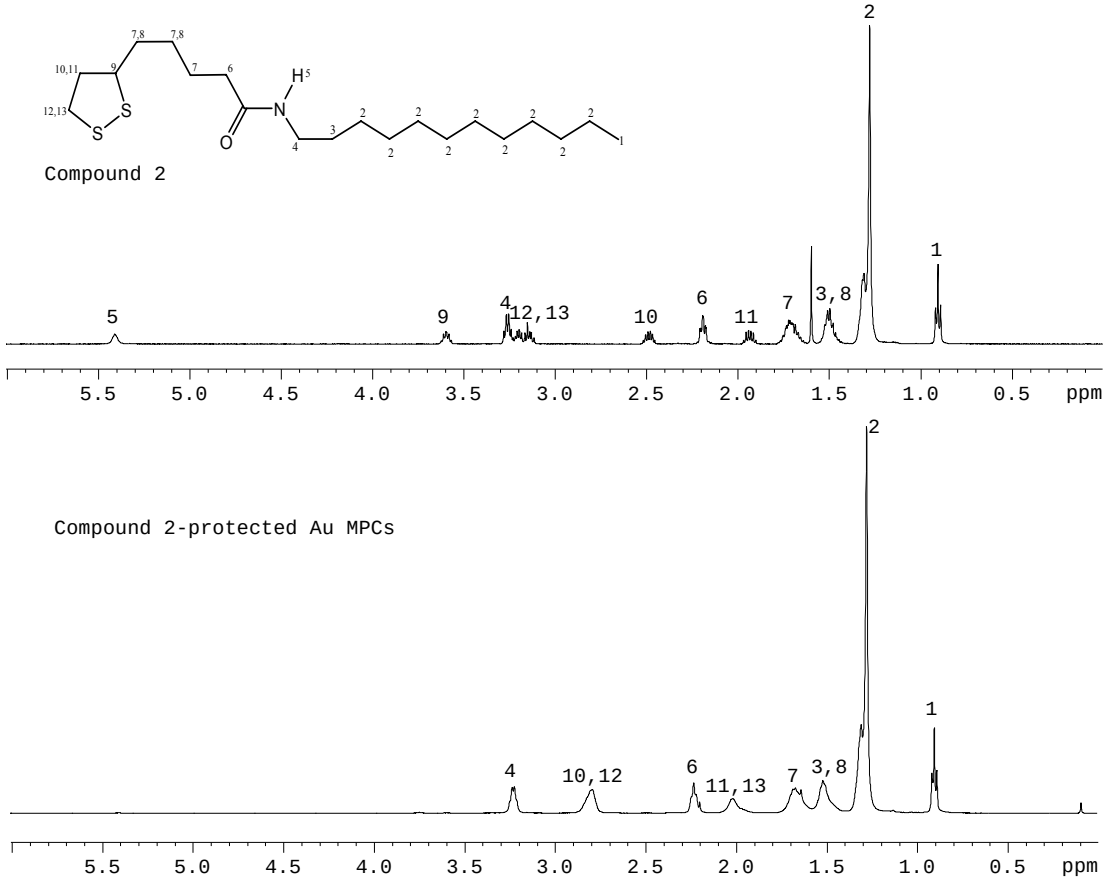

Figure 3.6. ^{1}H NMR of compound **2** (top) and compound **2**-protected Au MPCs (bottom). Assignments were verified by 2D COSY NMR.

3.3.4 Ligand Exchange Reactions

In an effort to make mixed-ligand species which have both thiolate and dithiolate stabilizers, attempts were made to ligand-exchange pure MPCs. 1-dodecanethiolate-protected Au MPCs were found to be quite stable in the presence of excess amounts of ligands **1** and **2**; after 24 h at room temperature, no ligand exchange products were observed by ^{1}H NMR. Attempts to heat up the MPCs to yield Au MPCs stabilized by mixed ligands led to complete decomposition of the Au MPCs. On the other hand, Au

MPCs stabilized by compound **2** were reactive in the presence of excess 1-dodecanethiol. After 24 h at room temperature, about 50% of the dithiolate ligands were replaced by 1-dodecanethiol (as observed by ^{1}H NMR), leading to the formation of Au MPCs with mixed ligand stabilizers. One plausible explanation for this reactivity is that compound **2** cannot pack densely on the surface of Au MPCs due to steric constraints. This allows 1-dodecanethiol ligands with a smaller volume to approach the surface and replace disulfide ligands via a ligand exchange mechanism. On the other hand, the dodecanethiolate-protected MPCs have dodecanethiolate ligands packed tightly on their surfaces, which does not allow for the bulky disulfide to attack the surface and replace 1-dodecanethiol. Figure 3.7 shows the UV-Vis spectrum of the mixed 1-dodecanethiolate/dithiolate-protected Au MPCs. The shape and position of the plasmon band is similar to that of dithiolate-protected Au MPCs, which indicates the size of mixed 1-dodecanethiolate/dithiolate-protected Au MPCs should be between 2 and 4 nm [19-21]. The TEM image in Figure 3.8 shows that their average size is 4.1±1.3 nm.

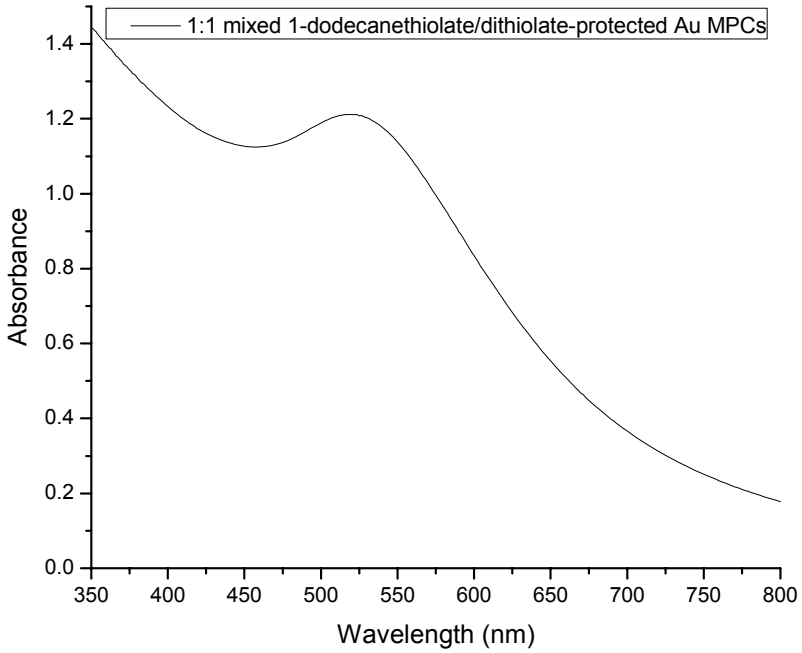

Figure 3.7. UV-Vis spectrum of Au MPCs stabilized by mixed 1-dodecanethiolate/dithiolate-protected Au MPCs.

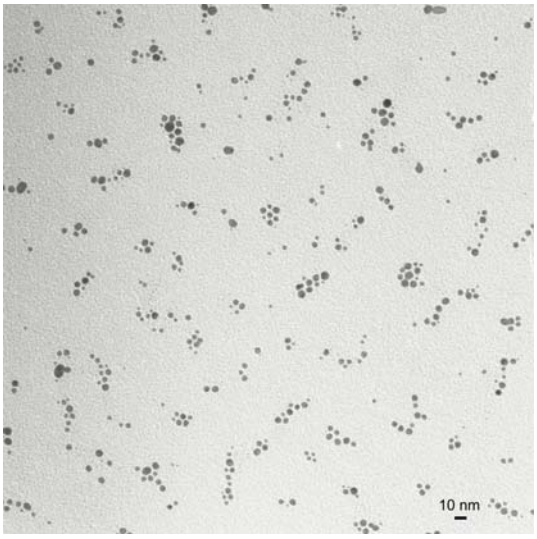

Figure 3.8. TEM image of mixed 1-dodecanethiolate/dithiolate-protected Au MPCs.

3.3.5 Thermal Stability of 1-dodecanethiolate-, Dithiolate- and 1:1 Mixed 1-dodecanethiolate/dithiolate-protected Au MPCs

The thermal stability of the Au MPCs was studied by using thermogravimetric analysis (TGA). The mass change was plotted against temperature to generate the thermogravimetric profiles. Such mass losses reflect the decomposition and removal of thiolate ligands from the gold surface [12]. Figure 3.9 shows percentage weight loss curves for the three MPCs; the percentage mass of ligands is 28.0% in 1-dodecanethiolate-protected Au MPCs, 56.8% in dithiolate-protected Au MPCs and 24.6% in 1:1 mixed 1-dodecanethiolate/dithiolate-protected Au MPCs. It should be noted that each of these samples did not contain free thiols/disulfides or other impurities as determined by ^{1}H NMR. Combining these data and the average particle sizes that were obtained by TEM, we can calculate, on average, how many gold atoms and ligand molecules constitute individual Au MPC in each sample. The results are summarized in Table 3.1. The number of Au atoms in one cluster for three Au MPCs was calculated using Equation (3.1) as follows, where n is the number of atoms per cluster, R is the nanoparticle diameter and V_g is the molar volume of Au, 10.2 cm^3/mole [23]. The number of ligands in one cluster for each of the three Au MPCs was estimated using Equation (3.2) below, where n is the number of atoms per cluster, N is the number of ligands per cluster, AW is the atomic weight of Au, MW is the molecular weight of one thiolate ligand (Equation 3.2 is derived from Weight % Ligand = (N×MW)/(N×MW + n×AW), followed by rearrangement to solve for N).

$$n = 4\pi R^3/3V_g \quad (3.1)$$

$$N = (n \times AW \times \text{Weight \% of Ligand})/(MW \times \text{Weight \% of Au}) \quad (3.2)$$

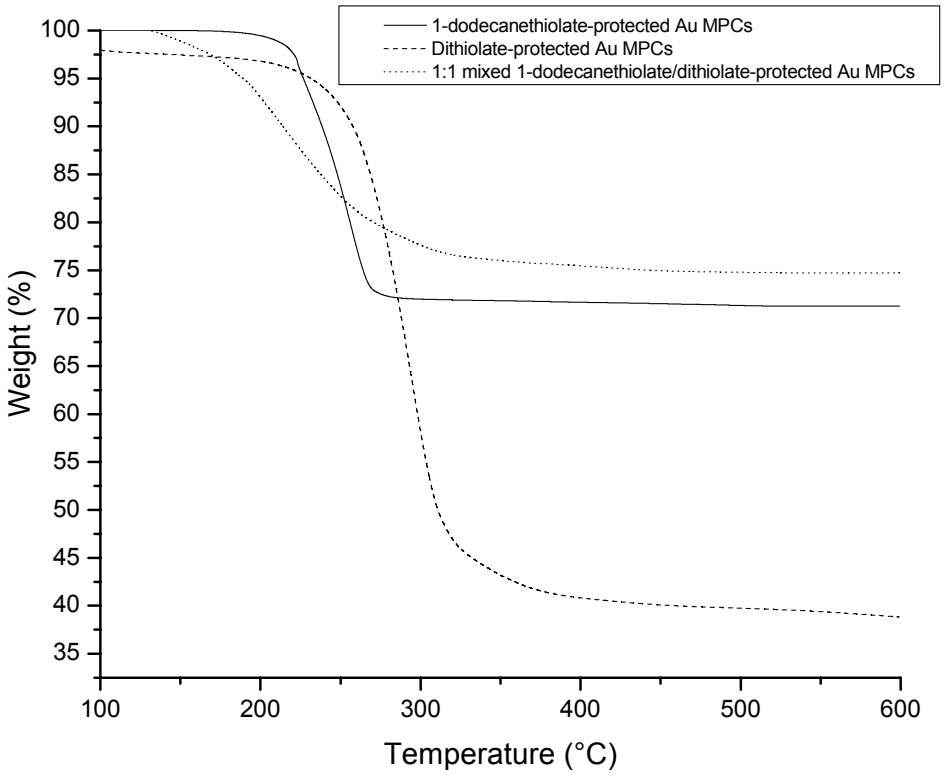

Figure 3.9. Weight loss versus temperature curves of 1-dodecanethiolate-, dithiolate-, and 1:1 mixed 1-dodecanethiolate/dithiolate-protected Au MPCs.

Table 3.1. Number of Au atoms and number of ligands of a single nanoparticle for each of the three Au MPCs based on TEM and TGA results.

Au-MPC stabilizer	TEM R (nm)	TGA Weight % of ligands	# of Au atoms and ligands in one cluster
1-dodecanethiolate	0.9±0.2	28.0	$Au_{180}L_{m68}$
Dithiolate	1.5±0.5	56.8	$Au_{834}L_{d579}$
1:1 mixed 1-dodecanethiolate/dithiolate	2.05±0.65	24.6	$\sim Au_{2130}L_{m238}L_{d238}$

L_m: monothiolate (1-dodecanethiolate) ligands; L_d: dithiolate (compound 2) ligands. Relative amounts of each ligand in mixed system were assumed to be 50/50, which was the ratio estimated from ^{1}H NMR using the integrated areas of methylene α-H (9) signals and methyl (1) signals.

The diameter of 1-dodecanethiolate-protected Au MPCs measured by TEM is 1.8±0.4 nm and the weight loss of adsorbed 1-dodecanethiolate ligands determined by TGA is 28.0%. This is consistent with the results obtained by Murray *et al.* (28.8% weight loss for 2.2 nm dodecanethiolate-protected Au MPCs) [21]. However, the weight losses seen for the 3.0±1.0 nm dithiolate- (56.8%) and 4.1±1.3 nm mixed 1-dodecanethiolate/dithiolate- (24.6%) stabilized Au MPCs (56.8%) are significantly larger than earlier results obtained by Murray *et al.* (16.9% weight loss for 2.8 nm and 12.8% weight loss for 4.0 nm Au nanoparticles covered by dodecanethiolate) [21], even when the difference of molecular weights of the different ligands has been considered.

We are currently unsure as to why the dithiolate-stabilized Au MPCs have such a large weight % of ligand; several possibilities are that impurity phases are present that were not accounted for (although the samples were clean by ^{1}H NMR), or there are a large fraction of sub 1 nm nanoparticles present that are not observable by TEM. Finally, the mixed thiolate/dithiolate- stabilized Au MPCs have a weight loss of 24.6%, which is higher than the value of 9.6% seen by Roux *et al.* for 5.5 nm Au nanoparticles stabilized by dihydrolipoic acid [13].

Figure 3.10 shows the derivative curves for TGA mass losses for the three Au MPCs. From the positions of the derivative peaks, it is clear that the dithiolate-protected Au MPCs have the highest decomposition temperature. The positions of the derivative peaks reflect the thermal stability of the thiolate ligands. The dithiolate ligand is bulkier and has two thiolate attachments to the Au surface, thus it is significantly more thermally stable than 1-dodecanethiolate-protected MPCs. The derivative peak of 1:1 mixed 1-dodecanethiolate/dithiolate-protected Au MPCs is quite broad, indicating decomposition of two kinds of thiolate ligands over a wide temperature range.

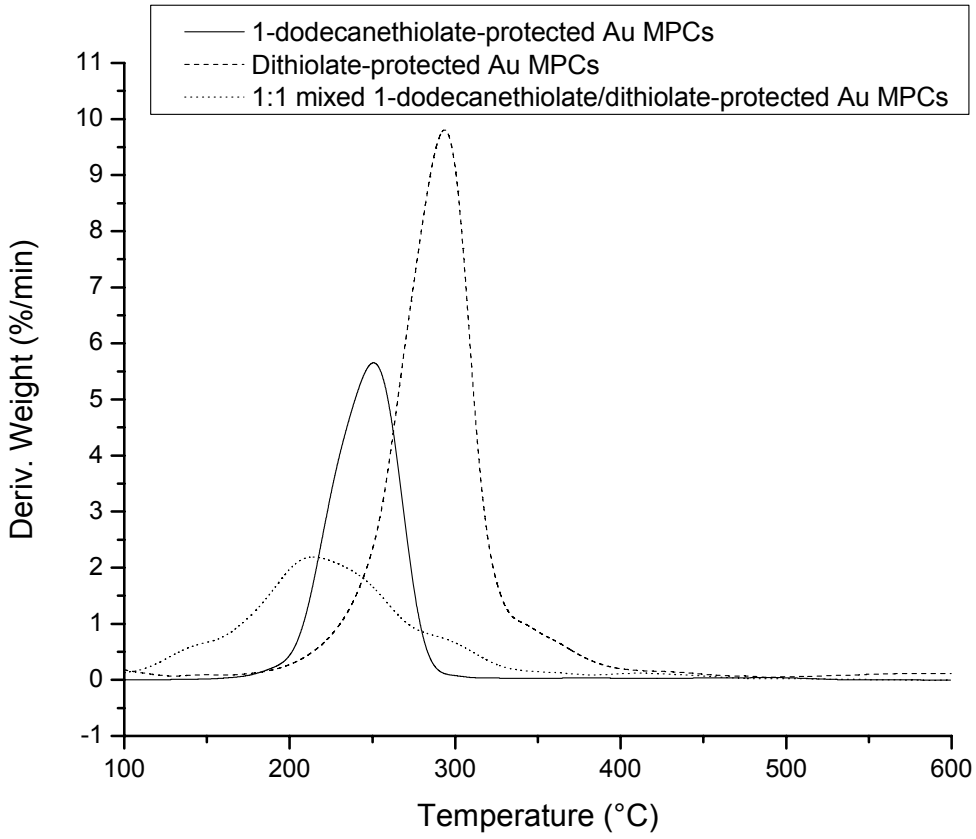

Figure 3.10. Derivative thermogravimetric curves of 1-dodecanethiolate-, dithiolate-, and 1:1 mixed 1-dodecanethiolate/dithiolate-protected Au MPCs.

3.3.6 Oxidative Stabilities of 1-dodecanethiolate-, Dithiolate- and 1:1 Mixed 1-dodecanethiolate/dithiolate-protected Au MPCs

Pure 1-dodecanethiolate-protected Au MPCs are fairly stable in the presence of oxygen over 72 hours, a result which was observed previously in our group (dodecanethiolate-stabilized Au MPCs are stable in air in the absence of halide impurities) [8]. UV-Vis data in Figure 3.11 shows a weak plasmon band before and after exposure to oxygen, indicating little or no change in particle sizes. However, TEM

measurements show that particle sizes increased after exposure to oxygen from 1.8±0.4 nm to 3.3±0.9 nm (Figure 3.12a and 3.12a'), which suggests that some thiolate oxidation is occurring, likely due to trace amounts of TOAB present [8].

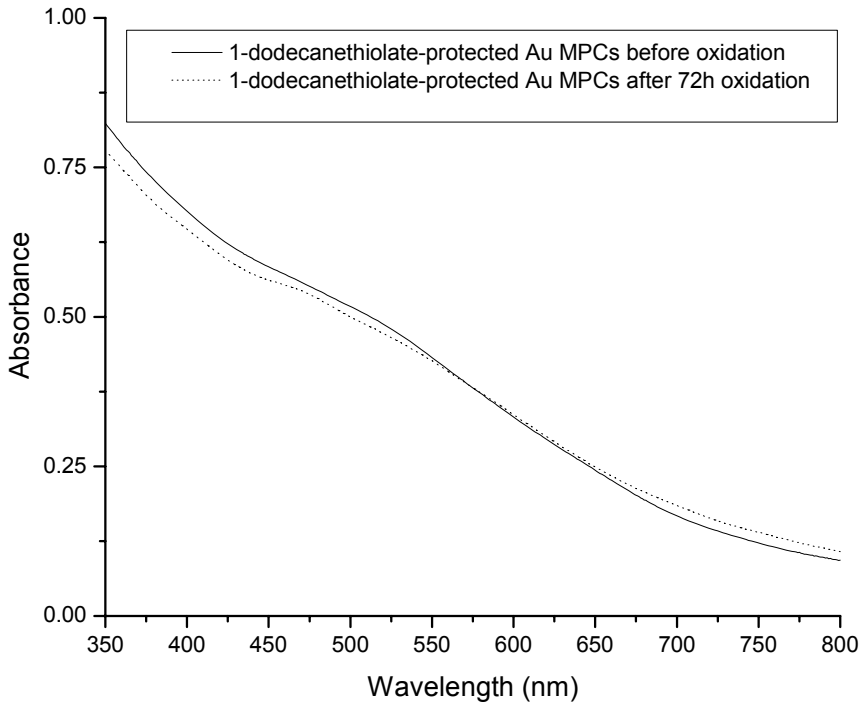

Figure 3.11. UV-Vis spectra of 1-dodecanethiolate-protected Au MPCs before (solid) and after (dot) exposure to oxygen for 72 h.

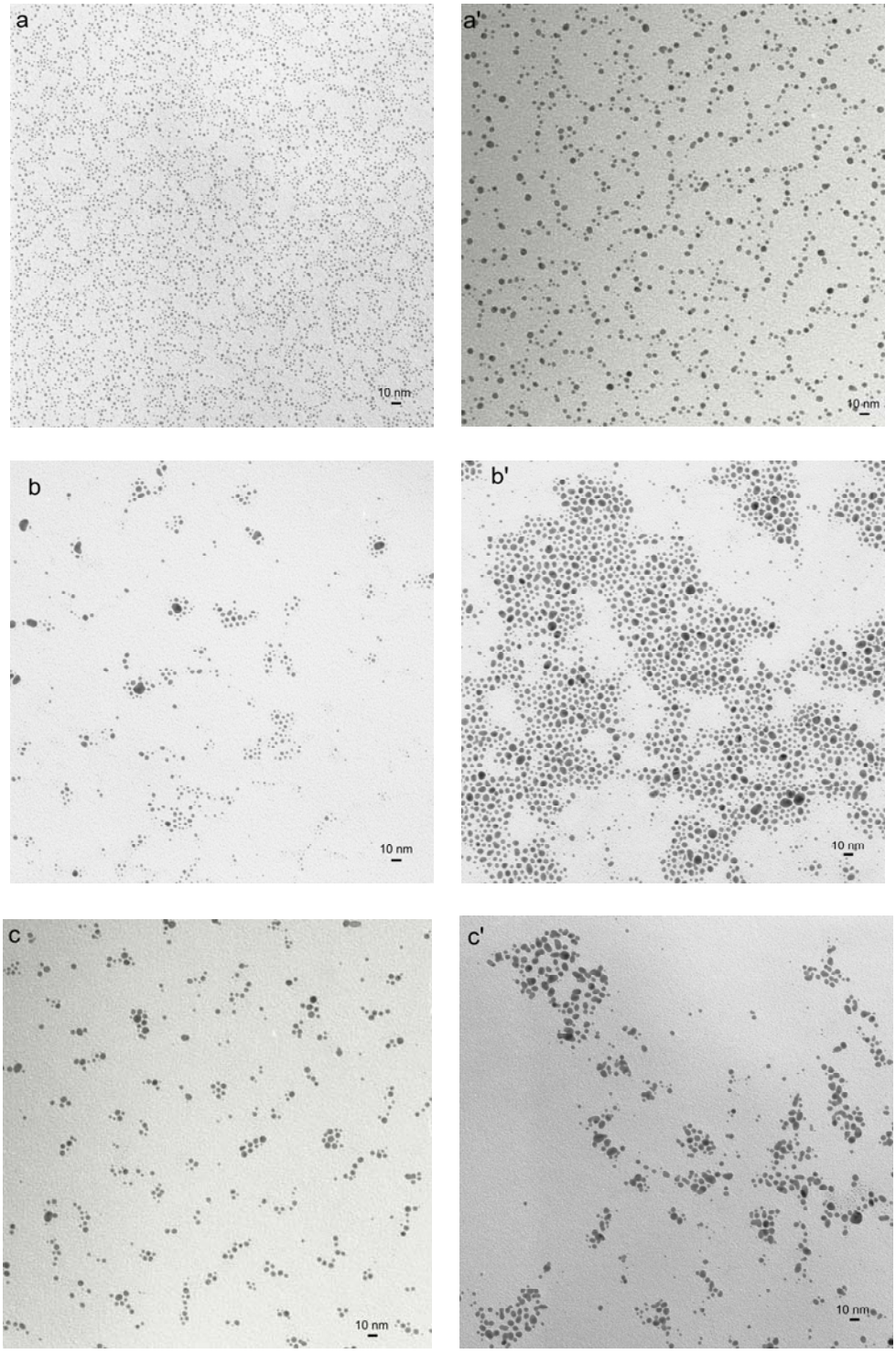

Figure 3.12. TEM images of 1-dodecanethiolate-, dithiolate-, and mixed 1-dodecanethiolate/dithiolate-protected Au MPCs before (a, b and c) and after exposure to oxygen for 72 h (a', b', and c').

Purified dithiolate-protected Au MPCs (synthesized from compound **2**) which were exposed to oxygen showed changes in their ^{1}H NMR spectra (Figure 3.13) over time, as the anchored dithiolate ligands were oxidized to the free disulfide, **2**. The peaks labeled by an asterisk in the bottom part of Figure 3.13 are attributed to free disulfide **2**. Table 3.2 shows the percentage amounts of anchored dithiolate and/or 1-dodecanethiolate oxidized calculated from integration of ^{1}H NMR spectra over different time intervals during the oxidation of each of the three Au MPCs. Compared with the oxidation of 1-dodecanethiolate-protected Au MPCs, the oxidative stability of the dithiolate-protected Au MPCs is poor, as 12.5% of the dithiolate ligands were oxidized to form free disulfides (compound **2**) after only 2 hours. The oxidation process slowed down after 2 hours and only 19% dithiol ligands were oxidized after 72 hours. Figure 3.14 shows the UV-Vis spectra of the dithiolate-protected Au MPCs before and after exposure to oxygen, the plasma band at 523 nm shifts to 526 nm after exposure to oxygen and increases significantly in intensity. This result suggests the average size of dithiolate-protected Au MPCs increases upon oxygen exposure. TEM results confirm this hypothesis, as shown in Figure 3.12b and 3.12b'. The average nanoparticle size of the dithiolate-protected Au MPCs before oxidation is 3.0±1.0 nm, while the size after oxidation is 4.6±1.2 nm. The difference of the oxidative stabilities between 1-dodecanethiolate- and dithiolate-protected Au MPCs can be explained by considering that 1-dodecanethiolate-protected Au MPCs have dense packing on their surface, thus making it difficult for oxygen to access the Au surface, while the dithiolate ligands on the dithiolate-protected Au MPCs do not pack well, allowing for oxygen to access the surface. In addition, as the dithiolate to disulfide oxidation is an intramolecular reaction

(compared to the intermolecular reaction needed to form disulfides from 1-docanethiolate ligands), it may be a kinetically-favourable oxidation process.

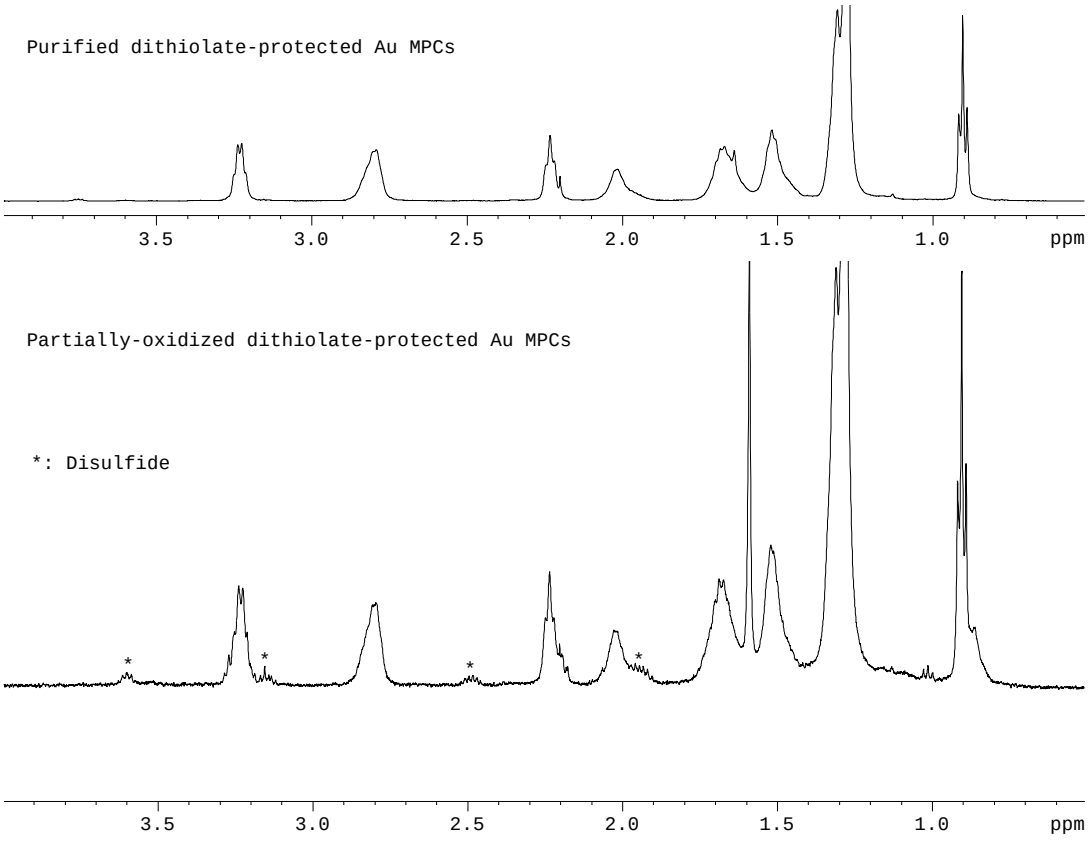

Figure 3.13. ^{1}H NMR spectra of dithiolate-protected Au MPCs before (top) and after (bottom) exposure to oxygen for 21 h.

Table 3.2. Percentage of anchored dithiol or 1-dodecanethiol oxidized at different time intervals for Au MPCs, as determined by ^{1}H NMR.

Time (h)	Percentage Amounts of Anchored Ligands Oxidized			
	Dithiolate-protected Au MPCs	1-dodecanethiolate-protected Au MPCs	Mixed 1-dodecanethiolate/dithiolate-protected Au MPCs	
			Compound **2**	1-dodecanethiolate
0	0%	0%	0%	0%
2	12.5%	0%	6.5%	1.7%
24	13.7%	0%	6.7%	1.5%
48	16.1%	0%	9.4%	2.8%
72	19.0%	0%	28.7%	4.0%

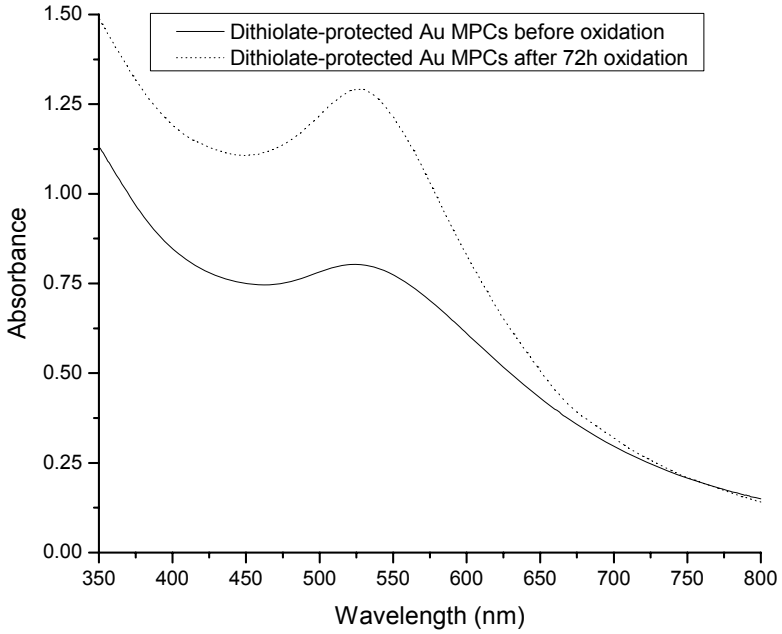

Figure 3.14. UV-Vis spectra of dithiolate-protected Au MPCs before (solid) and after (dot) exposure to oxygen for 72 h.

1:1 mixed 1-dodecanethiolate/dithiolate-protected Au MPCs are also unstable in the presence of oxygen, and both anchored 1-dodecanethiolate and dithiolate were oxidized, as verified by ^{1}H NMR. However, only 4.0% of the 1-dodecanethiolate ligands were oxidized, while 28.7% of the dithiolate ligands were oxidized after 72 h. UV-Vis spectra of 1:1 mixed 1-dodecanethoilate/dithiolate-protected Au MPCs before and after exposure to oxygen are shown in Figure 3.15. No shift and the intensity change of plasmon band indicate little or no change in average particle size. TEM measurements indicate that the particle sizes increase slightly from 4.1±1.3 nm to 4.8±1.3 nm (see Figure 3.12c and 3.12c').

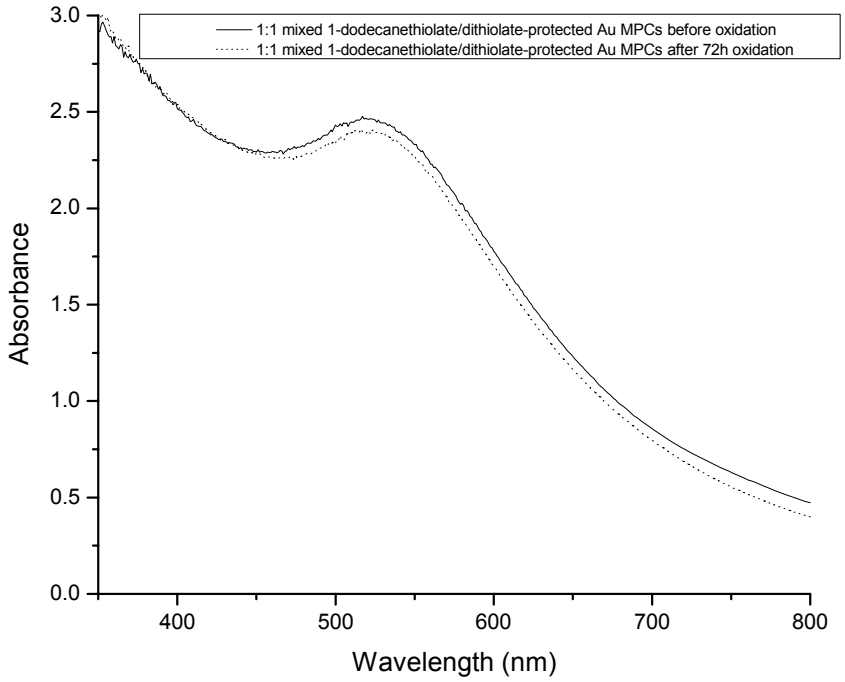

Figure 3.15. UV-Vis spectra of 1:1 mixed 1-dodecanethiolate/dithiolate-protected Au MPCs before (solid) and after (dot) exposure to oxygen for 72 h.

Based on these results, we expect that the sequence of catalytic activity of three Au MPCs should be dithiolate ~ mixed 1-dodecanethiolate/dithiolate- >> 1-dodecanethiolate-protected Au MPCs, as it proved to be the most difficult to remove ligands from the surface of 1-dodecanethiolate-protected Au MPCs. Somewhat surprisingly, dithiolate ligands could be oxidized from Au MPCs rather readily under oxygen, suggested that this might be a viable strategy to synthesize catalytically-active Au MPCs. It should be noted that the mixed thiolate/dithiolate-protected Au MPCs had the lowest change in particle size upon oxidation, we will explore the catalytic activity of this system in more detail in later sections.

3.3.7 Au MPC Cyanide Etching Studies

The surface accessibility of 1-dodecanethiolate-, dithiolate-, partially-oxidized dithiolate-(in which ~10% attached dithiolate ligands were oxidized) and 1:1 mixed 1-dodecanethiolate/dithiolate-protected Au MPCs was further probed by examining cyanide-induced etching of the gold cores. The solutions of Au MPCs were all etched in the presence of KCN to give colourless solutions comprising of $Au(CN)_2^-$ complexes, disulfides and alkyl cyanides [12]. The reaction kinetics were obtained by monitoring the absorption changes of the MPC solutions (4.8 μM of nanoparticles for 1-dodecanethiolate-protected Au MPCs and 1.0 μM of nanoparticles for dithiolate-protected Au MPCs) at 520 nm every minute in the presence of an excess amount of an aqueous solution of KCN (1.43 mM). Figure 3.16 shows a typical etching experiment of dithiolate-stabilized Au MPCs; the Au plasmon band decreased gradually over time as the Au cores were etched.

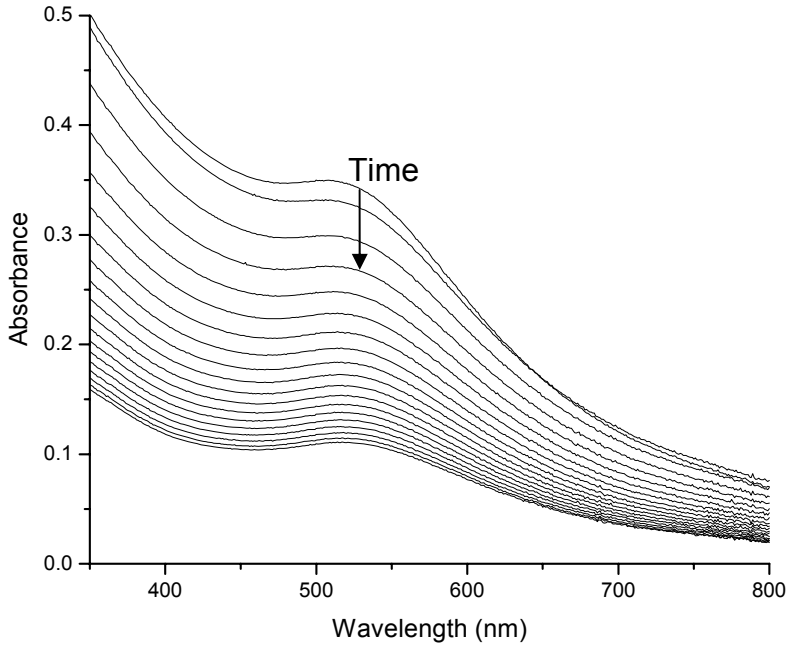

Figure 3.16. UV-Vis spectra of dithiolate-protected Au MPCs upon exposure to KCN. Each plot represents a 1 minute interval.

Representative etching profiles, as followed by UV-Vis spectroscopy, for the four MPCs (1-dodecanethiolate-, dithiolate-, partially-oxidized dithiolate- and 1:1 mixed 1-dodecanethiolate/dithiolate-protected MPCs) are depicted in Figure 3.17. The concentration of KCN was treated as a constant during the reaction course given its concentration was much higher than the concentration of Au MPCs. The absorption data of all four MPCs follow a general first-order reaction function, as can be seen in Figure 3.17. R^2 values for fits of for all four Au MPCs are larger than 0.985. Figure 3.18 shows an example of a fit for experimental data based on 1st order function for dithiolate-protected Au MPCs. The fit for the larger 1-dodecanethiolate/dithiolate-protected Au MPCs is the poorest, which is likely due to the fact that the absorbance of Au plasmon

band is not 100% correlated with the concentration of Au clusters, especially for larger Au clusters. Similar first-order kinetics of cyanide-induced etching of Au MPCs was previously reported by other groups [10, 12].

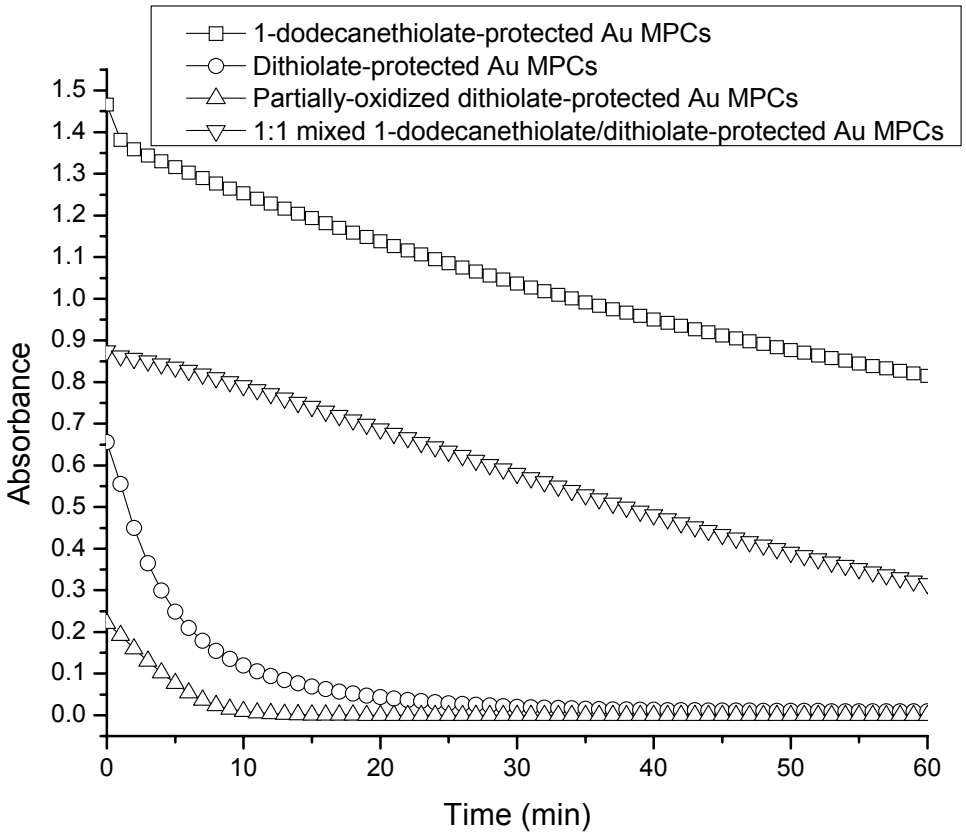

Figure 3.17. UV-Vis absorption changes of Au MPCs at 520 nm in the presence of KCN at room temperature.

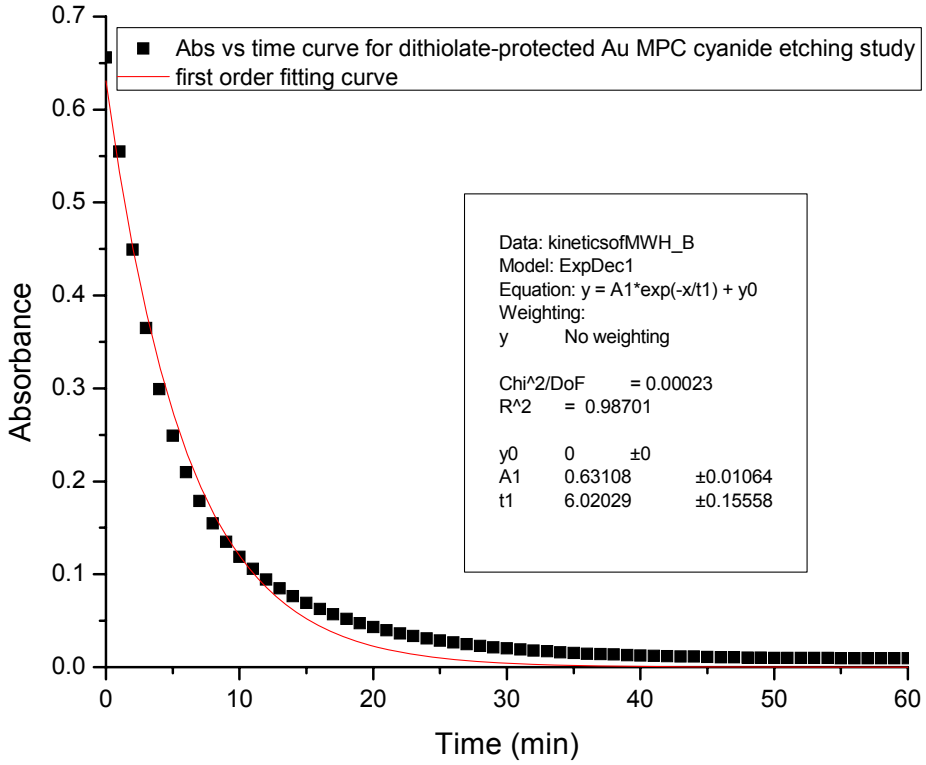

Figure 3.18. UV-Vis absorption changes of dithiolate-protected Au MPCs at 520 nm in the presence of KCN at room temperature with the 1st order fit shown (R^2=0.987).

The pseudo-first-order and second-order rate constants for the KCN etching are summarized in Table 3.3; they reveal that partially-oxidized dithiolate-protected Au MPCs have the highest Au core etching rate and 1-dodecanethiolate-protected Au MPCs are the most stable to KCN etching, despite their smaller particle size. The relative etching rates of the Au MPCs are likely governed primarily by the surface accessibility of Au MPCs, as cyanide anions need first to access the surface to etch Au MPCs [12]. Thus, the surfaces of dithiolate-protected Au MPCs are more accessible than 1-dodecanethiolate-protected Au MPCs, which agrees with oxidation data from the last

section. The partially-oxidized dithiolate-protected Au MPCs have the highest etching rate since they have the most accessible surface, given that ~10% of the anchored dithiolate ligands have been oxidized and detached from the surface of gold core. The 1:1 mixed 1-dodecanethiolate/dithiolate-protected Au MPCs have intermediate etching kinetics, as their surfaces are less accessible than those of pure dithiolate-protected Au MPCs.

Table 3.3 The pseudo-first-order (k_1) and second-order rate constants (k_2) for the decomposition of Au MPCs by KCN at room temperature.

Au-MPC Stabilizer	k_1/min^{-1}
1-dodecanethiolate	$9.16\times10^{-3}\pm1.0\times10^{-4}$
Dithiolate	0.166±0.004
Partially-oxidized dithiolate	0.245±0.007
1:1 mixed 1-dodecanethiolate/dithiolate	$1.64\times10^{-2}\pm2.4\times10^{-4}$

We postulate that the sequence of cyanide etching reaction rates should agree with the sequence of catalytic activity given both of them are related to the substrate-accessible surface area. For example, partially-oxidized dithiolate-protected Au MPCs would be expected to have highest catalytic activity as they showed the fastest cyanide etching rate constants as can be seen in Table 3.3. On the other hand, 1-dodecanethiolate-protected Au MPCs should have poor catalytic activity since they have the lowest KCN etching rate constant, and thus the least substrate-accessible surfaces.

3.3.8 Catalytic Activity of Au MPCs

The catalytic activity of 1-dodecanethiolate-, dithiolate-, and 1:1 mixed 1-dodecanethiolate/dithiolate-protected Au MPCs was examined using the reduction of 4-nitrophenol by $NaBH_4$ to 4-aminophenol as a model reaction. 4-nitrophenol reduction in the presence of the Au MPCs was monitored by UV-Vis spectroscopy. Figure 3.19 shows the UV-Vis spectra for the 4-nitrophenol reduction catalyzed by dithiolate-protected Au MPCs. The peak at 400 nm has been attributed to the presence of 4-nitrophenolate ions [17, 24]. After the addition of freshly prepared $NaBH_4$, this peak decreased in intensity until it finally disappeared, and a new peak at 300 nm, which has been attributed to 4-aminophenol, appeared and grew in intensity [24]. The concentration of Au MPCs was very low (50 μM in Au) and do not absorb significantly in this region of the spectra at this concentration [17, 24]. Control experiments were carried out to ensure that the Au MPCs were acting as catalysts; the intensity of the peak at 400 nm did not decrease upon $NaBH_4$ addition to 4-nitrophenol in the absence of the Au MPCs.

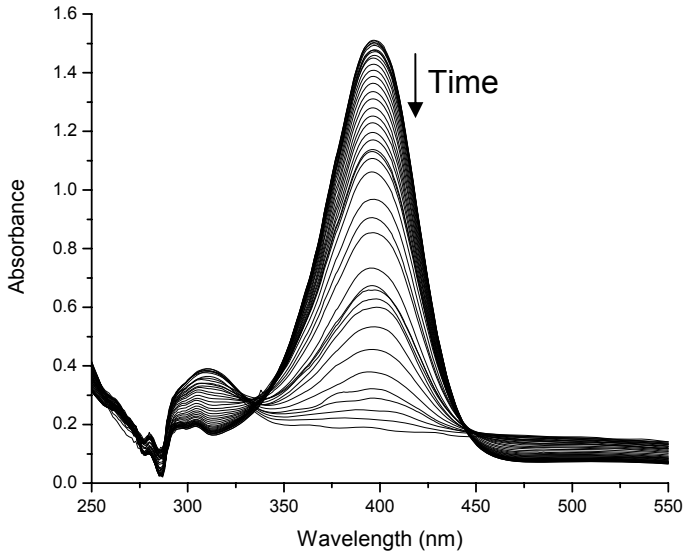

Figure 3.19. UV-Vis spectra for 4-nitrophenol reduction by $NaBH_4$ catalyzed by dithiolate-protected Au MPCs.

The kinetics of 4-nitrophenol reduction in the presence of the Au MPCs was studied by plotting absorption changes at 400 nm vs. time, as seen in Figure 3.20. The concentration of $NaBH_4$ is 1000 times as the concentration of 4-nitrophenol and remains essentially constant during the reaction. There is an induction time in all the cases. The induction time is typically between 9-10 minutes (see Table 3.4), after which the reaction is quite fast and finished in less than 30 min. Some other groups [17, 25] also reported that induction times were found for nitrophenol reductions under air, and attributed the induction times to the reduction of oxygen present in the system, thus the reduction reaction of 4-nitrophenol only starts after all the oxygen in the system has been reacted [17]. Control experiments were carried out to prove this point. No

induction times were observed when reactions were carried out in N_2 (and reaction kinetics were similar otherwise).

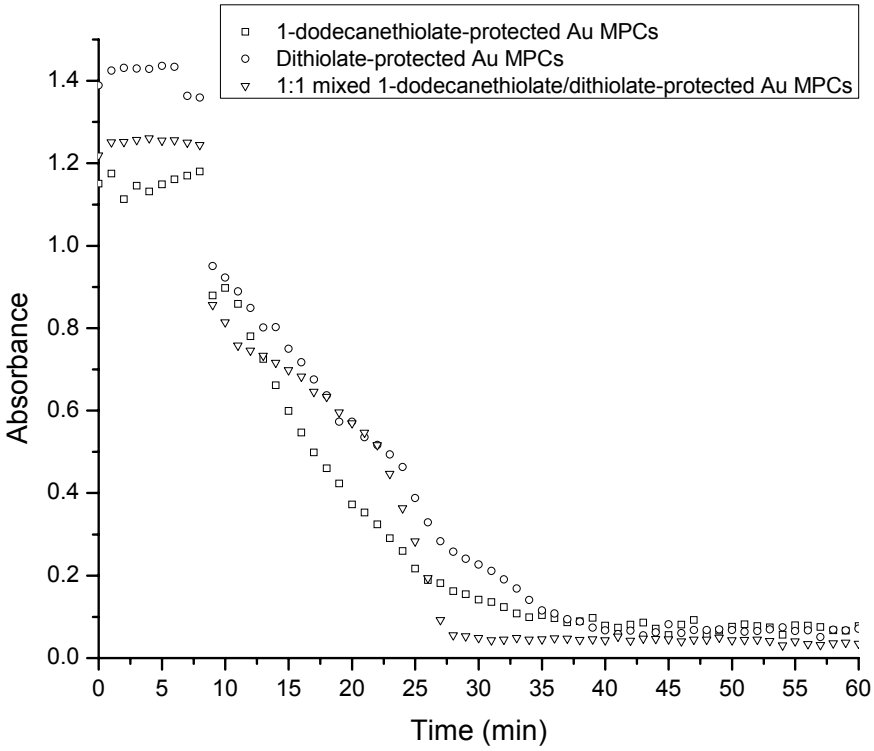

Figure 3.20. UV-Vis absorption changes at 400 nm vs. time for 4-nitrophenol reduction by $NaBH_4$ catalyzed by Au MPCs.

Pseudo-first-order kinetics with respect to 4-nitrophenol were used to evaluate the catalytic activity of the three Au MPCs [17, 24]. Pseudo-first-order rate constants were obtained by plotting the absorbance changes vs. time (after removing the induction time) and are shown in Table 3.4. As can be seen in Table 3.4, all three Au MPC samples have a high catalytic activity for the reduction of 4-nitrophenol. Dodecanethiolate-stabilized MPCs fit well to a pseudo-first order fit. However, the other

MPCs started with slow kinetics for nitrophenol reduction, followed by a transition to faster kinetics at longer time intervals; thus these MPCs were fit to two successive pseudo-first order fits. Figure 3.21 shows the fit of the experimental data for the nitrophenol reduction using 1-dodecanethiolate-protected Au MPCs, the fits for the other MPCs can be found in the Appendix (See Figure A4-A5 in Appendix).

Table 3.4. The pseudo-first-order rate constants (k_1) for 4-nitrophenol reduction catalyzed by Au MPCs at room temperature.

Au-MPC Stabilizer	Induction Time (min)	k_1/min^{-1}
1-dodecanethiolate	10	0.096 ± 0.001
Dithiolate	9	0.050 ± 0.001 (first 15 minutes) 0.115 ± 0.003 (after 15 minutes)
1:1 mixed 1-dodecanethiolate/dithiolate	9	0.035 ± 0.002 (first 12 minutes) 0.28 ± 0.03 (after 4 minutes)

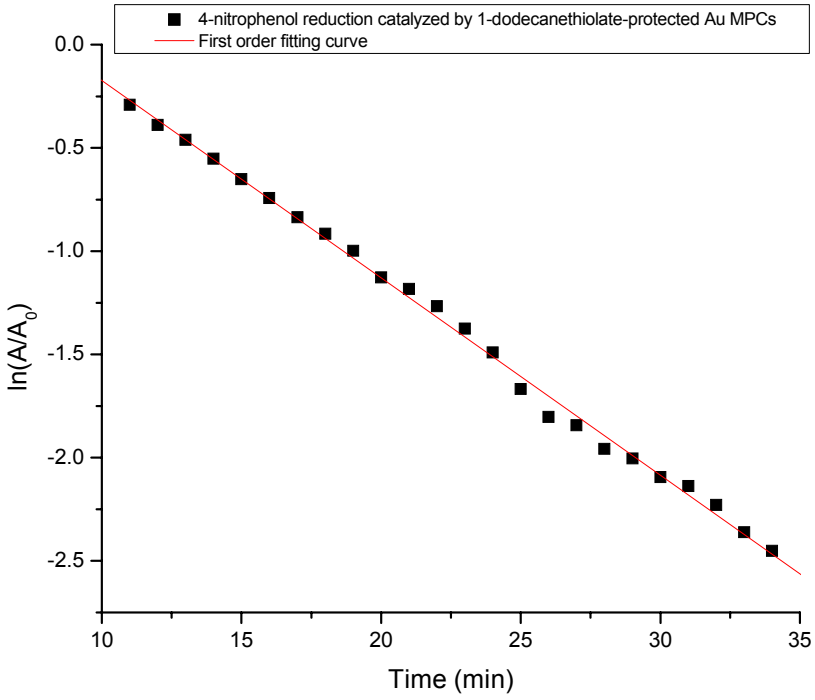

Figure 3.21. UV-Vis absorption changes at 400 nm vs. time for 4-nitrophenol reduction by $NaBH_4$ catalyzed by 1-dodecanethiolate-protected Au MPCs with the 1st order fit shown (R^2=0.997). The data were fitted to first order kinetics after removing the induction time.

The catalytic results are somewhat surprising in that all three Au MPCs have a high catalytic activity for 4-nitrophenol reduction reaction, despite major differences in their surface accessibility as noted in previous sections. Early in the reaction, the 1-dodecanethiolate-protected Au MPCs have a higher catalytic activity than any of the dithiolate-protected Au MPCs for the nitrophenol reduction reaction, despite having the least accessible surface according to cyanide etching studies. However, it should be noted that while dithiolate and mixed 1-docanethiolate/dithiolate Au MPCs show slow

reaction kinetics over short time periods, this is followed by a transition to rapidly increasing activity. These findings must be due to the mechanism(s) involved in the 4-nitrophenol reduction reaction. We postulate that the mechanism involves two steps. The first step is the process of reductively removing thiolates from the surface of gold nanoparticle via reaction with $NaBH_4$, while the second step is the reduction of 4-nitrophenol over the Au surface. The 4-nitrophenol reduction catalyzed by 1-dodecanethiolate-protected Au MPCs is fastest at the beginning as only one sulfur-Au bond needs to be reduced in the first step of the reaction, and the MPCs have extremely high surface areas due to their small size. However, for the dithiolate ligands the reduction reaction begins to proceed as the first sulfur-Au bond is reduced off the Au MPC surface, and rapidly accelerates as the second bond is reduced and the dithiolate desorbs, leaving an extremely accessible surface for nitrophenol reduction. However, this mechanism is speculative only, and more work needs to be done to verify that reductive thiolate desorption is indeed occurring during this reaction.

Finally, long-term stability of the catalysts also seems to be problematic. After the catalytic reaction, only the 1-dodecanethiolate-protected Au MPCs were still dispersed in the solution; the dithiolate- and 1:1 mixed 1-dodecanethiolate/dithiolate-protected Au MPCs precipitated out of the solution. We believe that the smaller dodecanethiolate-protected Au MPCs may be partially stabilized by the product of the reduction reaction, 4-aminophenol; however the ability to recycle and reuse Au MPC catalysts for nitrophenol reductions need be further studied.

3.4 Conclusions

1-dodecanethiolate-, dithiolate-, and 1:1 mixed 1-dodecanethiolate/dithiolate-protected Au MPCs have been synthesized and their thermal and oxidative stability in the presence of oxygen and cyanide anions has been studied. These systematic investigations have revealed the stability of Au MPCs can be tuned by choosing different thiolate-based ligands and oxidation conditions. The catalytic activity of 1-dodecanethiolate-, dithiolate-, and 1:1 mixed 1-dodecanethiolate/dithiolate-protected Au MPCs for the 4-nitrophenol reduction has also been studied, with Au MPCs showing high catalytic activity for this reaction. Somewhat surprisingly, the nitrophenol reduction results showed that even stable 1-dodecanethiolate-protected Au MPCs can be used as catalysts for such reactions, with excellent activity and stability. These results are very important first step for designing Au MPC catalysts with high catalytic activity and selectivity for specific products.

The stability results for the Au MPCs revealed that thiolate-protected Au MPCs, especially partially-oxidized thiolate-protected Au MPCs, could be promising catalysts. Future studies will examine their catalytic activity for aerobic alcohol oxidation reactions. Oxygen, which is used as the oxidant in this reaction, will oxidize thiolate ligands and remove them from the surface of gold core, followed by alcohol oxidation reactions that could be catalyzed by partially-oxidized thiolate-protected Au MPCs. However, the stability of Au MPCs might be problematic when they are used as catalysts for alcohol oxidation reactions. How to choose suitable conditions which allow for both sufficient catalytic activity and catalyst stability will be a key to use this

catalytic system for catalytic oxidation reactions. Another problem that will arise is how to separate products from catalytic system after reaction.

3.5 References

[1] L.S. Ott, and R.G. Finke, Coordination Chem. Rev. 251 (2007) 1075-1100.

[2] F. Lu, J. Ruiz, and D. Astruc, Tetrahedron Lett. 45 (2004) 9443-9445.

[3] S.E. Eklund, and D.E. Cliffel, Langmuir 20 (2004) 6012-6018.

[4] K.R. Gopidas, J.K. Whitesell, and M.A. Fox, Nano Lett. 3 (2003) 1757-1760.

[5] L. Strimbu, J. Liu, and A.E. Kaifer, Langmuir 19 (2003) 483-485.

[6] J. Alvarez, J. Liu, E. Roman, and A.E. Kaifer, Chem. Comm. (2000) 1151-1152.

[7] Y. Murakami, and K. Konishi, J. Am. Chem. Soc. 129 (2007) 14401-14407.

[8] M. Dasog, and R.W.J. Scott, Langmuir 23 (2007) 3381-3387.

[9] M.H. Schoenfisch, and J.E. Pemberton, J. Am. Chem. Soc. 120 (1998) 4502-4513.

[10] A.C. Templeton, M.J. Hostetler, C.T. Kraft, and R.W. Murray, J. Am. Chem. Soc. 120 (1998) 1906-1911.

[11] J.S. Choi, Y.W. Jun, S.I. Yeon, H.C. Kim, J.S. Shin, and J. Cheon, J. Am. Chem. Soc. 128 (2006) 15982-15983.

[12] S.S. Agasti, C.C. You, P. Arumugam, and V.M. Rotello, J. Mater. Chem. 18 (2008) 70-73.

[13] S. Roux, B. Garcia, J.L. Bridot, M. Salome, C. Marquette, L. Lemelle, P. Gillet, L. Blum, P. Perriat, and O. Tillement, Langmuir 21 (2005) 2526-2536.

[14] W. König, and R. Geiger, Chem. Ber. 103 (1970) 788.

[15] M. Brust, M. Walker, D. Bethell, D.J. Schiffrin, and R. Whyman, J. Chem. Soc., Chem. Commun. (1994) 801-802.

[16] M. Zheng, F. Davidson, and X.Y. Huang, J. Am. Chem. Soc. 125 (2003) 7790-7791.

[17] S. Panigrahi, S. Basu, S. Praharaj, S. Pande, S. Jana, A. Pal, S.K. Ghosh, and T. Pal, J. Phys. Chem. C 111 (2007) 4596-4605.

[18] T.G. Schaaff, M.N. Shafigullin, J.T. Khoury, I. Vezmar, R.L. Whetten, W.G. Cullen, P.N. First, C. GutierrezWing, J. Ascensio, and M.J. JoseYacaman, J. Phys. Chem. B 101 (1997) 7885-7891.

[19] C. Burda, X.B. Chen, R. Narayanan, and M.A. El-Sayed, Chem. Rev. 105 (2005) 1025-1102.

[20] S. Link, and M.A. El-Sayed, Int. Rev. Phys. Chem. 19 (2000) 409-453.

[21] M.J. Hostetler, J.E. Wingate, C.J. Zhong, J.E. Harris, R.W. Vachet, M.R. Clark, J.D. Londono, S.J. Green, J.J. Stokes, G.D. Wignall, G.L. Glish, M.D. Porter, N.D. Evans, and R.W. Murray, Langmuir 14 (1998) 17-30.

[22] O. Kohlmann, W.E. Steinmetz, X.A. Mao, W.P. Wuelfing, A.C. Templeton, R.W. Murray, and C.S. Johnson, J. Phys. Chem. B 105 (2001) 8801-8809.

[23] M. Dasog, A. Kavianpour, M.F. Paige, H.B. Kraatz, and R.W.J. Scott, Can. J. Chem. 86 (2008) 368-375.

[24] K. Hayakawa, T. Yoshimura, and K. Esumi, Langmuir 19 (2003) 5517-5521.

[25] G. Sharma, and M. Ballauff, Macromol. Rapid Commun. 25 (2004) 547-552.

CHAPTER 4

Summary and Future Work

4.1 Summary and Future Work for Alcohol Oxidation Catalysts

In this project, we have shown that PVP-stabilized 1:3 Au:Pd nanoparticles have higher catalytic activities than pure Au, pure Pd nanoparticles and other ratio bimetallic nanoparticles for alcohol oxidation reactions. These particles have been shown to catalyze the aerobic oxidations of aliphatic, allylic, phenylic alcohols, and diols in aqueous solution under mild conditions. In most cases, selective oxidations to aldehydes (or ketones) were seen; however, alkanoic acids were the major products for primary aliphatic alcohols and γ-butyrolactone was the only product observed for the oxidation of 1,4-butanediol. Even though we have already had success with this project, there are still several problems that still need solutions for this system. The first problem is the stability of the PVP-stabilized nanoparticle catalysts. Upon catalyzing the aerobic oxidation reaction of benzyl alcohol and 1-butanol, the stability was poor and the nanoparticles often precipitated out of the solution after the reaction. Routes that can lead to the improvement of nanoparticle stability for such reactions have been investigated, and some preliminary results have been obtained (see Sections 4.1.1 and 4.1.2 below). The second problem involves the selectivity for desired products, as will be detailed in Section 4.1.3.

4.1.1 Trapping AuPd Nanoparticles in TiO_2 to Improve Stability

In order to improve the stability, metal nanoparticle catalysts usually are typically trapped in or dispersed onto support materials and used as heterogeneous catalysts; for example, nanoparticles have been successfully incorporated into oxide(TiO_2 [1-3], SiO_2 [4, 5], Al_2O_3 [6], CeO_2 [7, 8]), activated carbon [9, 10], and clay [11, 12] supports, as well as many other supports. Thus we attempted to trap 1:3 Au:Pd nanoparticles into TiO_2 to improve the stability. TiO_2-supported 1:3 Au:Pd nanoparticles were prepared according to the following procedure. 0.26 g of PVP was dissolved into 14 ml of methanol, followed by the sequential addition of 0.75 ml of a K_2PdCl_4 aqueous solution (6.3 mg of K_2PdCl_4 in 0.75 ml of deionized water) and 1 ml of a $HAuCl_4 \cdot 3H_2O$ methanolic solution (3.6 mg of $HAuCl_4 \cdot 3H_2O$ in 1 ml of methanol). 14.4 mg of $NaBH_4$ was added to the metal salts to form 1:3 Au:Pd nanoparticles, followed by stirring for 15 min. Finally, 1.10 ml of $Ti(O^iPr)_4$, dissolved in 4 ml of methanol freshly dried over molecular sieves, was added slowly to the PVP-stabilized nanoparticle solution. Within 15-20 s, a gel was formed and was left overnight. The powder was then dried in an oven at 150 ^oC for 3h, followed by calcination in a furnace at 500 ^oC for 5h in air, followed by 2.5 hrs at 500 ^oC under a H_2 flow.

The catalytic activity for the aerobic oxidation of benzyl alcohol and 1-butanol was tested and results are shown in Table 4.1. As can be seen, TiO_2-supported 1:3 Au:Pd nanoparticles were less active for benzyl alcohol oxidation and inert for 1-butanol oxidation. These results are not necessarily surprising since a major disadvantage of heterogeneous catalysts, particularly for solid catalysts in solution, is low catalytic activity due to mass-transfer limitations. Therefore trapping 1:3 Au:Pd nanoparticles into

supporting materials was not an effective way to improve the stability due to the low catalytic activity of the resulting materials.

Table 4.1. Turnover frequency, conversion and selectivities for benzyl alcohol oxidation with 1:3 Au:Pd nanoparticles trapped into TiO_2.

Time (h)	Turnover Frequency (h^{-1})	Conversion (%)	Selectivity	
			Benzaldehyde (%)	Benzoic Acid (%)
1	20	4.0	87.9	12.1
2		4.0	84.8	15.2
3		3.8	82.4	17.6
4		3.7	80.6	19.4
6		3.4	77.1	22.9
8		3.3	75.7	24.3

4.1.2 Using Ionic Liquids as Solvents to Improve Nanoparticle Stability

As detailed in section 1.2.5, ionic liquids can provide electrosteric stabilization for metal nanoparticles (Figure 1.1) [13, 14], such that the anions of the ionic liquid electrostatically stabilize the electrophilic nanoparticle surface and cations offer steric stabilization due to their bulky volume [13, 14]. Therefore, ionic liquids as media can further stabilize metal nanoparticles, that is nanoparticles can be dispersed evenly in ionic liquid solvents to form quasi-homogeneous catalysts with high activities. Moreover, it is easy to recycle and reuse nanoparticle catalysts using ionic liquids as the reaction media [15-18]. Our group has shown that PVP-stabilized Au, Pd and bimetallic

AuPd nanoparticles in 1-butyl-3-methylimidazolium hexafluorophosphate [BMIM][PF_6] ionic liquids have decent catalytic activity and selectivity for hydrogenation reactions [18]. Catalysts could easily be recycled then reused for further catalytic reactions with only a minimal loss in activity, simply by extracting products from the ionic liquid phase and/or pumping off all volatile species from the ionic liquid. Inspired by this achievement, we wished to investigate whether PVP-stabilized 1:3 Au:Pd nanoparticles in [BMIM][PF_6] ionic liquids would also show high activity and significantly enhanced nanoparticle stability for aerobic alcohol oxidations.

PVP-stabilized 1:3 Au:Pd nanoparticles in [BMIM][PF_6] ionic liquid were synthesized following a phase transfer procedure from methanol, in which a methanolic solution of PVP-stabilized nanoparticles was added to the ionic liquid, followed by removal of methanol via vacuum [18]. The catalytic activity and stability of the nanoparticles were tested using benzyl alcohol oxidation as the model reaction. Aerobic alcohol oxidations catalyzed by PVP-stabilized 1:3 Au:Pd nanoparticles in aqueous solution are usually carried out in very basic conditions (pH ~11-12), using potassium carbonate as the base. However, in the case of [BMIM][PF_6] ionic liquid, 1-methylimidazole was first examined as the base (1-methylimidazole is a common impurity in BMIM based ionic liquids). However, the catalytic results showed that the PVP-stabilized 1:3 Au:Pd nanoparticles in [BMIM][PF_6] ionic liquid were inert for benzyl alcohol oxidation under these conditions, likely because 1-methylimidazole was oxidized quickly in the presence of oxygen. When the reaction was carried out with the addition of 78.1 mg of K_2CO_3 (final concentration: 0.057 M) as base, the PVP-stabilized 1:3 Au:Pd nanoparticles in [BMIM][PF_6] ionic liquid have a small but appreciable

catalytic activity for benzyl alcohol oxidation, as shown in Table 4.2. After 20 h, the conversion reached 23%, however the nanoparticles precipitated out of the solution after this time. We are still not certain as the reasons behind the low stability of the nanoparticles in the ionic liquid solvent; PVP oxidation by O_2 at temperatures used might be a possible reason. Alternatively, K_2CO_3 was sparingly soluble and may not act as an effective base in the [BMIM][PF_6] ionic liquid. Nevertheless, the results showed that alcohol oxidations are indeed possible in [BMIM][PF_6] ionic liquids.

Table 4.2. PVP-stabilized 1:3 Au:Pd nanoparticles as the catalyst for benzyl alcohol oxidation in [BMIM][PF_6] ionic liquid in the presence of O_2 at 62^{o}C with K_2CO_3 as base.

Time (h)	Conversion (%)	Selectivity	
		Benzaldehyde (%)	Benzoic Acid (%)
2	0	0	0
20	23	69.6	30.4

Several other attempts were made to improve the stability and activity of the PVP-stabilized 1:3 Au:Pd nanoparticles. The first attempt was to lower the reaction temperature to room temperature and use air as the oxidant instead of O_2. However, while the resulting nanoparticles were much more stable, nearly negligible catalytic activities were seen under these conditions, as shown in Table 4.3. After 26 hours, the conversion is only 3.25% which is much lower than 23% in the presence of O_2 at 62 ^{o}C. Finally, 31.7 mg of KOH (final concentration: 0.057 M) was used as the base to replace

K_2CO_3, to see if a stronger base would lead to improvements in the activity of the catalysts. Under the mild conditions, the catalytic activity is still low and the conversion is 3.1% after 24 hours, as shown in Table 4.4. Upon increasing the temperature to at 62 ^oC and using O_2 as the oxidizing agent, the conversion increased slightly to 7.05% (Table 4.5).

Table 4.3. PVP-stabilized 1:3 Au:Pd nanoparticles as the catalyst for benzyl alcohol oxidation in [BMIM][PF_6] ionic liquid under air at room temperature with K_2CO_3 as base.

Time (h)	Conversion (%)	Selectivity	
		Benzaldehyde (%)	Benzoic Acid (%)
2	1.94	68.2	31.8
26	3.25	78.6	21.4

Table 4.4. PVP-stabilized 1:3 Au:Pd nanoparticles as the catalyst for benzyl alcohol oxidation in [BMIM][PF_6] ionic liquid in the presence of O_2 at room temperature with KOH as base.

Time (h)	Conversion (%)	Selectivity	
		Benzaldehyde (%)	Benzoic Acid (%)
2	0.95	50.0	50.0
24	3.07	61.2	38.8

Table 4.5. PVP-stabilized 1:3 Au:Pd nanoparticles as the catalyst for benzyl alcohol oxidation in [BMIM][PF_6] ionic liquid in the presence of O_2 at 62 ^oC with KOH as base.

Time (h)	Conversion (%)	Selectivity	
		Benzaldehyde (%)	Benzoic Acid (%)
2	3.77	67.3	32.7
24	7.05	75.0	25.0

To date the highest catalytic activity for the PVP-stabilized AuPd nanoparticles for benzyl alcohol oxidation was obtained under O_2 at 62 ^oC with K_2CO_3 as base. Further studies will be carried out to improve both catalytic activity and stability by changing the conditions and the base. The ability to recycle and reuse PVP-stabilized AuPd nanoparticle catalysts in [BMIM][PF_6] ionic liquids will also be investigated.

4.1.3 Using Bimetallic Core/shell Structures to Improve Catalytic Oxidation Selectivity

In chapter two, it was noted that when the catalytic activity of the 1:3 Au:Pd nanoparticles towards 2-buten-1-ol was examined, three products were observed in the first hour of the reaction: the oxidation product of 2-buten-ol (crotonaldehyde), the hydrogenation product of 2-buten-1-ol (1-butanol), and an isomerization product of 2-buten-1-ol (3-buten-1-ol). However, after one hour, only the oxidation product was observed. Similar C=C double bond isomerization and hydrogenation products were reported by Abad *et al*.[7, 8], who suggested that Pd-H species are formed during the

aerobic alcohol oxidations which can promote C=C double bond isomerization and hydrogenation. Based on these results, nanoparticle catalysts with core/shell structures will be synthesized, which will not only have improved catalytic activities due to synergetic electronic interactions between Au and Pd atoms in the individual nanoparticles, but also should be specific to oxidation reactions, because only Au atoms would reside on the surface and no Pd-H species would be formed. This proposed research plan includes synthesis of Pd/Au core/shell nanoparticles using a sequential loading method and testing the resulting catalytic activity of such nanoparticles towards the oxidation of allylic alcohols (for example, allyl alcohol, 2-buten-1-ol, 1-hexen-3-ol, trans-2-hexen-1-ol and cinnamyl alcohol). In addition, Au/Pd core/shell nanoparticles will be synthesized and their catalytic activities towards allylic alcohol oxidation will be examined in order to compare with the catalytic activities of Pd/Au core/shell nanoparticles.

In addition, Extended X-ray Absorption Fine Structure (EXAFS) spectroscopy has been found to be a valuable technique for the examination of the structure of bimetallic nanoparticles [19, 20]. Future plans include the collection of EXAFS data at the Canadian Light Source (CLS) to characterize Pd/Au core/shell and Au/Pd core/shell structure nanoparticles. These systems will also be thoroughly characterized by TEM and UV-Vis spectroscopy, and attempts will be made to tie the structures of the nanoparticles with their resulting catalytic activity.

4.2 Summary and Future Work for Au Monolayer-Protected Cluster Catalysts

As detailed in Chapter 3, 1-dodecanethiolate-, dithiolate-, and 1:1 mixed 1-dodecanethiolate/dithiolate-protected Au MPCs have been synthesized and their thermal stability and oxidative stability in the presence of oxygen and cyanide anions has been studied. In addition, all of the Au MPCs showed high catalytic activity for 4-nitrophenol reduction by $NaBH_4$. However, there is still much work to be done on elucidating the mechanism of this catalytic reduction. Future work will focus both on elucidating the mechanism(s) of catalytic reduction of 4-nitrophenol, as well as these Au MPCs for aerobic alcohol oxidations. The investigation of catalytic activity and selectivity of partially-oxidized thiolate-protected Au MPCs will be the major part of the future work. More work needs to be done to establish control of the catalytic sites available on the gold core by varying the oxidation conditions and the types of ligands used. Partially-oxidized thiolate-protected Au MPCs with moderate free surface area could, in principle, have substantial selectivity for specific substrates, which would allow for design of nanoparticle catalysts with extremely high selectivity. However, as my work has shown in Chapter 3, routes towards catalytically-active Au MPCs via partial oxidation of thiolates from their surface are full of pitfalls, and much more work needs to be done before dreams of highly-selective MPC catalysts can become reality.

4.3 References

[1] M. Haruta, and M. Date, Appl. Catal. A: Gen. 222 (2001) 427-437.

[2] M. Valden, X. Lai, and D.W. Goodman, Science 281 (1998) 1647-1650.

[3] D.I. Enache, J.K. Edwards, P. Landon, B. Solsona-Espriu, A.F. Carley, A.A. Herzing, M. Watanabe, C.J. Kiely, D.W. Knight, and G.J. Hutchings, Science 311 (2006) 362-365.

[4] Z.S. Hou, N. Theyssen, and W. Leitner, Green Chem. 9 (2007) 127-132.

[5] B. Karimi, S. Abedi, J.H. Clark, and V. Budarin, Angew. Chem. Int. Ed. 45 (2006) 4776-4779.

[6] M.S. Kwon, N. Kim, C.M. Park, J.S. Lee, K.Y. Kang, and J. Park, Organic Letters 7 (2005) 1077-1079.

[7] A. Abad, C. Almela, A. Corma, and H. Garcia, Chem. Commun. (2006) 3178-3180.

[8] A. Abad, C. Almela, A. Corma, and H. Garcia, Tetrahedron 62 (2006) 6666-6672.

[9] S. Cahen, G. Furdin, J.F. Mareche, and A. Albiniak, Carbon 46 (2008) 511-517.

[10] S. Dominguez-Dominguez, W. Berenguer-Murcia, B.K. Pradhan, A. Linares-Solano, and D. Cazorla-Amoros, J. Phys. Chem. C 112 (2008) 3827-3834.

[11] N. Kakiuchi, Y. Maeda, T. Nishimura, and S. Uemura, J. Org. Chem. 66 (2001) 6620-6625.

[12] T. Nishimura, N. Kakiuchi, M. Inoue, and S. Uemura, Chem. Commun. (2000) 1245-1246.

[13] D. Astruc, F. Lu, and J.R. Aranzaes, Angew. Chem. Int. Ed. 44 (2005) 7852-7872.

[14] L.S. Ott, and R.G. Finke, Coordination Chem. Rev. 251 (2007) 1075-1100.

[15] X.D. Mu, D.G. Evans, and Y.A. Kou, Catal. Lett. 97 (2004) 151-154.

[16] C.W. Scheeren, G. Machado, J. Dupont, P.F.P. Fichtner, and S.R. Texeira, Inorg. Chem. 42 (2003) 4738-4742.

[17] J. Dupont, G.S. Fonseca, A.P. Umpierre, P.F.P. Fichtner, and S.R. Teixeira, J. Am. Chem. Soc. 124 (2002) 4228-4229.

[18] P. Dash, N.A. Dehm, and R.W.J. Scott, J. Mol. Catal. A: chem. 286 (2008) 114-119.

[19] N. Toshima, M. Harada, T. Yonezawa, K. Kushihashi, and K. Asakura, J. Phys. Chem. 95 (1991) 7448-7453.

[20] N. Toshima, M. Harada, Y. Yamazaki, and K. Asakura, J.Phys. Chem. B 96 (1992) 9927-9933.

APPENDIX

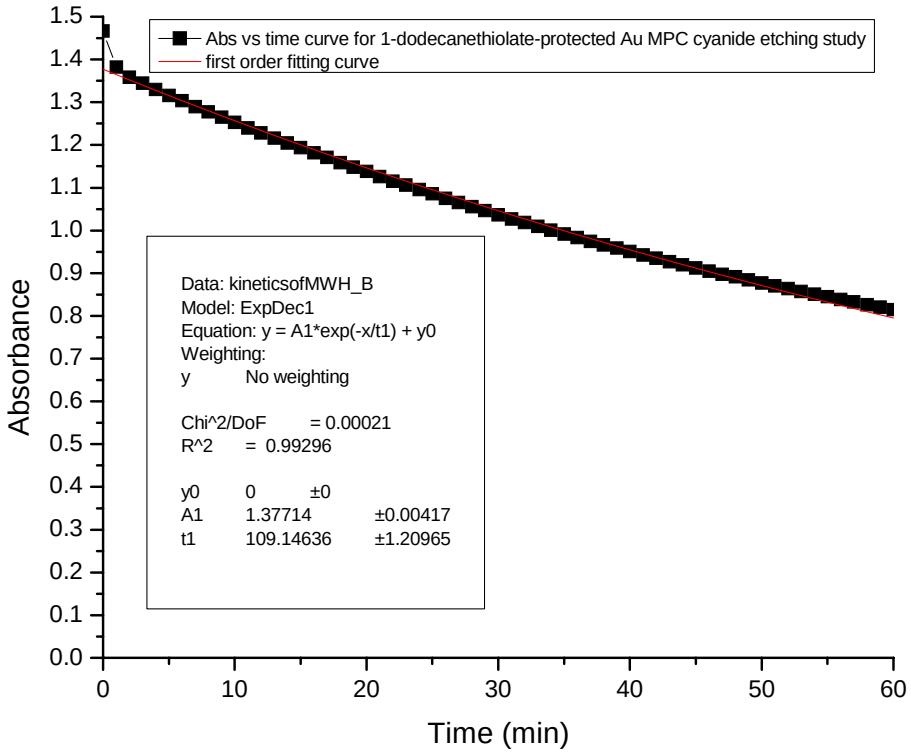

Figure A1. UV-Vis absorption changes of 1-dodecanethiolate-protected Au MPCs at 520 nm in the presence of KCN at room temperature with the 1st order fit shown (R^2=0.993).

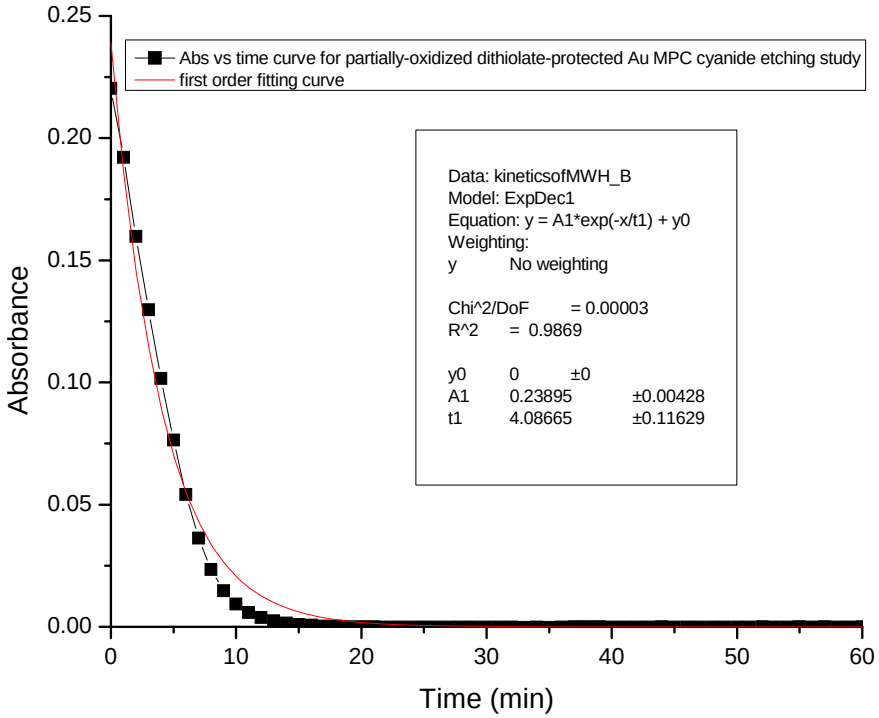

Figure A2. UV-Vis absorption changes of partially-oxidized dithiolate-protected Au MPCs at 520 nm in the presence of KCN at room temperature with the 1st order fit shown (R^2=0.987).

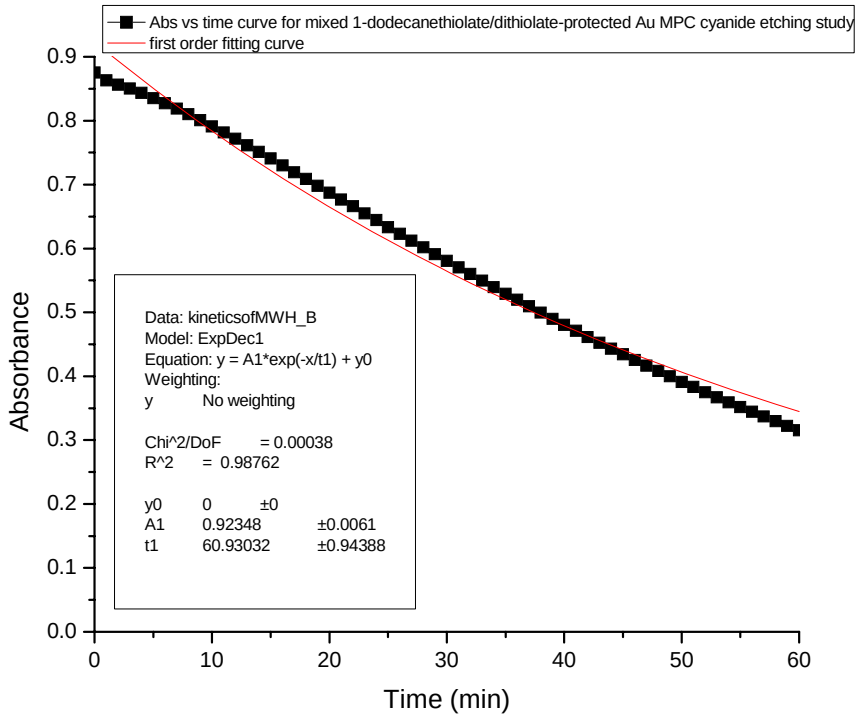

Figure A3. UV-Vis absorption changes of mixed 1-dodecanethiolate/dithiolate-protected Au MPCs at 520 nm in the presence of KCN at room temperature with the 1st order fit shown (R^2=0.988).

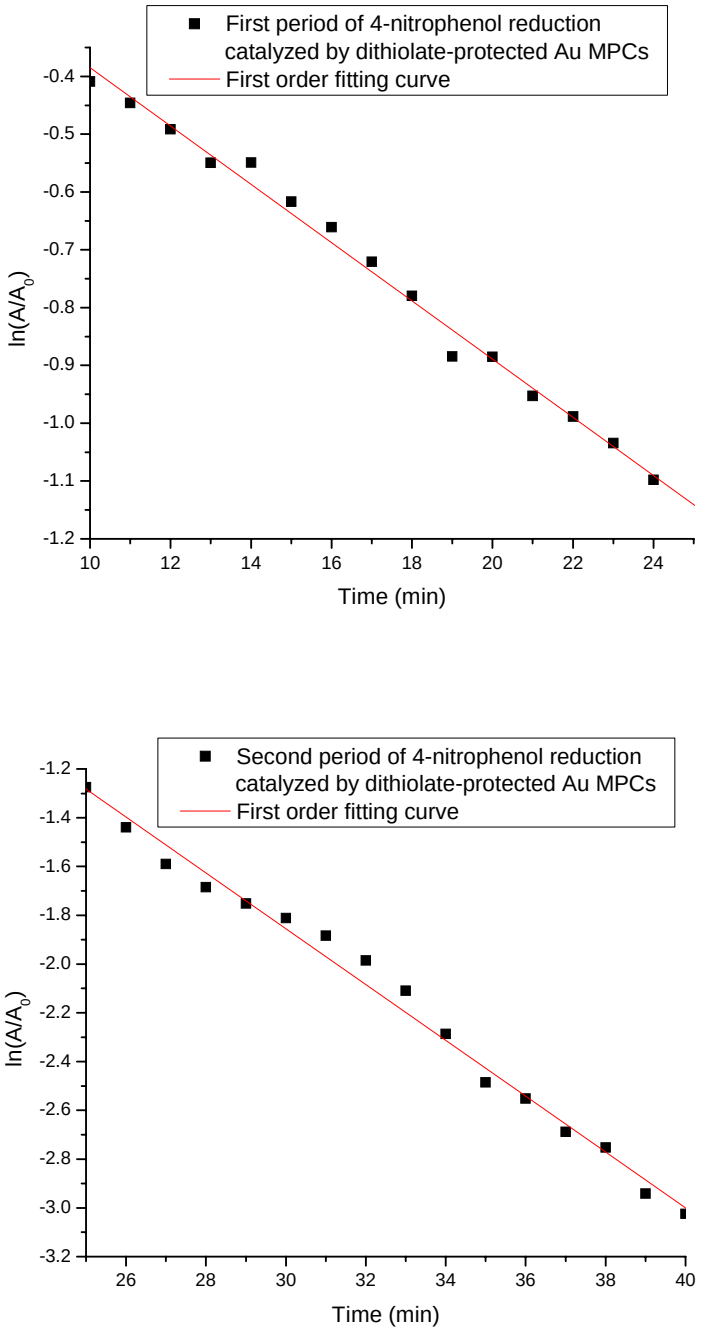

Figure A4. UV-Vis absorption changes at 400 nm vs. time for 4-nitrophenol reduction by $NaBH_4$ catalyzed by dithiolate-protected Au MPCs with the 1st order fit shown (R^2=0.991, 0.989). The data were fitted to first order kinetics after removing the induction time.

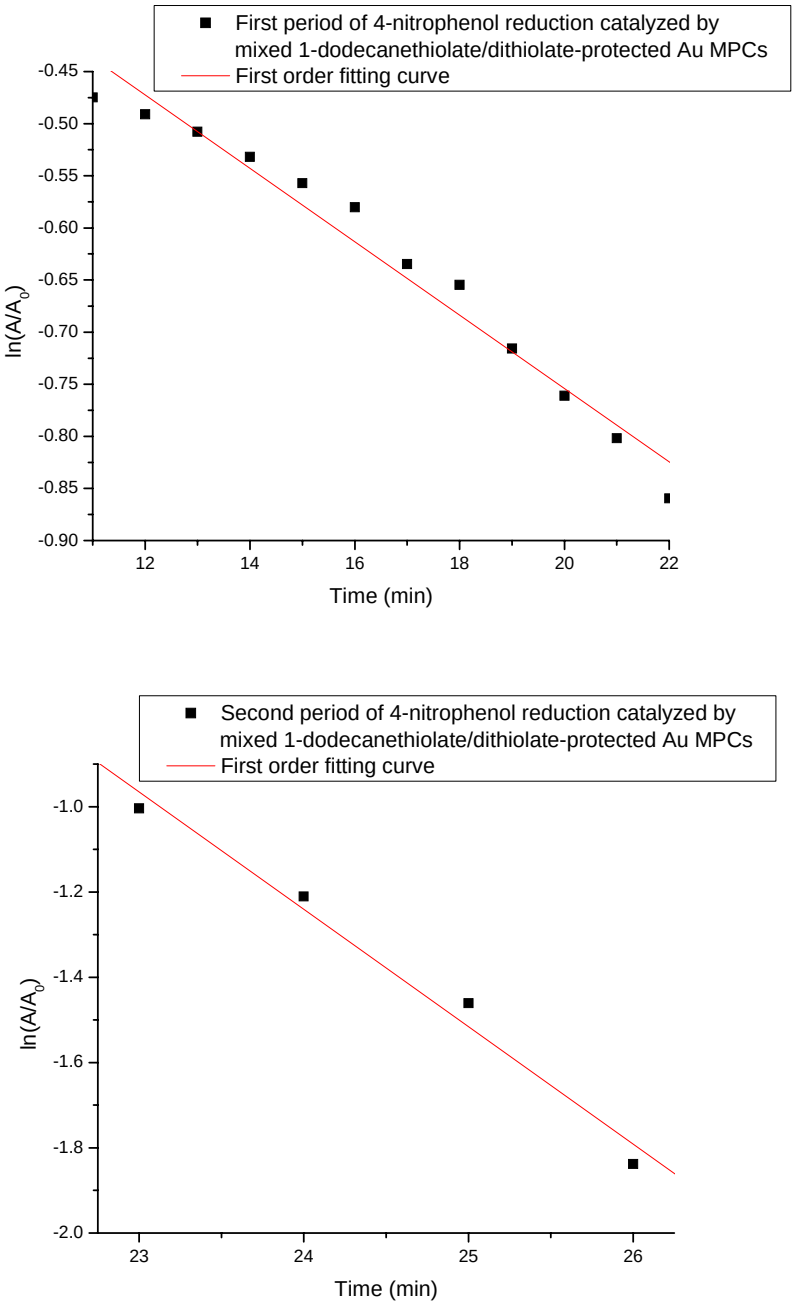

Figure A5. UV-Vis absorption changes at 400 nm vs. time for 4-nitrophenol reduction by $NaBH_4$ catalyzed by mixed 1-dodecanethiolate/dithiolate-protected Au MPCs with the 1st order fit shown (R^2=0.974, 0.980). The data were fitted to first order kinetics after removing the induction time.